A PSEUDO-2D HYDRODYNAMIC MODEL FOR A TIDAL RIVER-WETLAND SYSTEM

Final Report

DECEMBER 1996

JHR 96-253 Project 93-4

Principal Investigators:

J. D. Lin, Emeritus Professor
Michael W. Lefor, Assitant Professor
J. S. Hua, K. J. Qiu and W. G. Liao

This research was sponsored by the Joint Highway Research Advisory Council (JHRAC) of the University of Connecticut and the Connecticut Department of transportation and was carried out in the Civil and Environmental Engineering Department of the University of Connecticut.

The contents of this report reflect the view of the author (s) who are responsible for the facts and accuracy of the date presented herein. The contents do not necessarily reflect the official views or policies of the University of Connecticut or the Connecticut Department of Transportation. This report does not constitute a standard, specifications, or regulations.

Technical Report Documentation Page

1. Report No. JHR 96-253	2. Government Accession No.	3. Recipient's Catalog No.
4. Title and Subtitle A Pseudo-2-D Hydrodynamic Model for a Tidal River-Wetland System		5. Report Date December 1996
		6. Performing Organization Code
7. Author(s) J. D. Lin, M. W. Lefor, J. S. Hua, K. J. Qiu & W. G. Liao		8. Performing Organization Report No. JHR 96-253
9. Performing Organization Name and Address University of Connecticut Department of Civil and Environmental Engineering 191 Auditorium Road, Box U-37 Storrs, CT 06269		10. Work Unit No. (TRAIS)
		11. Contract or Grant No.
12. Sponsoring Agency Name and Address Connecticut Department of Transportation 280 West Street Rocky Hill, CT 06067-0207		13. Type of Report and Period Covered Final Report
		14. Sponsoring Agency Code
15. Supplementary Notes		

16. Abstract

A Pseudo-2-D hydrodynamic model has been developed for a coastal river and wetland-marsh system. The two-dimensional tidal flow field over a marsh is calculated by combining the St. Vennant equations for the river and marsh in the longitudinal direction and the continuity and the approximated momentum equations in the transverse direction. Calibration and validation of the model were carried out using tidal stage and current data acquired at the Oyster River in Old Saybrook, Connecticut, under low tide and spring high tide conditions. Model simulation can provide water depth and velocity over the marsh that will allow the transportation engineers to quantitatively assess the effects of highway structures on tidal flushing. The exchange of water between the main river and the marsh provides the transport of salinity, sediment, and nutrients over the marsh. The model was applied a number of scenarios due to the construction of the U. S. Route 1 bridge crossing over the Oyster River. The simulation results indicate that the present U. S. Route 1 bridge has little or no impact on the tidal flushing in the Oyster River-Marsh system.

17. Key Words	18. Distribution Statement		
19. Security Classif. (of this report) Unclassified	20. Security Classif. (of this page) Unclassified	21. No. of Pages 182	22. Price

Form DOT F 1700.7 (8-72) Reproduction of completed page authorized

SI* (MODERN METRIC) CONVERSION FACTORS

APPROXIMATE CONVERSIONS TO SI UNITS

Symbol	When You Know	Multiply By	To Find	Symbol
	LENGTH			
in	inches	25.4	millimetres	mm
ft	feet	0.305	metres	m
yd	yards	0.914	metres	m
mi	miles	1.61	kilometres	km
	AREA			
in^2	square inches	645.2	millimetres squared	mm^2
ft^2	square feet	0.093	metres squared	m^2
yd^2	square yards	0.836	metres squared	m^2
ac	acres	0.405	hectares	ha
mi^2	square miles	2.59	kilometres squared	km^2
	VOLUME			
fl oz	fluid ounces	29.57	millilitres	mL
gal	gallons	3.785	Litres	L
ft^3	cubic feet	0.028	metres cubed	m^3
yd^3	cubic yards	0.765	metres cubed	m^3

NOTE: Volumes greator than 1000 L shall be shown in m^3.

	MASS			
oz	ounces	28.35	grams	g
lb	pounds	0.454	kilograms	kg
T	short tons (2000 lb)	0.907	megagrams	Mg
	TEMPERATURE (exact)			
°F	Fahrenheit temperature	5(F-32)/9	Celcius temperature	°C

*SI is the symbol for the International System of Measurement

APPROXIMATE CONVERSIONS TO SI UNITS

Symbol	When You Know	Multiply By	To Find	Symbol
	LENGTH			
mm	millimetres	0.039	inches	in
m	metres	3.28	feet	ft
m	metres	1.09	yards	yd
km	kilometres	0.621	miles	mi
	AREA			
mm^2	millimetres squared	0.0016	square inches	in^2
m^2	metres squared	10.764	square feet	ft^2
ha	hectares	2.47	acres	ac
km^2	kilometres squared	0.386	square miles	mi^2
	VOLUME			
mL	millilitres	0.034	fluid ounces	fl oz
L	litres	0.264	gallons	gal
m^3	metres cubed	35.315	cubic feet	ft^3
m^3	metres cubed	1.308	cubic yards	yd^3
	MASS			
g	grams	0.035	ounces	oz
kg	kilograms	2.205	pounds	lb
Mg	megagrams	1.102	short tons (2000 lb)	T
	TEMPERATURE (exact)			
°C	Celcius temperature	1.8C + 32	Fahrenheit temperature	°F

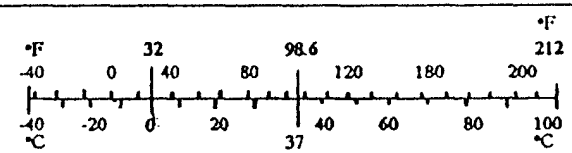

Achnowledgments

This work is sponsored by Connenticut Department of Transportation under project JHRAC 93-4, " Hydrodynamic and Transport Models of Coastal Water for Use in the Design and Management of Highway Structures ". Field surveying was conducted by Roger Ferguson at the Oyster River site and the maps were prepared by Roger Ferguson and Phil Caron. We thank Bruce Davies, U. S. Geological Survey, Connecticut Field Office, for use of the stream gaging equipment.

Table of Contents

Abstract ii

Acknowledgements iv

Table of Contents v

List of Figures vii

List of Tables x

1. Introduction 1

2. Pseudo 2-D Hydrodynamic Model 4

2.1 Background 4

2.2 Formulation 6

2.3 Numerical Method 12

2.4 Calculation Procedure 16

2.5 Relevant Treatments 25

2.6 Computer Programs 28

3. Field Work 40

3.1 Description of Research Site at the Oyster River, Old Saybrook, Connecticut 41

3.2 Surveying and Datum Establishment 46

3.3 Layout for Longitudinal Flow Calculation 50

3.4 Layout for Transverse Flow Calculation 51

3.5 Tidal Stage Measurements 51

3.6 Current Measurements 52

3.7 Measurement of Influent Fresh Water 53

3.8 Results of Field Measurements 53

3.9 Results of Detailed Vegetation Surveying Work 54

4. Model Calibration and Simulation 72

4.1 Transition Loss Coefficient 72

4.2 Manning's Roughness Coefficient for the Main Channel 74

4.3 Manning's Roughness Coefficient for the Overbank Regions 75

4.4 Calibration Results 76

4.5 Comparisons of Simulation Results With Measured Data 86

5. Model Applications 100

5.1 The Effect of Overbank Flow 100

5.2 Tidal Flow in the Oyster River-Marsh System 101

5.3 The Effect of Bridge Crossings 104

5.4 The Impact of the U.S. Route 1 Bridge 125

6. Summary and Conclusions 140

References 142

Appendices: 145

A. Cross Sections of the Oyster River 145

B. Tidal Stage and Current Data 155

List of Figures

2.1 Overbank Flow Notation 8

2.2 Coordinate System for Overbank Flow 10

2.3 Different Overbank Flow Conditions 11

2.4 Node System on x-t Plane 14

2.5 Flow Chart for Longitudinal Flow Calculation 22

2.6 Flow Chart for Transverse Flow Calculation 23

2.7 Flow Chart for Overall Calculation 24

2.8 Junction in a River Channel 26

2.9 Meandering Stream 27

2.10 Treatment of Lateral Flow During Ebb Tide 33

2.11 P2DHY1 Input and Output File Structure 37

3.1 Locations of Old Saybrook and Westbrook, Connecticut 55

3.2 Copy of State Road Map Showing Political Boundaries and Major Roads 56

3.3 U.S.G.S. Topographic Mapping for the Oyster River Region, Old Saybrook 57

3.4 Major Bedrock Boundaries 58

3.5 Bedrock Surface Distribution 59

3.6 U.S.G.S. Surficial Mapping 60

3.7 Cross-section Showing Bedrock and Surficial Deposits (from Flint, 1972) 61

3.8 Drainage Basins (State of Conn. Drainage Basin Atlas, 1982) 62

3.9 Digitized Topography Used in the Computer Simulation 63

3.10 Basin Convergences 64

3.11 Locations of Tide Staff 65

3.12 Schematic Cross-sections of Salt Marsh Channels 66

3.13 Locations of Cross-sections for Model Calculation 67

3.14 System Storage Areas 68

3.15 Current Measurements at the Rte. 1 Bridge Section 69

3.16 Current Measurements at the ConnRail Bridge Section 70

3.17 Locations For Fresh-Water Runoff Measurements 71

4.1 Influence of K_e on Discharge Process 77

4.2 Influence of K_e on Water Elevation Distribution 78

4.3 Influence of n_c on Discharge at Section 6 Near Rte. 1 Bridge 79
4.4 Influence of n_c on Water Surface Elevation at Section 6 Near Rte. 1 Bridge 80
4.5 Influence of n_c on Water Surface Elevation Profile During Flood Tide 80
4.6 Influence of n_c on Water Surface Elevation Profile During Ebb Tide 81
4.7 Influence of n_s on Discharge at the Section 6 near Rte. 1 Bridge 82
4.8 Influence of n_s on Water Surface Elevation at Section 6 near Rte. 1 Bridge 83
4.9 Influence of n_s on Water Surface Elevation Profile During Flood Tide 84
4.10 Influence of n_s on Water Surface Elevation Profile During Ebb Tide 85
4.11 Comparison of Water Surface Elevation at Staff 2 87
4.12 Comparison of Water Surface Elevation at Staff 3 88
4.13 Comparison of Water Surface Elevation at Staff 5 88
4.14 Comparison of Water Surface Elevation at Staff 6 89
4.15 Comparison of Water Surface Elevation at Staff 7 89
4.16 Comparison of Water Elevation During Ebb Tide 90
4.17 Comparison of Water Elevation During Flood Tide 91
4.18 Comparison of Water Elevation at Staff 3 92
4.19 Comparison of Water Elevation at Staff 6 92
4.20 Comparison of Water Elevation at Staff 7 93
4.21 Comparison of Water Elevation Distribution During Flood Tide 94
4.22 Comparison of Water Elevation Distribution During Ebb Tide 95
4.23 Comparison of Water Elevation at Staff 7 96
4.24 Comparison of Discharge and Water Elevation at Section 6 97
4.25 Comparison of Water Elevation at Staff 4 98
4.26 Comparison of Water Elevation at Staff 7 98
4.27 Comparison of Discharges and Water Elevation at Section 6 99
5.1 Q-T Relation at Rte. 1 Bridge (Section 6) 106
5.2 Water Elevation and Discharge at Rte. 1 Bridge (Section 6) 107
5.3 Water Elevation and Discharge at the R.R. Bridge (Section 20) 108
5.4 Time Lag Analysis 109
5.5 Transverse Propagation of Water Surface at Section 14 110
5.6 Transverse Propagation of Tidal Fronts Over the Marsh 111
5.7 Velocity Distribution During Flood Tide Over the Marsh 112

5.8 Velocity Distribution During Ebb Tide Over the Marsh 113
5.9 Water Exchange between Main Channel and Left Marsh at Section 14 114
5.10 Comparison of Longitudinal and Transverse Velocity at Left Marsh at Section 14 115
5.11 Comparision of Longitudinal Velocity in Main Channel and Overbank Region 116
5.12 Comparision of Discharge in Main Channel and Overbank Region 117
5.13 Comparision of Discharge in Main Channel and Overbank Region 118
5.14 Comparison of Water Surface Elevations at Rte. 1 Bridge (Section 6) 119
5.15 Comparison of Discharge at Rte. 1 Bridge (Section 6) 120
5.16 Comparison of Longitudinal Water Elevation Distributions 121
5.17 Influence of Bridge Opening on Tidal Flow 122
5.18 Water Surface Elevation Near the River Mouth for the Spring High Tide in 1995 123
5.19 Influence of Bridge on Tidal Flow 124
5.20 1935 and 1972 Sites of U. S. Rte. 1 Bridge 127
5.21 Previous Cross Section 6 128
5.22 Previous Cross Section 7 129
5.23 Previous Cross Section 8 130
5.24 Water Surface Profiles for Spring Tide at 22:30 on May 15, 1995 131
5.25 Water Surface Profiles for Spring Tide at 1:30 on May 16, 1995 132
5.26 Water Surface Profiles for Spring Tide at 3:30 on May 16, 1995 133
5.27 Water Surface Profiles for Spring Tide at 6:00 on May 16, 1995 134
5.28 Discharge and Elevation at Rte. 1 Bridge for Spring Tide on May 15-16, 1995 135
5.29 Discharge and Elevation at Railroad Bridge for Spring Tide on May 15-16, 1995 136
5.30 Tidal Range for Spring Tide on May 15-16, 1995 137
5.31 Maximum Flood Tide Discharge for Spring Tide on May 15-16, 1995 138
5.32 Maximum Ebb Tide Discharge for Spring Tide on May 15-16, 1995 139

List of Tables

2.1 Values of Roughness Coefficient, n, for Natural Streams 35

3.1 Number of Stations Used in Transverse Flow Calculations 51

3.2 Tidal Stage Measurements 54

4.1 Suggested Values for K_e 73

4.2 Calibrated Parameters 76

1. Introduction

Coastal salt marshes have a broad global distribution (Chapman, 1974), forming a rich biological escosystem because of their interaction with the flow of nutrients between the terrestial and marine environment. Water is the primary conveyor of nutrient and salt, and a thorough knowledge of marsh hydrology is vital to understanding the transport mechanism involved and the environmental characteristics in the coastal marsh (Price, 1988).

The Connecticut shore of Long Island Sound is one of the most heavily developed coastal zones in the United States. Our coastal waters, including estuaries, harbors, coves and tidal wetlands, are used for transportation, fisheries, and as receiving waters for domestic and industrial effluents. Long Island Sound's water quality (badly impacted by excess nutrients) and the long-term ecology of its coastal wetlands have become sensitive environmental concerns, along with the ever-increasing social and environmental pressures arising from increasing population. On the other hand, there has been a continuing demand for maintenance, reconstruction, and new construction of highway facilities. The highway engineer not only has to deal with conventional design concerns, but also has to face problems of the environmental impacts of highways on coastal wetlands, tidal channels, and estuaries, especially in the process of applying for permits from state and federal environmental regulatory agencies.

Many projects along the Connecticut coast involve tidal marsh. Environmentalists

charge that restricted tidal openings imposed by highway and rail right-of-way facilities negatively impact flora and fauna because they alter natural tidal regimes.

Today, secondary roads, State routes, U. S. Route 1, Interstate 95, and the ConnRail (AmTrak) coastal rail corridor form a series of braided obstructions perpendicular to the Connecticut's natural drainages into Long Island Sound. There is a large number of river, stream, and wetland crossings that significantly restrict the full exchange of tidal waters in coastal salt marshes, further complicated by changes in the hydrographs of these streams and rivers due to filling, dredging, and diking of marshes. Salt and estuarine marshes are a vital part of the ecology of Long Island Sound and its water quality; their annual cycle of growth and decay rests on the type of vegetation they support and is principally linked to the elevation and frequency of flooding by tidal waters (Lefor, Kennard, and Civco, 1987; Miller and Egler, 1950). The slightest change in ambient surface elevation of tidal regime or marsh surface itself alters the vegetation and therefore the productivity of the system. The tidal salt waters of Long Island Sound are the principal and essential environmental factor in the existence of valuable salt marsh ecosystems in Connecticut.

In 1993, the Joint Highway Research Advisory Council (JHRAC) of the University of Connecticut awarded us a research grant to develop one- and two-dimensional hydrodynamic and transport models of tidal flows as an analytical framework to address the need for environmental assessment for permit applications as well as for use in

the design and maintainance of highway structures. The development of the pseudo-2D hydrodynamic model is the first step toward providing this framework and an analytical tool for the highway engineer to assess the impacts of highway structures on tidal flushing.

2. Pseudo 2-D Hydrodynamic Model

2.1 Background

Hydrodynamic models for a river system with overbank regions can be classified into two main types:

(1) A one-dimensional model treating overbank regions only as storage; the overbank flow is not considered in the longitudinal momentum equation (Lewandowski et al., 1993); and,

(2) A one-dimensional model taking both the main channel and overbank regions into consideration (Tingsanchali and Ackermann, 1976; Hoggan, 1988; Amein and Krans, 1991).

The first type of model is appropriate for a river system with limited shallow overbank regions. The second type of model is suitable for a river system in which water elevation does not change rapidly with time. Both these two types of models share the same assumptions: that transverse flow is not important, and that water surface level in the overbank regions changes simultaneously with that in the main channel. These models can not effectively account for the process of water exchange between the main channel and the overbank regions. Without transverse flow, it is not possible to trace solute transport due to the tide movement in overbank regions. The coastal tidal marsh is considerably wider than the flooded valley in a typical river system. Transverse flow must be considered during the wetting and drying process in a tidal cycle. Therefore, a two-dimensional model is needed for a tidal river-marsh system,

and this requires not only more computational resources, but more field data.

A tidal river and salt marsh system can be characterized as a narrow main channel meandering through a wide, nearly flat marsh on one or both sides of the channel. A variety of salt marsh vegetation inhabits this "shallow valley," inundated by diurnal tides as depicted in Figure 2.1. The spatial pattern of salt marsh vegetation likely depends in large part on microtopography, depth and period of inundation, salinity, and sedimentation among other factors. Tidal flows are mostly confined within the main channel, while overland flow spreads laterally over a nearly dry marsh during higher and highest high tides, and drains into the main channel during ebb tides. Therefore, the tidal motion in the system is in general two-dimensional, but it is dominated by longitudinal flow along the main channel. The pseudo 2-D hydrodynamic model has been formulated on the basis of these unique features, and couples the one-dimensional longitudinal flow in the main channel and over the marsh with the transverse overland flow on the marsh, with the following considerations:

(1) A one-dimensional flow analysis based on the mass continuity and momentum equations is used when the flow is confined within the main channel at the early stage of flood tide and at the late stage of ebb tide;

(2) When the overland flow occurs during flood tide, a one-dimensional flow analysis is carried out in the transverse direction on both banks to account for the spreading of wetting front over the marsh;

(3) Longitudinal flows in the main channel and the overbank regions are reanalysed

for overall mass and momentum balance;

(4) Iteration continues for (2) and (3) until the boundary conditions at the banks of the channel and at the edges of the overbank regions are satisfied;

(5) When the water recedes from the overbank regions into the main channel during ebb tide, (2), (3) and (4) are carried out until the water surface in the main channel drops below a critical elevation; and,

(6) Lateral flows from the overbank regions are added to (1) until the marsh surface is dry.

In short, the one-dimensional longitudinal and transverse flow analyses are carried out iteratively for the two-dimensional flow field in the main channel and overbank regions as a whole.

2.2 Formulation

Formulation of tidal flow in rivers, tidal marshes, and estuaries is based on shallow water flow theory. The governing equations are the depth-averaged equations of continuity and momentum in two dimensions (Tan, 1992). The pseudo-2D hydrodynamic model uses the one-dimensional continuity and momentum equations, known as St. Vennant equations for unsteady flow in open channel (Mahmood and Yevjevich, 1975; Amein and Kraus, 1991) in the longitudinal direction. In the transverse direction, the momentum equation is approximated by Manning's formula.

2.2.1 Governing Equations for Longitudinal Flow

The continuity equation is given by

$$\frac{\partial A}{\partial t} + \frac{\partial Q}{\partial x} + q_o = 0.0 \tag{2.1}$$

and the momentum equation by

$$\frac{\partial Q}{\partial t} + \frac{\partial}{\partial x}(\frac{Q^2}{A}) = -gA\frac{\partial Z}{\partial x} - gAS_f - gAS_e \tag{2.2}$$

where A= the cross-section area;

Q=the discharge;

q_o=the lateral outflow rate per unit length of channel;

Z=the water surface elevation;

S_f=the friction slope due to bottom resistance;

S_e=the rate of transition loss;

t=time;

x=the distance along the channel; and,

g=the gravitational acceleration.

The frictional slope and transition loss rate are represented by

$$S_f = \frac{Q|Q|n^2}{A^2R^{4/3}} \tag{2.3}$$

and

$$S_e = \frac{K_e}{2g}|\frac{\Delta(\frac{Q^2}{A^2})}{\Delta x}| \tag{2.4}$$

where n=Manning's roughness coefficient;

R=the hydraulic radius; and,

K_e=an empirical transition loss coefficient.

When overbank flow occurs as shown in Figure 2.1, the cross-section area is divided into $A = A_r + A_c + A_l$ with the corresponding discharge $Q = Q_r + Q_c + Q_l$ where subscripts r, c, and l refer to right overbank, main channel, and left overbank, respectively. Some approximations are introduced for Q^2/A, S_f, and S_e as follows. Assuming the conveyance

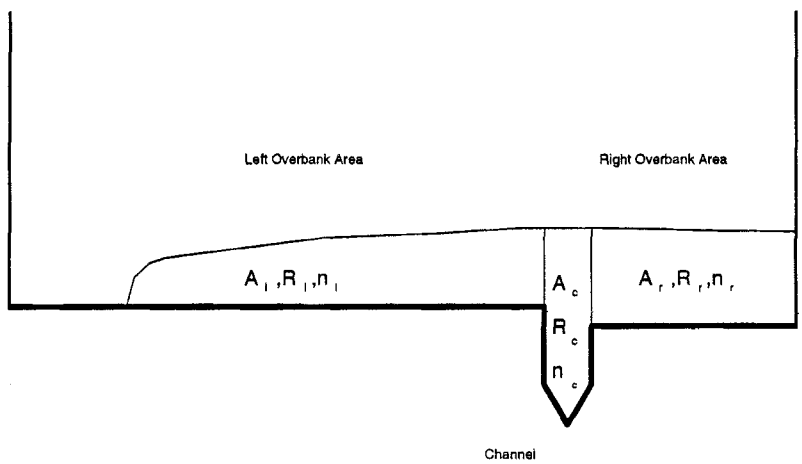

Figure 2.1: Overbank Flow Notation.

$$C = \frac{1}{n_l} R_l^{2/3} A_l + \frac{1}{n_c} R_c^{2/3} A_c + \frac{1}{n_r} R_r^{2/3} A_r \tag{2.5}$$

then the specific momentum flux, the friction slope and the rate of transition loss can be derived respectively as

$$\frac{Q^2}{A} = \left(\frac{\frac{1}{n_l^2} R_l^{4/3} A_l}{C^2} + \frac{\frac{1}{n_c^2} R_c^{4/3} A_c}{C^2} + \frac{\frac{1}{n_r^2} R_r^{4/3} A_r}{C^2}\right) Q^2 \tag{2.6}$$

$$S_f = \frac{Q|Q|}{C^2} \tag{2.7}$$

and

$$S_e = K_e \frac{\Delta(\frac{\frac{1}{n_l^2}R_l^{4/3}}{C^2} + \frac{\frac{1}{n_c^2}R_c^{4/3}}{C^2} + \frac{\frac{1}{n_r^2}R_r^{4/3}}{C^2})Q^2}{2g\Delta x} \tag{2.8}$$

In this case, A_l, A_r, R_l and R_r are provided by transverse flow calculations.

2.2.2 Boundary Conditions for Longitudinal Flow

In a well-posed mathematical problem, appropriate boundary conditions must be given at external boundaries. The external boundary conditions are prescribed by the stage, the discharge, and the relation between stage and discharge as a function of time. One or two of the above conditions could be given at an external boundary, such as the beginning or ending cross section. Since this model is designed for use in a tidal salt marsh system, the stage or water surface elevation near the mouth of the river is either derived from the tide tables or is provided by observed stage data. Any one of the above conditions may be used at the upstream external boundary (the beginning cross section) depending on the availablity of observed data for stage or discharge. In general, the non-steady relation between stage and discharge in a tidal river is difficult to derive; therefore, this boundary condition is not considered in the model.

2.2.3 Governing Equations for Transverse Flow

When an overbank flow occurs at a cross section of the main channel, the transverse flow calculation is begun immediately by using a set of unsteady flow equations for the spreading of water onto the overland surface during flood tide and the subsequent

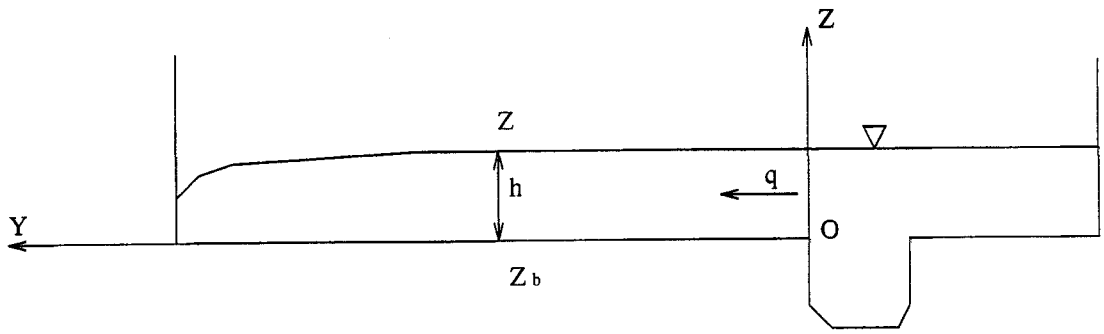

Figure 2.2: Coordinate System for Overbank Flow.

release of water during ebb tide. For each side of the overland region as shown in Figure 2.2, the continuity equation is given by

$$\frac{\partial h}{\partial t} + \frac{1}{w}\frac{\partial wq}{\partial y} = 0 \tag{2.9}$$

and the momentum equation is approximated by

$$q = \begin{cases} -\frac{1}{n}h^{\frac{5}{3}}(\frac{\partial z}{\partial y})^{\frac{1}{2}} & : \quad when\ \frac{\partial z}{\partial y} > 0 \\ \frac{1}{n}h^{\frac{5}{3}}(-\frac{\partial z}{\partial y})^{\frac{1}{2}} & : \quad when\ \frac{\partial z}{\partial y} < 0 \end{cases} \tag{2.10}$$

where q=the transverse discharge per unit width;

h=the water depth;

w=the width of floodplain between longitudinal sections;

n=Manning's roughness coefficient; and,

z=the water surface elevation $= z_b + h$.

In Figure 2.2 and the above equations, the subscripts r and l, for left and right overbank are omitted.

2.2.4 Boundary Conditions For Transverse Flow

Transverse overland flow is driven by the boundary condition at the bank of the main channel, and the boundary condition varies with time. The boundary conditions for the different cases illustrated in Figure 2.3 are the following:

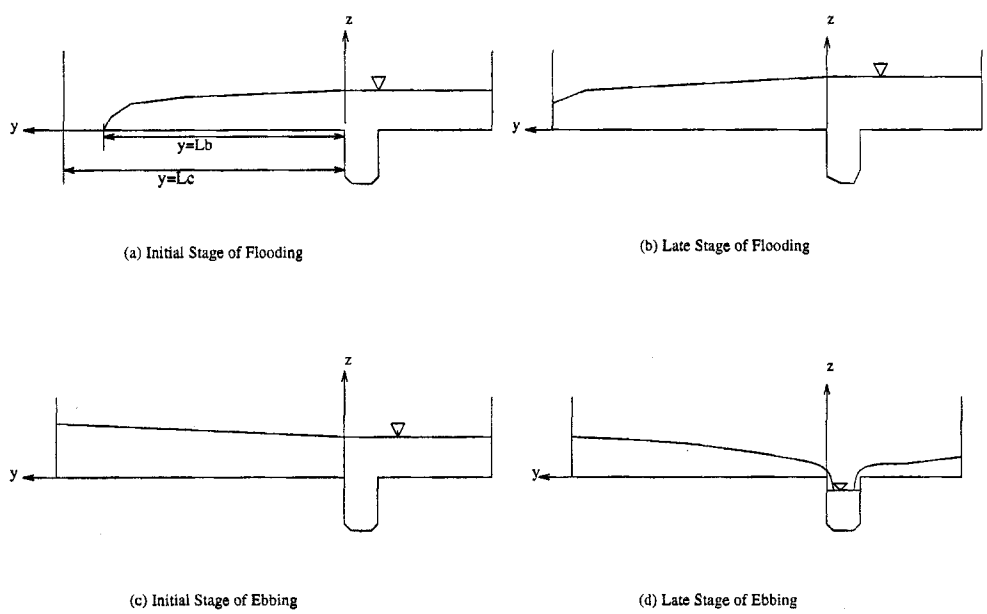

Figure 2.3: Different Overbank Flow Conditions.

Case (a): Initial flood stage when the front has not reached the outer boundary of the marsh

$$\begin{cases} z = Z_c, & at\ y = 0 \\ q = 0, & at\ y = L_f \end{cases}$$

where Z_c is the water surface elevation at the bank of the channel, given by the result of the longitudinal flow calculation. The location of L_f is not known *a priori* and is determined by a trial method.

Cases (b) and (c): Later flood stage and initial ebb stage

$$\begin{cases} z = Z_c & at\ y = 0 \\ q = 0 & at\ y = L_c \end{cases}$$

where L_c is the transverse distance of the outer marsh boundary from the bank of channel.

Case (d): Later ebb stage when the water surface elevation in the main channel drops below the control elevation on the bank

$$\begin{cases} h = f(q), & at\ y = 0 \\ q = 0, & at\ y = L_f \end{cases}$$

where $f(q)$ is a known function, for example, which can be derived from the critical depth condition at the control point on the bank of channel.

2.3 Numerical Method

The model uses a finite difference scheme based on the four-point implicit method (Amein and Kraus, 1991). The computational domain is first discretized longitudinally along the channel, including the tributaries. The cross sections at nodal points are then extended into the marsh to form the overland flow regions. The transverse discretization starts from the junctions (on the left and right banks, respectively) outward into the marsh as shown in Figure 2.2. The external boundary in the compu-

tational domain is chosen in such a way that the boundary condition can be provided by observed data or approximated by a no-flow condition on the bank.

2.3.1 Difference Scheme

The four point implicit method has been applied to a variety of unsteady flows in river systems (Amein and Kraus, 1991). The method has the following characteristics:

(1) good stability;

(2) its accuracy can be maintained to a certain standard with a large range of Δt and Δx;

(3) it is easy to use with a fixed irregular space mesh;

(4) the boundary condition can be easily given;

(5) it is relatively simple to apply to river systems with wide flood plains and tributaries; and,

(6) numerical results are concrete and easily comparable.

For the four-point implicit method, the function α(Q, Z, or A), and its partial derivatives with respect to x and t at a point, M, shown in Figure 2.4 can be expressed as

$$\alpha(M) = \frac{1}{2}[\alpha(i+1,n+1) + \alpha(i,n+1)]\theta + \frac{1}{2}[\alpha(i+1,n) + \alpha(i,n)](1-\theta) \quad (2.11)$$

$$\frac{\partial \alpha(M)}{\partial t} = \frac{1}{2\Delta t}\{[\alpha(i+1,n+1) + \alpha(i,n+1)] - [\alpha(i+1,n) + \alpha(i,n)]\} \quad (2.12)$$

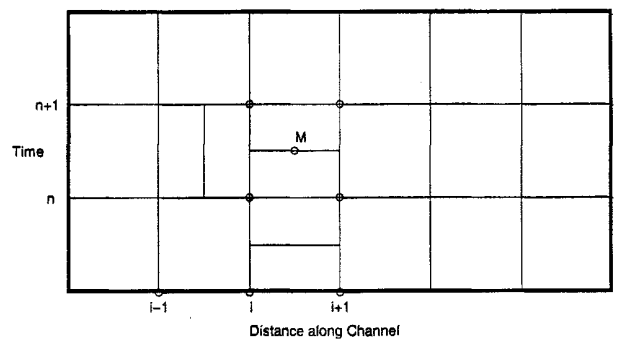

Figure 2.4: Node System on x-t Plane.

and

$$\frac{\partial \alpha(M)}{\partial x} = \frac{1}{\Delta x}\{[\alpha(i+1,n+1)-\alpha(i,n+1)]\theta+[\alpha(i+1,n)-\alpha(i,n)](1-\theta)\} \quad (2.13)$$

where θ is a weighting factor ranging from 0 to 1, $\theta = 0$ corresponds to the explicit scheme, $\theta = 0.5$ the implicit centered-in-time scheme, and $\theta = 1$ the fully implicit forward-in-time sheme. Thus, the implicit method corresponds to $\theta \geq \frac{1}{2}$.

2.3.2 Difference Equations for Lonitudinal Flow

Using the above scheme, the governing equations, Eqs. (2.1) and (2.2), can be converted into the following difference equations:

$$\begin{aligned}(Q_{i+1}^{n+1} - Q_i^{n+1})\theta + (Q_{i+1}^n - Q_i^n)(1-\theta) \\ +\frac{\Delta x}{\Delta t}(A_{i+1/2}^{n+1} - A_{i+1/2}^n) + \Delta x q_{o_{i+1/2}}^{n+1} \quad = \quad 0\end{aligned} \quad (2.14)$$

and

$$
\begin{aligned}
Q_{i+1/2}^{n+1} - Q_{i+1/2}^{n} + \frac{\Delta t}{\Delta x}\left(\frac{(Q_{i+1}^{n+1})^2}{A_{i+1}^{n+1}} - \frac{(Q_{i}^{n+1})^2}{A_{i}^{n+1}}\right)\theta \\
+\frac{\Delta t}{\Delta x}\left(\frac{(Q_{i+1}^{n})^2}{A_{i+1}^{n}} - \frac{(Q_{i}^{n})^2}{A_{i}^{n}}\right)(1-\theta) \\
+g\frac{\Delta t}{\Delta x}A_{i+1/2}^{n+1}(Z_{i+1}^{n+1} - Z_{i}^{n+1})\theta \\
+g\frac{\Delta t}{\Delta x}A_{i+1/2}^{n}(Z_{i+1}^{n} - Z_{i}^{n})(1-\theta) \\
+g\Delta t A_{i+1/2}^{n+1} S_{f_{i+1/2}}^{n+1}\theta + g\Delta t A_{i+1/2}^{n} S_{f_{i+1/2}}^{n}(1-\theta) \\
+g\Delta t A_{i+1/2}^{n+1} S_{e_{i+1/2}}^{n+1}\theta + g\Delta t A_{i+1/2}^{n} S_{e_{i+1/2}}^{n}(1-\theta) \quad = \quad 0.
\end{aligned}
\tag{2.15}
$$

In the above equations, the value of a variable $\alpha_{i+1/2}$ is taken as

$$
\alpha_{i+1/2} = \frac{1}{\Delta x}\int_{x_i}^{x_{i+1}} \alpha(x,t)dx \approx \frac{1}{2}(\alpha_i + \alpha_{i+1}). \tag{2.16}
$$

2.3.3 Difference Equations for Transverse Flow

The difference equations for Eqs. (2.9) and (2.10) are derived as

$$
\begin{aligned}
\frac{h_{j+1}^{n+1} + h_{j}^{n+1} - h_{j+1}^{n} - h_{j}^{n}}{2\Delta t} \\
+\frac{2[(w_{j+1}q_{j+1}^{n+1} - w_j q_j^{n+1})\theta + (w_{j+1}q_{j+1}^{n} - w_j q_j^{n})(1-\theta)]}{(w_j + w_{j+1})\Delta y} \quad = \quad 0.
\end{aligned}
\tag{2.17}
$$

In the case of $\frac{\partial z}{\partial x} < 0$,

$$
\frac{q_{j+1}^{n+1} + q_{j}^{n+1}}{2} - \frac{1}{n}\left(\frac{h_{j+1}^{n+1} + h_{j}^{n+1}}{2}\right)^{5/3}\left(\frac{z_{j}^{n+1} - z_{j+1}^{n+1}}{\Delta y}\right)^{1/2} = 0. \tag{2.18}
$$

In the case of $\frac{\partial z}{\partial x} > 0$,

$$
\frac{q_{j+1}^{n+1} + q_{j}^{n+1}}{2} + \frac{1}{n}\left(\frac{h_{j+1}^{n+1} + h_{j}^{n+1}}{2}\right)^{5/3}\left(\frac{z_{j+1}^{n+1} - z_{j}^{n+1}}{\Delta y}\right)^{1/2} = 0. \tag{2.19}
$$

2.4 Calculation Procedure

2.4.1 Calculation of Longitudinal Flow

In view of the nonlinear nature of Eq. (2.15), the Newton iteration method is applied to solve the nonlinear equations. Assuming N cross-sections in a river system, the finite-difference equations given by the system of Eqs. (2.14) and (2.15), together with the boundary conditions, constitute a system of 2N nonlinear algebraic equations for 2N unknowns. Let these equations be represented by

$$
\begin{aligned}
F_1(Z_1^{n+1}, Q_1^{n+1}, Z_2^{n+1}, Q_2^{n+1}) &= 0 \\
F_2(Z_1^{n+1}, Q_1^{n+1}, Z_2^{n+1}, Q_2^{n+1}) &= 0 \\
&\vdots \\
F_{2i-1}(Z_i^{n+1}, Q_i^{n+1}, Z_{i+1}^{n+1}, Q_{i+1}^{n+1}) &= 0 \\
F_{2i}(Z_i^{n+1}, Q_i^{n+1}, Z_{i+1}^{n+1}, Q_{i+1}^{n+1}) &= 0 \\
&\vdots \\
F_{2N-1}(Z_{N-1}^{n+1}, Q_{N-1}^{n+1}, Z_N^{n+1}, Q_N^{n+1}) &= 0 \\
F_{2N}(Z_{N-1}^{n+1}, Q_{N-1}^{n+1}, Z_N^{n+1}, Q_N^{n+1}) &= 0.
\end{aligned}
\tag{2.20}
$$

Let R_{2i-1}^k and R_{2i}^k be the residuals at the kth iteration of Eq. (2.20) corresponding to F_{2i-1} and F_{2i}. Then, according to the generalized Newton iteration method, the residuals and partial derivatives are related by the following system of equations with partial derivatives, evaluated at the kth iteration cycle:

$$
\begin{aligned}
\frac{\partial F_1}{\partial Z_1}dZ_1 + \frac{\partial F_1}{\partial Q_1}dQ_1 + \frac{\partial F_1}{\partial Z_2}dZ_2 + \frac{\partial F_1}{\partial Q_2}dQ_2 &= -R_1^k \\
\frac{\partial F_2}{\partial Z_1}dZ_1 + \frac{\partial F_2}{\partial Q_1}dQ_1 + \frac{\partial F_2}{\partial Z_2}dZ_2 + \frac{\partial F_2}{\partial Q_2}dQ_2 &= -R_2^k \\
&\vdots \\
\frac{\partial F_{2i-1}}{\partial Z_i}dZ_i + \frac{\partial F_{2i-1}}{\partial Q_i}dQ_i + \frac{\partial F_{2i-1}}{\partial Z_{i+1}}dZ_{i+1} + \frac{\partial F_{2i-1}}{\partial Q_{i+1}}dQ_{i+1} &= -R_{2i-1}^k \\
\frac{\partial F_{2i}}{\partial Z_i}dZ_i + \frac{\partial F_{2i}}{\partial Q_i}dQ_i + \frac{\partial F_{2i}}{\partial Z_{i+1}}dZ_{i+1} + \frac{\partial F_{2i}}{\partial Q_{i+1}}dQ_{i+1} &= -R_{2i}^k \\
&\vdots \\
\frac{\partial F_{2N-1}}{\partial Z_{N-1}}dZ_{N-1} + \frac{\partial F_{2N-1}}{\partial Q_{N-1}}dQ_{N-1} + \frac{\partial F_{2N-1}}{\partial Z_N}dZ_N + \frac{\partial F_{2N-1}}{\partial Q_N}dQ_N &= -R_{2N-1}^k \\
\frac{\partial F_{2N}}{\partial Z_{N-1}}dZ_{N-1} + \frac{\partial F_{2N}}{\partial Q_{N-1}}dQ_{N-1} + \frac{\partial F_{2N}}{\partial Z_N}dZ_N + \frac{\partial F_{2N}}{\partial Q_N}dQ_N &= -R_{2N}^k
\end{aligned}
\tag{2.21}
$$

where

$$
\begin{aligned}
dZ_1 &= Z_1^{k+1} - Z_1^k \\
dQ_1 &= Q_1^{k+1} - Q_1^k \\
&\vdots \\
dZ_i &= Z_i^{k+1} - Z_i^k \\
dQ_i &= Q_i^{k+1} - Q_i^k \\
&\vdots \\
dZ_N &= Z_N^{k+1} - Z_N^k \\
dQ_N &= Q_n^{k+1} - Q_N^k.
\end{aligned}
\tag{2.22}
$$

The solution of Eq. (2.21) will provide values of Z_1^{k+1}, Q_1^{k+1}, ..., Z_i^{k+1}, Q_i^{k+1}, ..., Z_N^{K+1}, Q_N^{k+1}, i.e., the values of the variables at the $k+1^{th}$ iteration. The procedure

can be repeated as many times as required until the difference between the values of any variable in two consecutive iterations falls below a specified tolerance limit. The values of the variables obtained in the last iteration cycle will be taken as the values of the variables for the time step n+1, and the computation will be advanced to the next time step, n+2. Through such a procedure, the variables at all sections along the channel can be obtained throughout the entire time period.

2.4.2 Calculation of Transverse Flow

Simular to the procedure for longitudinal flow, Eqs. (2.17), (2.18), and (2.19) for transverse flow with M calculation points can be written in the following form:

$$
\begin{aligned}
G_1(h_1^{n+1}, q_1^{n+1}, h_2^{n+1}, q_2^{n+1}) &= 0 \\
G_2(h_1^{n+1}, q_1^{n+1}, h_2^{n+1}, q_2^{n+1}) &= 0 \\
&\vdots \\
G_{2j-1}(h_j^{n+1}, q_j^{n+1}, h_{j+1}^{n+1}, q_{j+1}^{n+1}) &= 0 \\
G_{2j}(h_j^{n+1}, q_j^{n+1}, h_{j+1}^{n+1}, q_{j+1}^{n+1}) &= 0 \\
&\vdots \\
G_{2M-1}(h_{2M-1}^{n+1}, q_{2M-1}^{n+1}, h_{2M}^{n+1}, q_{2M}^{n+1}) &= 0 \\
G_{2M}(h_{2M-1}^{n+1}, q_{2M-1}^{n+1}, h_{2M}^{n+1}, q_{2M}^{n+1}) &= 0.
\end{aligned}
\tag{2.23}
$$

Again, using the Newton iteration method, h_j^{n+1} and q_j^{n+1} can be solved from

$$
\begin{aligned}
\frac{\partial G_1}{\partial h_1}dh_1 + \frac{\partial G_1}{\partial q_1}dq_1 + \frac{\partial G_1}{\partial h_2}dh_2 + \frac{\partial G_1}{\partial q_2}dq_2 &= -R_1^k \\
\frac{\partial G_2}{\partial h_1}dh_1 + \frac{\partial G_2}{\partial q_1}dq_1 + \frac{\partial G_2}{\partial h_2}dh_2 + \frac{\partial G_2}{\partial q_2}dq_2 &= -R_2^k \\
&\vdots \\
\frac{\partial G_{2j-1}}{\partial h_j}dh_j + \frac{\partial G_{2j-1}}{\partial q_j}dq_j + \frac{\partial G_{2j-1}}{\partial h_{j+1}}dh_{j+1} + \frac{\partial G_{2j-1}}{\partial q_{j+1}}dq_{j+1} &= -R_{2j-1}^k \\
\frac{\partial G_{2j}}{\partial h_j}dh_j + \frac{\partial G_{2j}}{\partial q_j}dq_j + \frac{\partial G_{2j}}{\partial h_{j+1}}dh_{j+1} + \frac{\partial G_{2j}}{\partial q_{j+1}}dq_{j+1} &= -R_{2j}^k \\
&\vdots \\
\frac{\partial G_{2M-1}}{\partial h_{M-1}}dh_{M-1} + \frac{\partial G_{2M-1}}{\partial q_{M-1}}dq_{M-1} + \frac{\partial G_{2M-1}}{\partial h_M}dh_M + \frac{\partial S_{2M-1}}{\partial q_M}dq_M &= -R_{2M-1}^k \\
\frac{\partial G_{2M}}{\partial h_{M-1}}dh_{M-1} + \frac{\partial G_{2M}}{\partial q_{2M-1}}dq_{2M-1} + \frac{\partial G_{2M}}{\partial h_M}dh_M + \frac{\partial G_{2M}}{\partial q_M}dq_M &= -R_{2M}^k
\end{aligned}
\tag{2.24}
$$

where

$$
\begin{aligned}
dh_1 &= h_1^{k+1} - h_1^k \\
dq_1 &= q_1^{k+1} - q_1^k \\
&\vdots \\
dh_j &= h_j^{k+1} - h_j^k \\
dq_j &= q_j^{k+1} - q_j^k \\
&\vdots \\
dh_M &= h_M^{k+1} - h_M^k \\
dq_M &= q_M^{k+1} - q_M^k.
\end{aligned}
\tag{2.25}
$$

The solution of Eq. (2.24) will provide the values of h_1^{k+1}, q_1^{k+1},...,h_j^{k+1}, q_j^{k+1},..., h_M^{k+1}, q_M^{k+1} through iterations which use the water depth and discharge at each transverse calculation point. As discussed in the section on the transverse flow boundary

conditions, if the flood front has not reached the outer boundary of the marsh, the location of the front is determined by a trial method that assumes an initial location of the flooding front and then seeks the successive convergence. In this model, a subprogram is provided to handle this case.

2.4.3 Coupling of Longitudinal and Transverse Flow

In the preceeding sections, it was mentioned that the coefficients for longitudinal flow calculation, such as cross-section area, friction slope, etc., are involved in the transverse flow calculations. Transverse flow calculations must use the results of the longitudinal flow calculations as the boundary condition at the channel bank. Therefore, transverse and longitudinal flow calculations cannot be carried out independently. These calculation processes must be coupled with each other iteratively, and this is the essence of the pseudo-2D hydrodynamic model. In this model, longitudinal and transverse flows are coupled through iteration as follows:

(1) Calculation starts with longitudinal flow at low tide. During this phase of the tidal cycle, the flow is entirely confined within the main channel. In addition, the initial condition over the whole length of the channel can simply be specified since the water surface is nearly level, particularly in view of the small lag time for a relatively small river-marsh system.

(2) When overbank flow occurs, the water surface elevations along the main channel are used as the boundary conditions for the transverse flow calculation. Calculation of the transverse flow is initiated by assuming a flooding front on the nearly dry

overland surface. Final water surface elevation and transverse discharge are obtained by successive trials of the front distance from the bank. This calculation is carried out for all sections with overbank flow.

(3) Using the transverse flow results, the cross-section area for the longitudinal flow is updated to include the overbank flow for all sections along the channel. The longitudinal flow is recalculated.

(4) Using the updated water surface elevation at the bank of the main channel, step three is repeated until the solutions converge. As the flooding front reaches the outer boundary of the marsh, the trial solution is no longer needed during flood tide and during the draining of ebb tide because of the no-flow boundary condition at the outer boundary of the marsh.

(5) Transverse flow calculation stops when the water surface elevation on the bank of the main channel drops to a control elevation, which may be taken at the critical depth. After this time, overland drainage is treated as lateral inflow into the main channel for the longitudinal flow calculation.

2.4.4 Flow Charts

The flow charts for longitudinal flow calculations, transverse flow calculations, and overall calculations are given in Figures 2.5, 2.6, and 2.7.

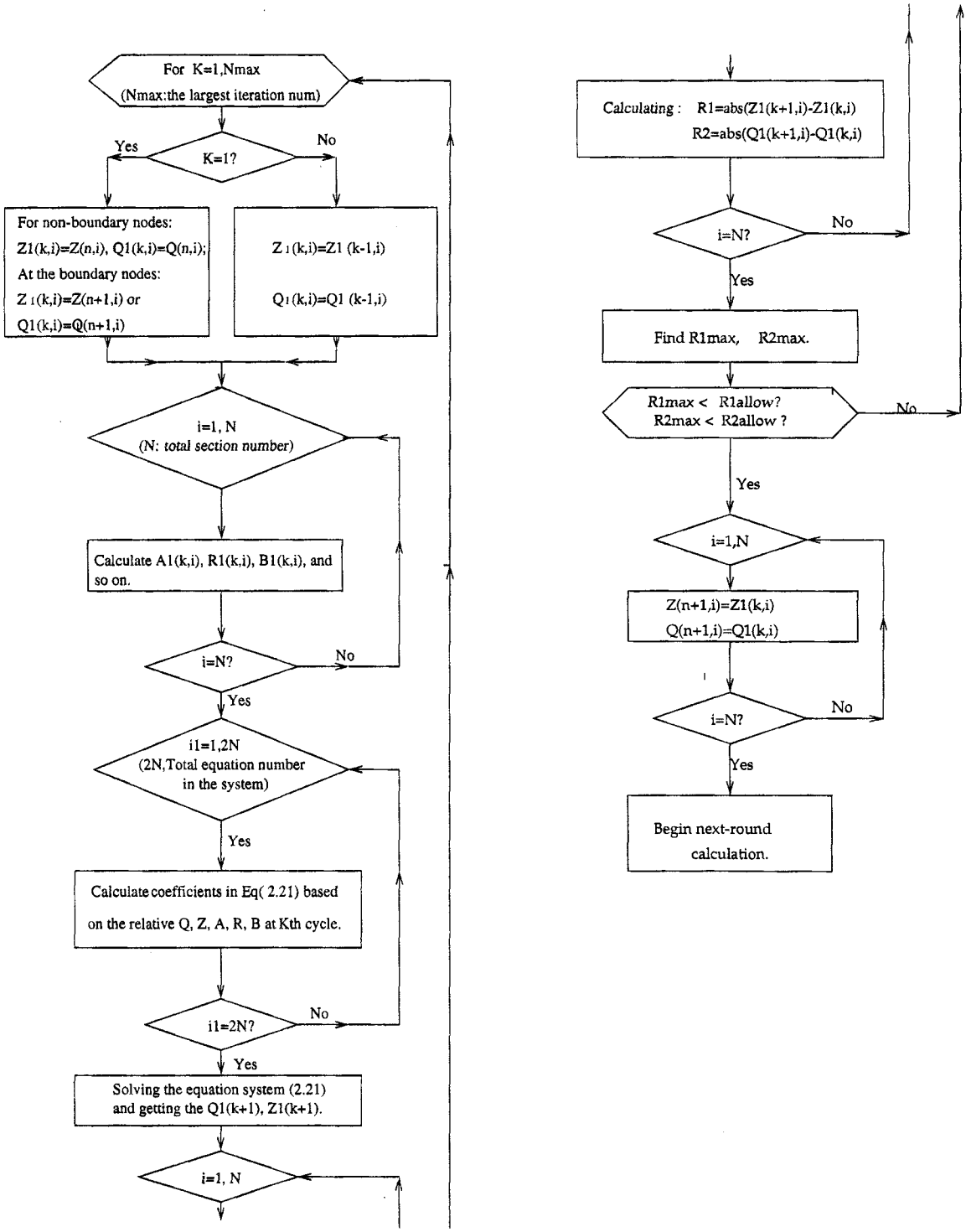

Figure 2.5: Flowchart For Longitudinal Flow Calculation

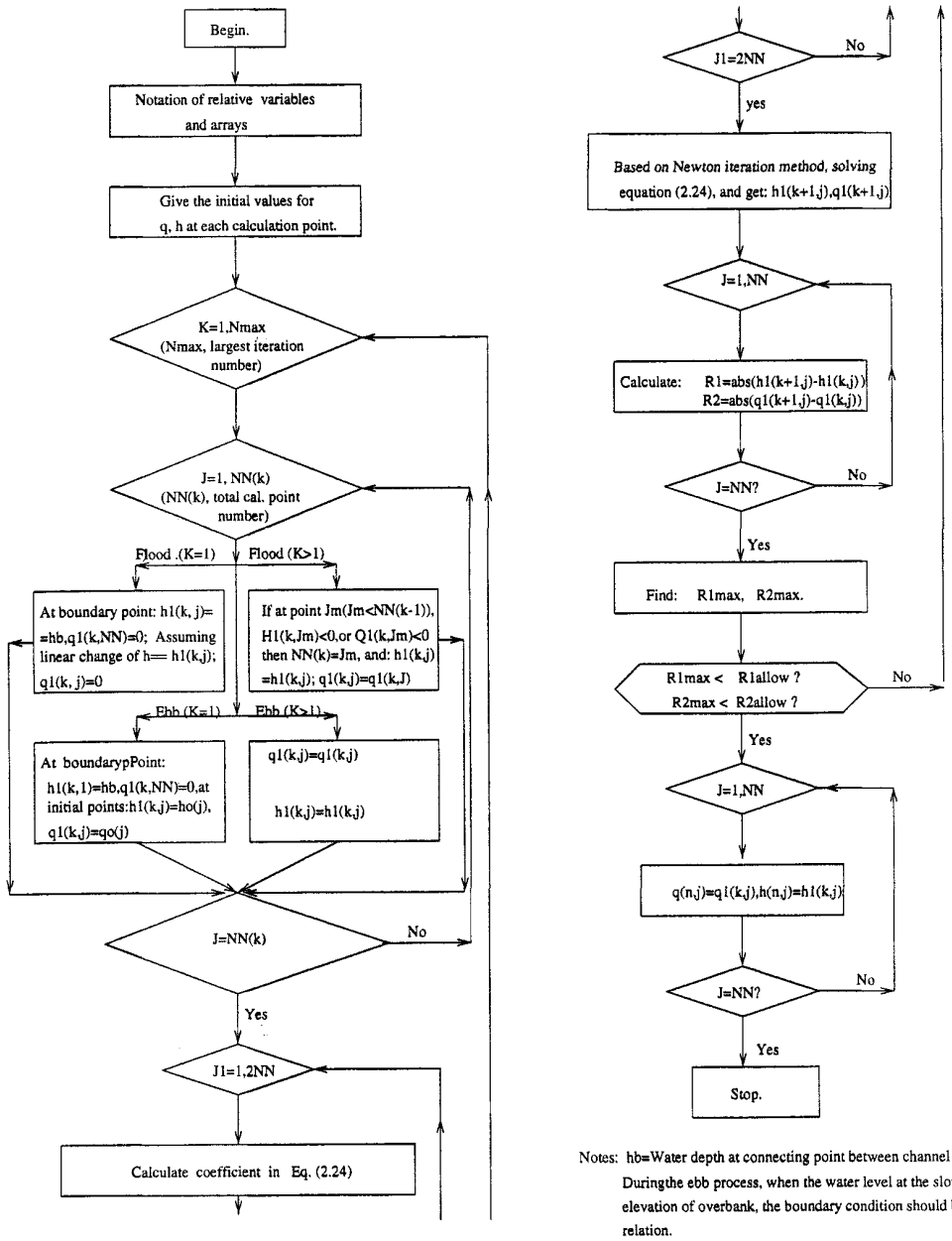

Notes: hb=Water depth at connecting point between channel and overbank region. Duringthe ebb process, when the water level at the slough channel < the bottom elevation of overbank, the boundary condition should be taken as the qb-hb relation.

Figure 2.6: Flowchart For Transverse Flow Calculation

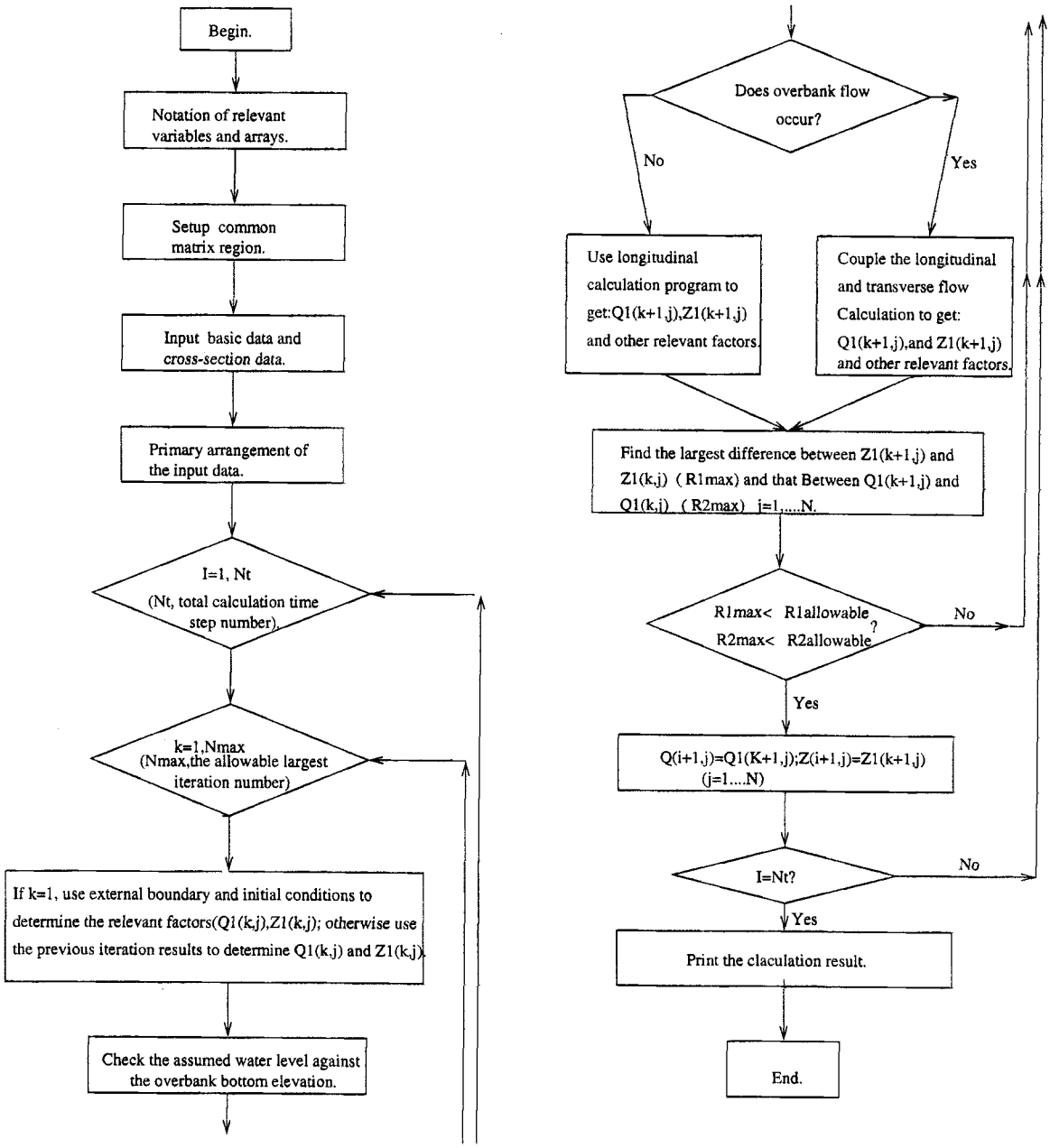

Figure 2.7: Flowchart For Overall Calculation

2.5 Relevant Treatments

2.5.1 External Boundary Conditions

For a properly-posed computation scheme, two external boundary conditions are required: either both of them at one external point, or one at each of two external points.

The boundary condition can be specified by the water surface elevation, expressed as

$$Z_b^{n+1} - (Z')_b^{n+1} = 0 \tag{2.27}$$

where $(Z')_b^{n+1}$ is the prescribed water surface elevation as a function of time at the external boundary node ib or jb, at time step n+1, or discharge expressed as

$$Q_b^{n+1} - (Q')_b^{n+1} = 0 \tag{2.28}$$

where $(Q')_b^{n+1}$ is the prescribed discharge as a function of time at the external boundary ib or jb at time-step n+1.

Other types of external boundary conditions include discharge expressed as a function of water surface elevation, e.g.,

$$Q_b^{n+1} = f(Z_b^{n+1}) \tag{2.29}$$

or the velocity and water surface elevation expressed as function of time, e.g.,

$$Q_b^{n+1} = V_b^{n+1} A_b^{n+1} = V_b^{n+1} f(Z_b^{n+1}) \tag{2.30}$$

In this model, any of the four boundary conditions above can be used at the external boundaries.

2.5.2 River Junctions

A junction is created at the confluence of two or more channels as shown in Figure 2.8. If the junction involves M channels (M$\geq$ 2), and assuming the node numbers of the channels are K(1), K(2),... K(M), the junction condition can be expressed in terms of the discharges as

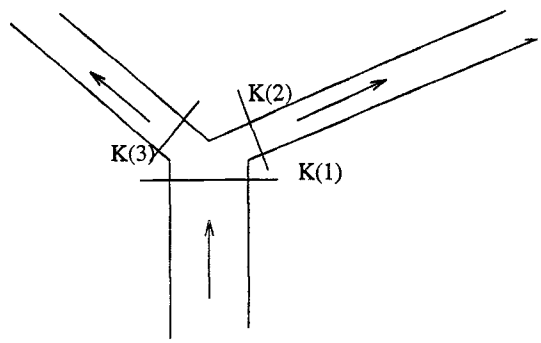

Figure 2.8: Junction in a River Channel.

$$\sum_{i=1}^{M} Q_{K(i)}^{n+1} = 0 \tag{2.31}$$

and the water surface elevations as

$$Z_{k(1)}^{n+1} = Z_{k(2)}^{n+1} = ... = Z_{k(M)}^{n+1}. \tag{2.32}$$

The junction condition then produces M independent equations.

2.5.3 Meandering Streams

In the one-dimensional flow analysis, the actual length of a meandering stream in

a reach such as that shown in Figure 2.9 is different from the reach length. An apparent reach length must be defined to represent the overall flow characteristics for the main channel and overbank regions as overbank flow occurs. In this model, the streamwise gradients in the main channel and overbank regions are assumed to be the same. Using a discharge-weighted method, the apparent reach length between two cross-sections is given by

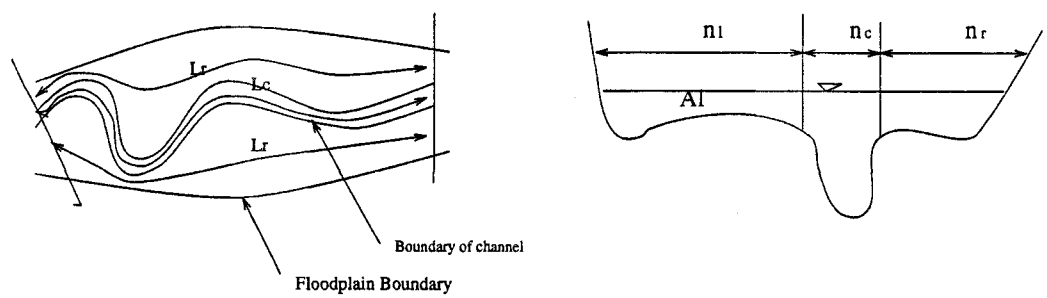

Figure 2.9: Meandering Stream.

$$L_s = \frac{\frac{A_l}{n_l} L_l^{1/2} R_l^{\frac{2}{3}} + \frac{A_c}{n_c} L_c^{1/2} R_c^{\frac{2}{3}} + \frac{A_r}{n_r} L_r^{1/2} R_r^{\frac{2}{3}}}{\frac{A_l}{n_l} R_l^{\frac{2}{3}} \frac{1}{L_l^{\frac{1}{2}}} + \frac{A_c}{n_c} R_c^{\frac{2}{3}} \frac{1}{L_c^{\frac{1}{2}}} + \frac{A_r}{n_r} R_r^{\frac{2}{3}} \frac{1}{L_r^{\frac{1}{2}}}} \tag{2.33}$$

where L_l, L_c and L_r are the flow path length for the left overbank, main channel and right overbank, respectively.

2.5.4 Determination of Overall Roughness

Based on Manning's formula, the discharge at the middle point (M) between the consecutive sections in the left overbank, the main channel, and the right overbank

can be expressed as

$$Q_l(M) = \frac{1}{n_l} R_l^{\frac{2}{3}} \frac{\Delta z^{\frac{1}{2}}}{L_l} \tag{2.34}$$

$$Q_c(M) = \frac{1}{n_c} R_c^{\frac{2}{3}} \frac{\Delta z^{\frac{1}{2}}}{L_c} \tag{2.35}$$

$$Q_r(M) = \frac{1}{n_r} R_r^{\frac{2}{3}} \frac{\Delta z^{\frac{1}{2}}}{L_r} \tag{2.36}$$

and the overall discharge by

$$Q(M) = \frac{1}{n} R^{\frac{2}{3}} \frac{\Delta z^{\frac{1}{2}}}{L_s} . \tag{2.37}$$

For $Q(M) = Q_l(m) + Q_c(M) + Q_r(M)$, the overall roughness can then be calculated by the following formula:

$$\frac{1}{n} = \frac{L_s^{1/2}}{R^{2/3}} \left(\frac{1}{n_l} \frac{R_l^{2/3}}{L_l^{1/2}} + \frac{1}{n_c} \frac{R_c^{2/3}}{L_c^{1/2}} + \frac{1}{n_r} \frac{R_r^{2/3}}{L_r^{1/2}} \right). \tag{2.38}$$

2.6 Computer Programs

The programs for this model have been coded using FORTRAN 7.7, and can be compiled and executed on any PC or Unix system which includes a FORTRAN package. The model consists of one main program and four sub-programs. Each sub-program is designed to handle a relatively independent problem and all of these sub-programs are connected through the main program. For details refer to the companion volume, "Documentation of Pseudo 2D Hydrodynamic Model".

2.6.1 Program Control Parameters

The parameters controlling the operation of the model consist of:

(1) Initial Time and Termination Time

The initial starting time and termination time of the event in hours decimal must be specified. The calculation stops at the termination time.

(2) Tolerance Values for Iteration Convergence

Tolerance values for water surface elevations and discharges determine the number of iterations required for the numerical solutions to satisfy a specified degree of accuracy. These values should be chosen based on a consideration of river geometry. If the cross-sections are highly irregular, the computation may not converge in a reasonable number of steps, or not at all if the tolerance values are too small. In this case, the calculation will stop and a message to this effect will be displayed. If the tolerance values are large, the calculation will finish rapidly, but the accuracy of the solution will be compromised. In this model, the water surface elevation tolerance is given by the absolute difference of water surface elevations between consecutive iterations; generally 0.001 to 0.05 ft is acceptable. The discharge tolerance is given by the relative difference. Generally, 0.01-1.00 percent is reasonable for this value.

(3) Temporal Weighting Coefficient

The temporal weighting coefficient θ can vary between 0 to 1. A weighting coefficient of 0.0 will transform the numerical procedure into an explicit method. However, the stability or the convergence of the procedure may cause problems in some cases when $\theta < 0.5$. The present model uses θ from 0.5 to 1. A value $\theta = 1.0$ is recommended in starting a simulation series, and this value is also generally recommended for simu-

lating field conditions. Numerical tests for idealized and severe situations have shown that the value of $\theta = 1.0$ may introduce damping, whereas $\theta = 0.5$ may introduce oscillation (Amein and Kraus, 1991). However, the damping effect is negligible in tidal flow.

(4) Computation Time Step

Tests of numerical models of the shallow-water equations (Price, 1974) have shown that the accuracy of the solution depends on the size of the computational step. In natural channels, a comparison with field observations (Amein and Chu, 1975) demonstrated that a time step can be selected commensurate with the resolution level of the available field data. For example, if boundary condition data are provided at hourly intervals, a time step of 1 or 0.5 hour is adequate. The use of small time steps does not improve the accuracy of the solution because the field data controls must be interpolated as input data. Because the numerical procedure used in this model is implicit, the computation is unconditionally stable, and a large time step is possible.

(5) Number of Iterations

The number of iteration steps to reach convergence during the longitudinal flow computation in the program depends on specified tolerance values selected for the variables. For a river-salt marsh system, convergence is usually attained within three to five iterations when there is no overbank flow. Additional iterations may be required at start-up, or when cross-sectional properties vary sharply between cross-sections

(such as the existence of overbank flow) or if there are rapid changes in water surface elevation and flow rate with time. Numerical experiments showed that 15 iterations may be necessary when overbank flow occurs. In view of these, a maximum limit of 30 iteration steps is recommended. If the solution does not converge within a reasonable number of iterations, one of the followings may be the cause:

A. the time step may be too large;

B. the tolerance values may be too small;

C. there is an error in the cross-section data, roughness coefficients, or transition loss coefficients; or,

D. the model fails because it has been applied to a physical situation violating the underlying assumptions of the model.

(6) External Boundary Conditions

Presently, this model accepts two types of external boundary conditions:

Type 1: values of water surface elevation as a function of time are tabulated as input data.

Type 2: values of discharge as a function of time are tabulated as input data. A tabulation of time-dependent input data is needed for every external boundary node.

(7) Internal Boundaries Internal boundaries exist at tributary junctions, and the model handles the boundary conditions internally. It determines how the junction nodes are located with respect to the channels, and applies the conservation of flow rate and the consistency of water stages at the nodes.

2.6.2 Nodal Parameters along the Main Channel

Nodal parameters must be assigned to all channel cross-sections as follows.

(1) Reference Longitudinal Distances of the Cross Sections

The longitudinal distance of a cross section is the streamwise distance from a reference point to the cross section. Generally, the longitudinal distances for the overbank regions and for the main channel are different due to meander characteristics. Thus, both longitudinal distances for the overbank regions and for the main channel must be given in the input data file.

(2) Lateral Flow

Lateral flow is that water which enters or leaves the main channel between two consecutive cross sections by overbank flow, seepage, evaporation, and precipitation. In addition, flow exchange with ponding reservoirs and minor tributary streams can be treated by specifying their values as lateral flow. During ebb tide, the transverse water surface elevation distribution over an overbank region can reach the case shown in Figure 2.10 after the water elevation at the main channel becomes lower than the elevation at the critical depth on the bank. In this case the water receeding from the overbank region can be taken as lateral flow for the main channel flow. The model can discriminate and handle this case automatically.

(3) Transition Loss Coefficient

The values of the transition loss coefficient, K_e (assigned to describe turbulent losses caused by expansion and contraction), must be specified at all nodes. If these losses

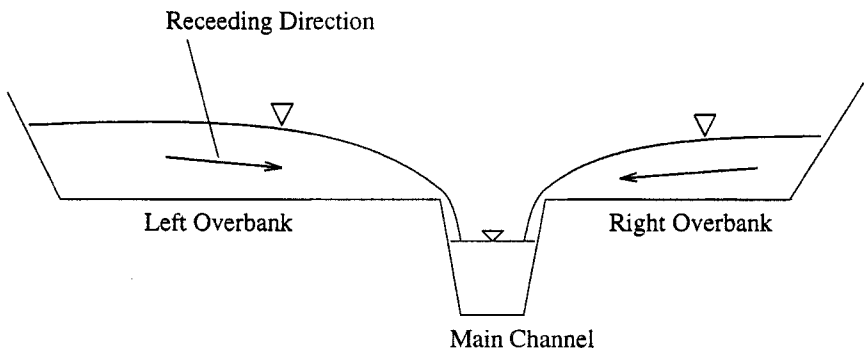

Figure 2.10: Treatment of Lateral Flow During Ebb Tide.

are to be omitted, K_e must be set to zero. However, such losses must be accounted for in order to accurately represent turbulent losses produced by sharp channel contraction or expansion, bridge pilings, culverts, etc. A cross section that produces flow contraction during ebb tide will produce flow expansion during flood tide. Generally, the values of K_e for contraction are different from those for expansion. In this model, the values of K_e are given in an input file; the model can distinguish the case and use the corresponding value of K_e. The maximum value for the contraction coefficient is 0.5, and the maximum value for the expansion coefficient is 1.0. In the presence of highway structures, such as a bridge, it may be necessary to calibrate the coefficient using field data. Generally, values for K_e can be obtained through a published manual (Hoggan, 1989).

(4) Storage Areas and Their Reference Elevations

Storage areas such as ponds, topographic depressions, etc., may exist in a reach between neighboring cross-sections. In this model, only the mass balance is accounted

for and the dynamics of lateral flow are neglected in the longitudinal flow calculation. Some regions become storage areas only if the water surface elevation is higher than some reference elevation. In this case, reference elevations must be provided in input data files.

(5) Overbank Elevations and Lengths

Average overbank elevations and lengths for both left and right overbank regions between cross-sections should be specified in input data files. These data are used to determine the occurence of overbank flow and in the transverse flow calculation.

(6) Manning's Roughness Coefficients

Manning's roughness coefficients, n, are specified for the main channel and overbank regions for all reaches. The values for overbank regions are generally greater than those for the corresponding main channel due to the presence of marsh vegetation. These values are estimated from previous studies, experience and judgement at this point. Table 2.1 (Hoggan, 1989) provides guidance for selecting the value of Manning's n according to physical conditions. Adjustment of the values at selected locations is accomplished via model calibration.

Table 2.1: Values of Roughness Coefficient, n, for Natural Streams (Hoggan, 1989)

Type of Channel and description	Minmum	Normal	Maximum
A-1 Minor streams (Top width at flood stage $\leq$100 ft).			
a. Streams on plain.			
1.Clean, straight, full stage, no rifts or deep pools.	0.025	0.030	0.033
2. Same as above,but more stones and weeds.	0.030	0.035	0.040
3.Clean, winding, some pools and shoals.	0.033	0.040	0.045
4.Same as above, but some weeds and stones.	0.035	0.045	0.050
5.Same as above, lower stage, more ineffective slopes and sections.	0.040	0.048	0.055
6.Same as 4, but more stones.	0.045	0.050	0.060
7.Sluggish reaches, weedy, deep pools.	0.050	0.070	0.080
8.Very weedy reaches, deeps pools or floodway with heavy stand of timber and underbrush.	0.075	0.100	0.150
b.Mountain streams, no vegetation in channel, bank usually steep, trees, and brush along banks submerged at high stages.			
1. Bottom: gravel, cobbles, and few boulders.	0.030	0.040	0.050
2. Bottom: cobbles with large bouders.	0.040	0.050	0.070
A-2. Floodplains.			
a. Pasture, no brush.			
1. Short grass.	0.025	0.030	0.035
2. High grass.	0.030	0.035	0.050
b. Cultivated areas.			
1. No crop.	0.020	0.030	0.040
2. Mature row crops.	0.025	0.035	0.045
3. Mature field crops.	0.030	0.040	0.050
c. Brush.			
1. Scattered brush, heavy weeds.	0.035	0.050	0.070
2. Light brush and trees, in winter.	0.035	0.050	0.060
3. Light brush and trees, in summer.	0.040	0.060	0.080
4. Medium to dense brush, in winter.	0.045	0.070	0.110
5. Medium to dense brush in summer.	0.070	0.100	0.160
d. Trees.			
1. Dense willows, summer, straight.	0.110	0.150	0.220
2. Cleared land with tree stumps, no sprouts.	0.030	0.040	0.050
3. Same as above, but with heavy growth of sprouts.	0.050	0.060	0.080
4. Heavy stand of timber, a few downed trees, little undergrowth flood stage below branches.	0.080	0.100	0.120
5. Same as above, but with flood stage reaching branches.	0.100	0.120	0.160
A-3. Major streams (top width at flood stages $\geq$ 100 ft). The n value is less than that for minor streams of similar description because banks offer less effective resistance.			
a. Regular section with no boulders or brush.	0.025		0.060
b. Irregular and rough section.	0.035		0.100

(7) Initial Values of Water Surface Elevations and Flow Rates

Values of water surface elevations and flow rates must be given at every node at the initial time. These values may be obtained from field measurements. For a "cold start," a horizontal water surface may be assumed at the initial time—for example, the average value of the water surafce elevations throughout a diurnal cycle at the external boundaries.

2.6.3 Channel Cross-Section Data

Channel cross-section data at all nodes along the main channel must be obtained from field surveys. The data are recorded as "distance" and "elevation," where the distance is a relative offset from the left bank and the elevation is the bottom elevation referred to the reference benchmark for the system.

2.6.4 Data Input Files

The program uses three input files: BP.DAT, NODE.DAT, and SECTION.DAT, and generates five output files as shown in Figure 2.11. The input files are described as follows.

(1) BP.DAT

All control parameters are introduced through the input data file BP.DAT. In BP.DAT, as many as 20 comment lines can be inserted at the beginning or header of the BP.DAT file; comment lines are identified by an asterisk in column 1. Titles, identifications, notes, and other useful information can be entered in these lines. After the header, the main file consists of data groups. Each data group consists of one or

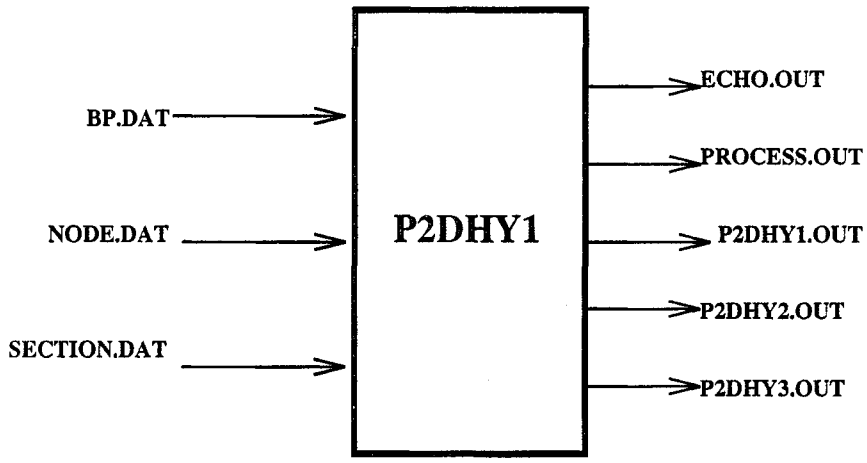

Figure 2.11: P2DHY1 Input and Output File Structure.

more data sets. A data set consists of a single identifier title line followed by lines of data. As many lines of data as needed may be added. All data are input in free format (irrespective of the number of digits or characters, locations on the lines, or spacing between entries on a line).

(2) NODE.DAT

All nodal parameters are entered through the input file NODE.DAT with a similar format for BP.DAT.

(3) SECTION.DAT

This input file contains detailed data of the cross-section geometry. The cross-section geometry is defined by data points identifying the channel boundary. Each data point is described by a pair of values for relative distance and elevation, for example,

SET.1: section node number (Node), number of elevation points at the cross-section (NNUM), station dividing the left overbank region and the main channel (NL), sta-

tion dividing the right overbank region and the main channel (NR), and,

SET.2: relative distance and elevation pairs (NNUM pairs of values).

The formats for BP.DAT, NODE.DAT, and SECTION.DAT for the Oyster River are given in the companion volume, "Documentation of Pseudo-2D Hydrodynamic Model".

2.6.5 Output Files

This program calculates the two-dimensional flow processes in a river-marsh system at the discrete longitudinal and transverse nodes (or points of calculation). The longitudinal flow results include water surface elevation, discharge, flow velocity, water interchange rate between the channel and overbank regions, and flow areas of the overbank regions for each section at each time step. The transverse flow results include water surface elevation, lateral flow rate, and transverse velocity at each lateral station when overbank flow exists. Output files, as shown in Figure 2.11, consist of ECHO.OUT, PROCESS.OUT, P2DHY1.OUT, P2DHY2.OUT, and P2DHY3.OUT, described as follows.

ECHO.OUT is an echo of the input data file. All the input data are printed out so the user can check input errors.

PROCESS.OUT supplies information for the calculation process. In this file, the maximum absolute difference of water surface elevations between consecutive iteration steps, the maximum relative difference in discharge, the corresponding sections in which the maximum water elevation difference and the maximum relative discharge

difference occur for each iteration step, and each time step are given. The total number of iteration steps executed by the program for each time step and the change trends of the relevant differences can be obtained from this file. When the calculation is interrupted due to non-convergence, the user will find the information in this file useful in respecifying inputs.

P2DHY1.OUT contains longitudinal flow results at all sections along the main channel.

P2DHY2.OUT contains longitudinal flow results at selected sections.

P2DHY3.OUT contains transverse flow results which include water surface elevation, lateral flow rate, and lateral velocity in overbank regions.

3. Field Work

Development of the mathematical model required that suitable coastal river-and-marsh sites be selected to provide field data for calibration and validation of the model. The entire Connecticut coast was travelled by project investigators over three days during the summer of 1993. Criteria for selection of research sites were:

1. The system should be fairly small (no more than 2 miles long);
2. The system should be fairly simple in initial appearance, e.g., main channel fairly straight and apparently free from complicated and flashy urbanized hydrology;
3. The system should be crossed by a causeway and(or) bridge at about the middle of the potential study area;
4. The system should be free of hydrological complications: multiple channels, excavations, other bridges or causeways, etc.;
5. The system should be in good apparent ecological health, free of noticeable short-term or long-term environmental impacts such as sewage outfalls, recent fills, etc.;
6. The system should possess the "typical" mixture of salt marsh higher plant species, with a minimum of incursion by Reed, *Phragmites australis;* and,
7. The system should be within 1.5 hrs. travel time from Storrs.

Few of the marshes fit all the above qualifications, but two came close: the Oyster River, Old Saybrook, and portions of the Menunketesuck River marshes in Clinton (Figures 3.1, 3.2). Initially it was decided to use the Oyster River for verification of a pseudo 2-D hydrodynamic model, and the Menunketesuck River for verification of

a two-dimensional hydrodynamic model.

3.1 Description of Research Site at the Oyster River, Old Saybrook, Connecticut

The Oyster River marsh is shown on the U.S. Geological Survey (U.S.G.S.) topographical mapping, 7.5 minute series, Essex quadrangle. The study area lies to the south of I-95 at Exit 67. The river crosses under the ConnRail tracks approximately 1 mile SW of the Old Saybrook train station, proceeds southward to cross under U. S. Rte. 1., and together with the Back River to the east, meets Long Island Sound at Indiantown Harbor. Conn. Rte 154 lies to the east, and the Saybrook Village district lies to the west (Figure 3.3).

The study area is underlain by bedrock of the Clinton granite gneiss at its southern extremity, by the Monson gneiss (with outcrops) northward to a short distance above the Rte. 1 Crossing, and by rocks of the Brimfield formation up to the railroad. North of the railroad the area is underlain by the Putnam Gneiss - Sillimanite formation. The above units are shown on the U.S.G.S. bedrock geological mapping (Lundgren, 1994) trending in a WSW-ENE direction in the study area (Figures 3.4, 3.5). Dissociation of these rocks is generally acid.

USGS surficial geological mapping and a surficial geologic cross-section (Figures 3.6, 3.7) shows the southern half of the study area (below the Rte. 1 bridge) as covered by end moraine deposits, with locally conspicuous concentrations of boulders. The tidal wetlands themselves are mapped as "swamp deposits." Artificial fills are shown

on the western and southern extremities of till and outwash sediments, and in fact, a large water-filled basin now exists as a result of a sand-mining operation, apparently dug to supply sand to the construction industry and(or) for the construction of I-95. A north-south cross-section of the surficial geology of the Oyster River area is given here, redrawn from Flint's section C (Figure 3.7).

In Hill and Shearin's *Tidal Marshes of Connecticut and Rhode Island,* (1970) the Oyster River and its marshes are shown as peaty sediments lying over glacially-derived outwash and gneiss bedrock. The area apparently developed in and over outwash in a glacially-eroded, north-south trending bedrock drainage channel.

According to the standard explanations of salt marsh development in our region (Miller and Egler, 1950), the annual growth of the rhizome-mat of salt marsh plants and their entrained sediments accreted vertically, and proceeded horizontally up the glacial sediment slope, keeping pace with isostatic rebound and the increase in adjacent sea-level associated with Long Island Sound as it grew from an inland glacial lake into an arm of the sea. Offshore nearby, shifting bathymetry has caused changes in shoreline erosion and deposition patterns, and has resulted in changes in local tidal hydrology (Lefor, Kennard and Civco, 1987; Niering and Warren, 1980).

Within the limited spectrum of higher plant species available to colonize this saline intertidal environment, distribution patterns of salt marsh plants change with disturbance, the state of the tidal epoch, and with changes in hydrology, among other factors still under investigation (Lefor, Kennard and Civco, 1987; Miller and Egler,

1950; Niering and Warren, 1977, 1980). Just as at other areas along Connecticut's coast and in salt marshes generally, vegetation distribution has changed sometimes gradually, sometimes quickly over the last 4-5,000 years of its development, as has been revealed by gridded peat-core sampling of the Pattagansett marshes in East Lyme, Connecticut, by Niering and Warren (1977).

The first human users of the Oyster River were the native Americans, whose considerable population (Cronon, 1985) made frequent use of salt marshes and their channels for trapping fish, for plant fibres, and for shellfishing. Summer encampments near salt marshes were frequent in Native American times.

Uses by the European colonists were eventually less benign. Colonial European shipbuilders regularly dredged small harbours and boat slips for fishing vessels through marshes to reach adjacent navigable channels. Further, most travel between New York and Boston developed (quite naturally) along the flatter coast on a southwest-northeast axis, crossing the State's tidal streams with numerous ferries, and eventually, causeways and toll roads, and then railroads. Later, the coastal zone was in effect separated by the rest of the mainland by the Connecticut Turnpike (Rte. I-95). Initial investigations indicate that a bridge or other crossing of some sort has been present at the Oyster River Rte. 1 Bridge site since at least 1857. The present bridge was constructed in 1970-1972, replacing an earlier structure from the 1930's. In the 1970-72 work, the Oyster River channel and bridge crossing were moved less than 100 ft to the east, leaving a rectangular, shallow, muddy-bottomed embayment im-

mediately to the north of the Rte. 1 bridge causeway.

The surface of the area is irregular, rising northward from the shoreline to a maximum altitude of 210 ft. National Geodetic Vertical Datum (NGVD) near the northeastern corner of the basin. Locally, large contrasts in topographic expression and altitude occur between adjacent facies of a single geologic/topographic unit (Figures 3.5, 3.9).

The Oyster River Drainage Basin empties into Long Island Sound on the Western side of the Town of Old Saybrook (Figure 3.8).

The drainage area controlled by the Oyster River is about 6.31 square miles. Figure 3.10 shows the convergences and sub-watersheds in the region.

Proceeding from north to south, the Oyster River watershed is crossed by Rte. 153, by Ingham Hill Road, by the Connecticut Turnpike (I-95), by the ConnRail tracks, and by U.S. Rte. 1, as well as by a variety of subsidiary roads and driveways. Impervious surface increases as one moves lower in the watershed, but most of the area above the railroad tracks (with the exception of I-95) is in second-and third-growth forest. Upper reaches of the contributing streams are all impounded. Two streams join immediately above the ConnRail Tracks at the northern limit of the model verification area, Fishing Brook from the west, and a brook leading out of Ingham Pond to the north. Most of the fresh-water stream input to the Oyster River is from the eastern of the two streams, Fishing Brook, which drains a large area of wetlands and upland to the north and east. A second sub-drainage, that of Mill Meadows, an occluded wetland lying southeast of I-95 and northeast of the ConnRail tracks, occasionally

feeds the Oyster River from the northeast; but an old control structure (probably designed as a floodgate) appears to stop any significant flow into the Oyster River from this area.

On the west side of the upper reaches of the study area, and immediately adjacent to the ConnRail tracks, lies a large water -filled basin that has resulted from a sand and gravel mining operation. Based on our observations and on the surficial geology map, this water is probably mostly derived from the local ground-water. The edge of the former upland in which this hole was dug now remains as a sand and till vegetated dike varying in height from about 4 ft. to over 10 ft. above the surface of the adjacent Oyster River marsh. The dike has been breached in the middle of its north-facing length, and only exchanges water with the marsh (in either direction) after heavy rains or at monthly high tides. Its connection with the ground-water of the adjacent salt marsh is an object of further study. The basin was the subject of a groundwater study by DeLeuw-Cather Engineers, East Hartford, Connecticut (DeLeuw-Cather, 1985). According to this study, the water in this basin is largely groundwater that has entered through the locally previous substrates.

Maps and other drawings on file in the University of Connecticut (UConn) Map Library and Connecticut Department of Transportation (ConnDOT) Archives reveal that a bridge crossing has existed at the Oyster River and Rte. 1 at least since about the 1850. It is likely that some sort of crossing, at least a ferry, has existed in this location since the 1700's. Evidence of this may be found in local archives and in the

British Admiralty Records (Wm. Keegan, Dept. of Anthropology, Univ. of Conn., 1995, pers. comm.), which have not been consulted so far in this study, however.

3.2 Surveying and Datum Establishment

Exhaustive and detailed survey work and vegetation mapping have been completed to permit field verification of the mathematical model:

1. Horizontal and vertical control benchmarks north and south of the Rte. 1 bridge have been established. The positions of these benchmarks are shown on sheet 1 in the map pocket. These elevations are referenced to a ConnDOT highway benchmark located on the south side of Rte. 1, some 1000 ft east of the Rte. 1 bridge (sheet 2, pocket). An infrared-actuated total station/theodolite (Lietz SAT3) and self-levelling level (Wild NA233) were used in transferring and checking all elevations. Elevations and positions are referenced to the Connecticut Coordinate Grid System and NGVD throughout.

2. Using the established base elevations, additional benchmarks and control points were established approx. 1500 ft. north and south of the Rte. 1 bridge, and on the abutment walls and railings of the Railroad bridge at the northern system limit, and south of and adjacent to the Rte. 1 bridge at the top of a cast concrete pipe at the southwestern corner of the abutment. Surveyor's brass-topped monument posts, drills holes, and (or) pins were installed as appropriate, and their positions are shown on AutoCAD-generated on files with the authors, and available for examination.

3. Twenty tide staffs were constructed as follows: 2in x 4in, 10ft long spruce, pressure-

treated timbers were purchased, pointed at one end, and given numerous coats of high-grade polyurethane varnish. Surveyor's rod ribbon, graduated in feet and hundredths, was purchased, and 8 ft. of contiguous ribbon was glued and stapled to the staffs with stainless-steel staples. The staffs were individually numbered, labelled with organization and phone number, and varnished repeatedly again.

4. The staffs were placed in the Oyster River channel adjacent to marsh upstream and downstream of the Railroad and Rte. 1 bridges; near the mouth of the Oyster River; and, in several positions along the channel easily reachable from shore and near the apices of channel curves (Figure 3.11).

5. Horizontal and vertical positions of the staffs were determened with the above mentioned surveying instruments, and correction factors for staff scales were noted.

6. Channel cross-sections were taken at a variety of positions along the channel and under the Railroad and Rte. 1 bridges as shown in Figure 3.13. Figures A.1 through A.20 in Appendix show the results of field surveys of the channel cross-sections, in which the horizontal distance is measured from the left (west) bank (looking upstream); the elevations are in reference to the common datum.

7. Current measurements were taken at the Railroad and Rte. 1 Bridges through at least one-half tidal cycle, as discussed below.

8. A photointerpreted map was made of the marsh north and south the Rte. 1 bridge, extending south to the mouth of the system and northward to the Railroad bridge (Figure 3.16). Vegetation mapping units were selected on the basis of (1) discernable

differences in tone and texture on the aerial photograph enlargements (1 in. = 200 ft.) and (2) the vegetation as observed in the field.

9. All mapping, both survey data and the photointerpretations, were entered into an AutoCad mapping base. Since the photointerpretation and the aerial photograph are uncontrolled and unrectified, a best fit was applied by the CAD operator. Note that while survey data was necessary for the model verification, area and patterns–not edges–of vegetation mapping units are critical to this portion of the study, not their precise location (at this scale).

10. Detailed mapping of four regions of marsh was performed immediately north and south of the railroad bridge, near the mouth, and below the railroad bridge, to determine the mean elevations of the different mapping units and to assess the feasibility of preparing small-interval topographic maps by an automated procedure in AutoCAD. Boundaries of vegetation mapping units were walked in the field, and horizontal and vertical positions of the vegetation unit boundaries, along with spot elevations of salient surface features (e.g., ditch margins) were taken. One hundred-fourteen points were mapped in "Area 4" (near the mouth), 94 in "Area 5" (south of the Rte.1 bridge), 82 in "Area 6," and 83 in "Area 7" for a total of 373 points and plotted on AutoCAD-generated maps (available for examination from the authors). Vegetation was noted for each point to aid in correlating the field-mapped boundaries with the photointerpreted vegetation boundaries, and to be used in summary statistics on vegetation and elevation distributions applicable to the model verifica-

tions. These maps indicate any differences in upstream-downstream elevations and help indicate potential mechanisms for those differences, e.g., obstructions to tidal exchange by the Rte. 1 bridge and causeway.

In general, a typical cross-section of the marsh surface perpendicular to the channel ("overbank region" of the model) (see Figure 3.12) in a so-called "low" marsh with large tidal amplitude looks like "THEN" in Figure 3.12. On the other hand, the Oyster River marshes have a slight levee adjacent to the main channel and along the channel-ward portions of the bounding, perpendicular mosquito ditches ("NOW" in Fig. 3.12). Generally this is caused by increased sedimentation in those regions (Miller & Egler, 1950). This condition is exacerbated by greater sediment influx from the perpendicular side-ditches. In the Oyster River, the channel margins support *Spartina patens* and *S. alterniflora*-tall form as opposed to the *Juncus gerardi* of the Egler model. *Juncus* is usually found as an upland boundary species or in raised patches in the centers of areas bounded by ditches (in somes marshes, but not here) as an indicator of increased elevation caused by increased sedimentation. At the Oyster River, patches of *Spartina patens* line the main channel above eroding banks with variable populations of *S. alterniflora*-tall form, and are occasionally found intermixed with plants of *S. alterniflora*-short form and *S. alterniflora* intermediate form, forms commonly found in stagnant pannes (depressions) and at lower elevations in the marsh. In a typical perpendicular section at the Oyster River, the marsh is highest at the riverbank, grades lower to a semi-stagnant lower area near the

landward boundary, and then upward through a boundary of *S. patens* and *Juncus gerardi* to Reed (*Phragmites australis*) or High-tide Bush, *Iva frutescens*, inverting somewhat the normal sequence (see Table 3.1). Presently this indicates that ambient water-levels may have increased over time through sea-level rise or via a retention of waters, an increase in ambient salinity, or a combination of some or all of these factors.

Referring to the photointerpreted cover map (in pocket), one can note the greater patchiness of the ditch-bounded blocks of salt marsh north of the Rte. 1 Bridge vs. the somewhat more regular patterning of vegetation in marsh blocks below the bridge. While this pattern may also be due to decreasing ambient salinity as one proceeds upstream, no systematic salinity data exists at present, and any conclusions as to the major environmental influences on the vegetation here are premature. Salinity will be measured in FY 96-97.

3.3 Layout for Longitudinal Flow Calculation

Based on the objectives, the reach of the Oyster River, lying between Sections 1 and 28 in Figure 3.13, was selected as the simulation region. It was necessary to extend the study area to regions further upstream where boundary conditions could be easily determined. The extended study area and locations of cross-sections are shown in Figure 3.13.

The U. S. Route 1 bridge is located approximately at the middle of the reach. The cross-sections to be used in the model have been laid out as shown in Figure 3.14 to

effectively simulate tidal flows in both the main channel and the overbank regions. Some parts of the river are not suitable for longitudinal flow calculation, and these regions are treated as storage areas in the model. The storage region is shown in Figure 3.15.

For the additional region shown in Figure 3.15, the boundary conditions at the upstream exterior boundary can be assumed to correspond to influent fresh water.

3.4 Layout for Transverse Flow Calculation

Considering that the overbank regions have only a small degree of relief and that the trend in geographic change is somewhat random, the surface of the overbank region is assumed to be flat, and therefore, the average elevations used in the calculations were determined by our survey data. The number of stations necessary for transverse flow calculation depends on the transverse extent of the overbank region. In this model, the total number of stations for the overbank region is given and decribed in Table 3.1.

Table 3.1: Number of Stations Used in Transverse Flow Calculations.

Length of Transverse Overbank Region (BL)	Number of Stations
BL $\leq$ 60 ft	5
60 ft $\geq$ BL $\leq$ 200 ft	10
BL $\geq$ 200 ft	20

3.5 Tidal Stage Measurements

Nine tide staffs were installed along the river for water surface measurements throughout the diurnal tides, as shown in Figure 3.11 and described above. The stage records of staffs 1 and 9 were generally used as the external boundary conditions, while the remaining staffs were used for model calibration, validation, or simulation. Stages were recorded over four sessions during highest high tides over at least a 12-hour period, including one 22 hour period, with readings of all staffs taken every 50 minutes, and at least 20 and 10-minute intervals at staffs 1, 9, and 13 during the period two hours to either side of the peak tidal elevation.

3.6 Current Measurements

Current measurements were carried out with a Price current meter on loan from the U. S. Geological Survey (Hartford, Connecticut). Measurements were taken at the U. S. Rte. 1 bridge near the middle of the Oyster River, and at the ConnRail railroad near the upstream end of the system. Fresh-water runoff was measured by means of a midget Price current meter (also on loan from the USGS) at the cross-sections of the several upstream branches.

In each current measurement cross-section, the cross-section geometry was determined first, and the number of vertical depth sampling lines was then ascertained. One-point velocity measurement was adopted for each vertical line. The discharge at the section can be obtained through the weighted-area method. Typical current measurement sampling arrangements at the U.S. Rte. 1 Bridge and the ConnRail

railroad bridge sections are shown in Figure 3.16 and Figure 3.17.

3.7 Measurement of Influent Fresh Water

Influent fresh water was measured at locations not influenced by system tidal flow. Locations of influent fresh-water measurements are shown in Figure 3.17.

Numerical solutions based on the finite difference method require one-dimensional discretization of the computional domain. The reach of the Oyster River between Section 1 near the mouth and Section 20 at the Railroad Bridge was chosen for modelling. A total of 20 sections were used for longitudinal or streamwise flow calculations.

Some parts of the river with extensive surface area or with certain meandering patterns are not well-modelled by the one-dimensioinal approach. These regions were treated as storage areas in our model. The storage regions are those shown in Figure 3.14.

3.8 Results of Field Measurements

Four runs of field measurements were conducted under various conditions, as shown in Table 3.2. The first two runs were conducted under low tide conditions, while the last two runs were conducted under high tide conditions.

Table 3.2: Tidal Stage Measurements.

Run No.	Date	Climate Cond.	Over-bank Flow	Measurement	Nd. of Cycles
1	Oct.26-27,1994	Clear	No overbank flow	Water Elev.	2
2	Dec1-2,1994	Clear	Small-scale	Water Elev.	1
3	Apr19-20,1995	Clear	Middle-scale	Water Elev./Current	1
4	May15-16,1995	Clear	Spring High tide	Water Elev./Current	1

Raw data from the tidal stage and current measurements are given in Appendix B.

3.9 Results of Detailed Vegetation Surveying Work

Results of the detailed field mapping for marsh surface elevations and the elevations of the vegetation mapping units were produced as AutoCAD maps available for examination from the authors. A statistical analysis of the vegetation types and their relative elevations on the marsh surface is in progress.

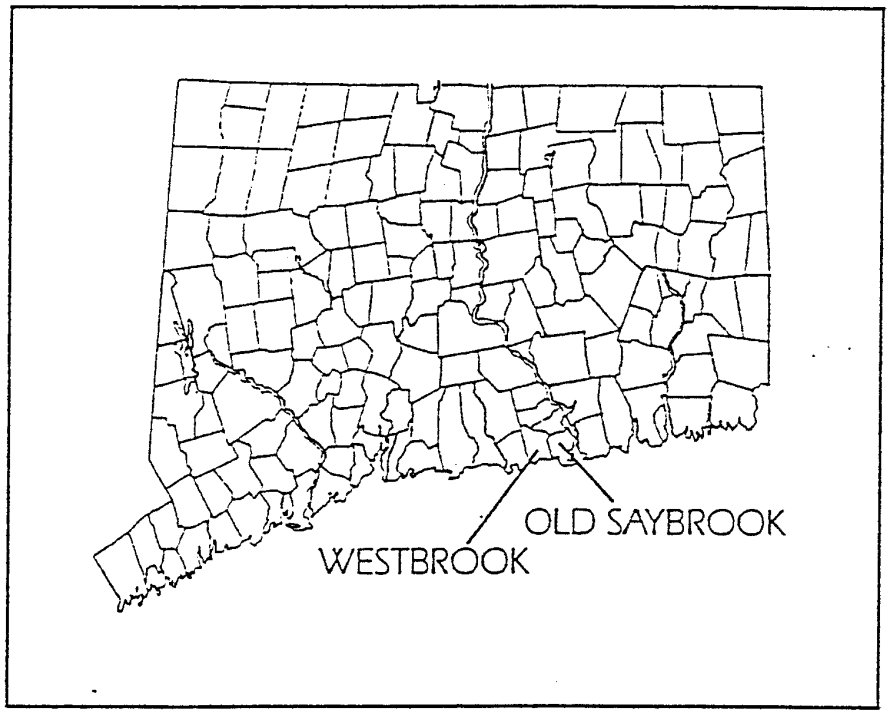

Figure 3.1: Locations of Old Saybrook and Westbrook, Connecticut.

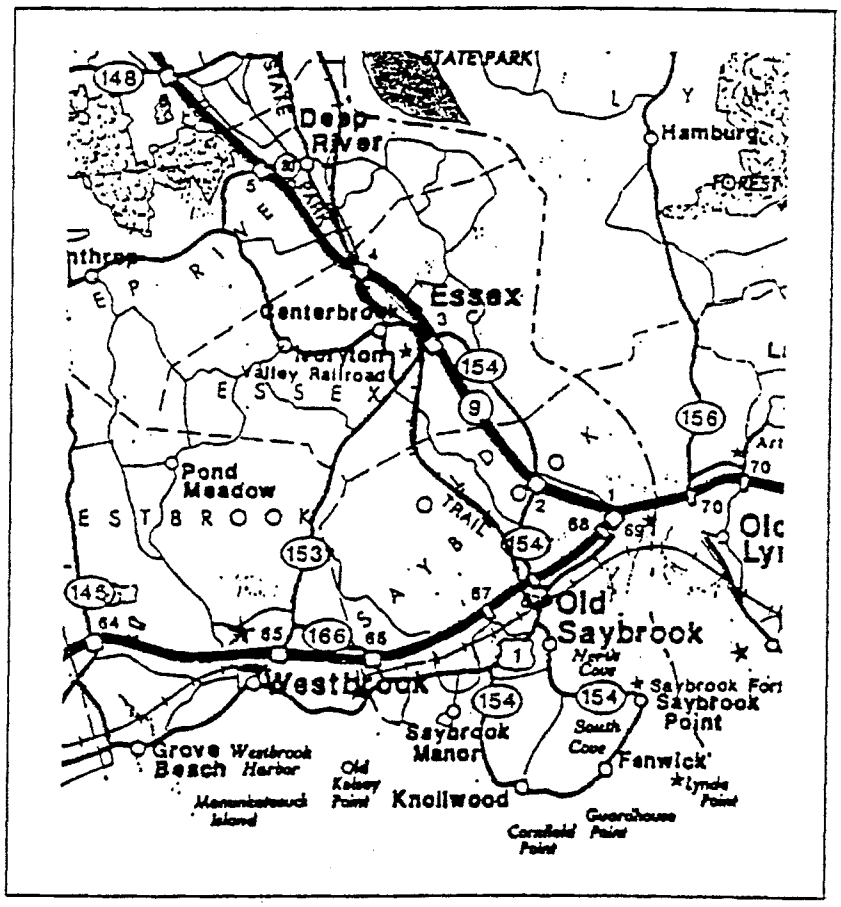

Figure 3.2: Copy of State Road Map Showing Political Boundaries and Major Roads.

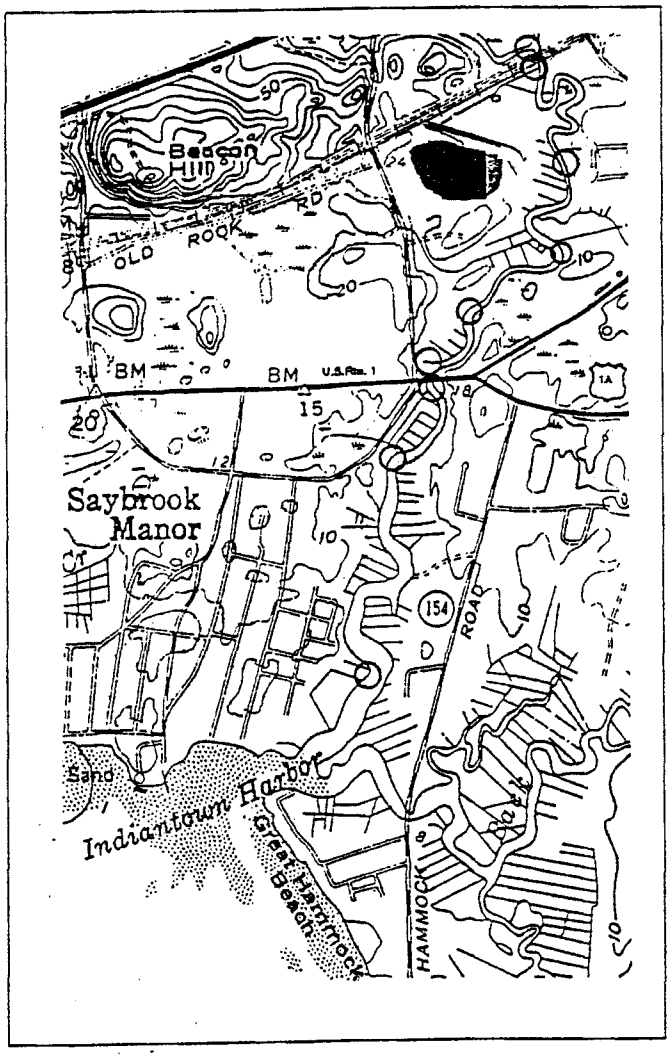

Figure 3.3: U.S.G.S. Topographic Mapping for the Oyster River Region, Old Saybrook.

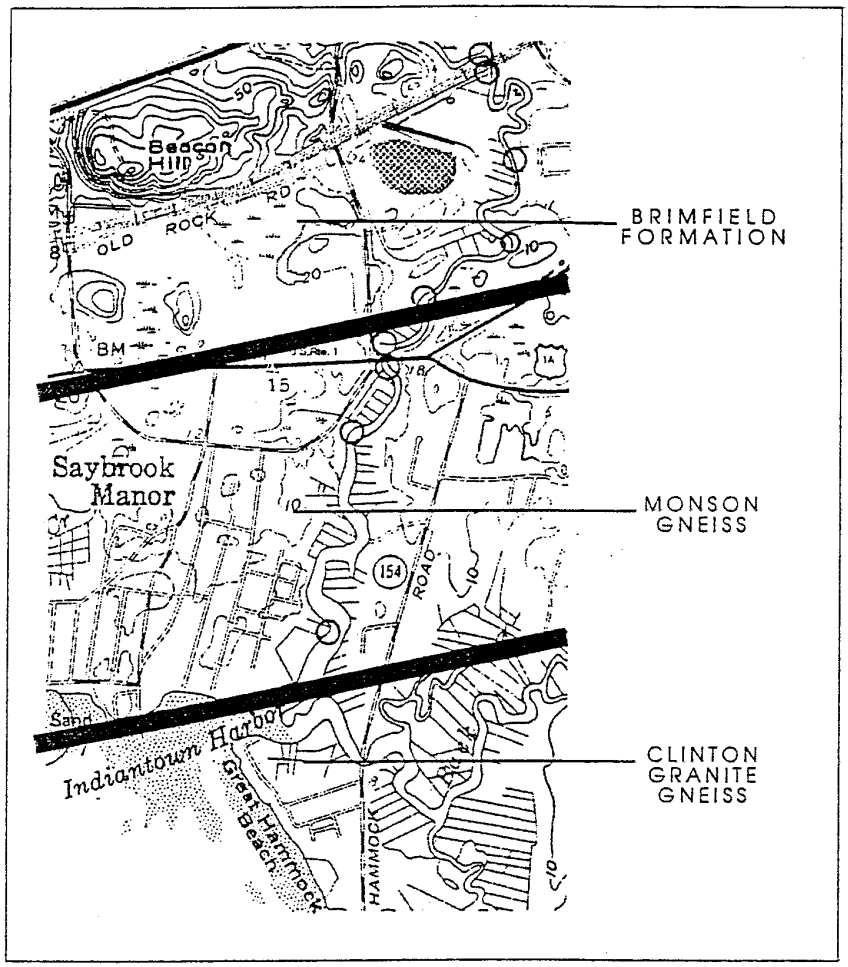

Figure 3.4: Major Bedrock Boundaries.

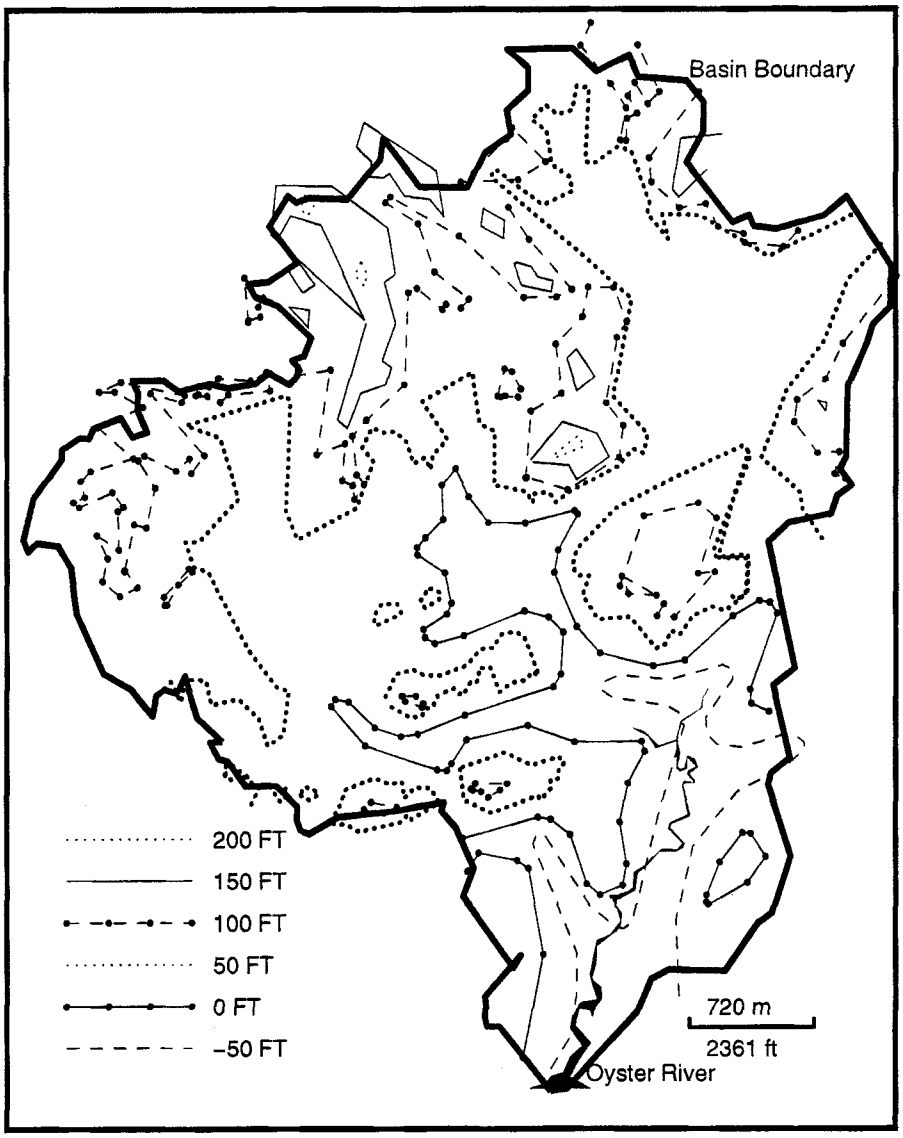

Figure 3.5: Bedrock Surface Distribution.

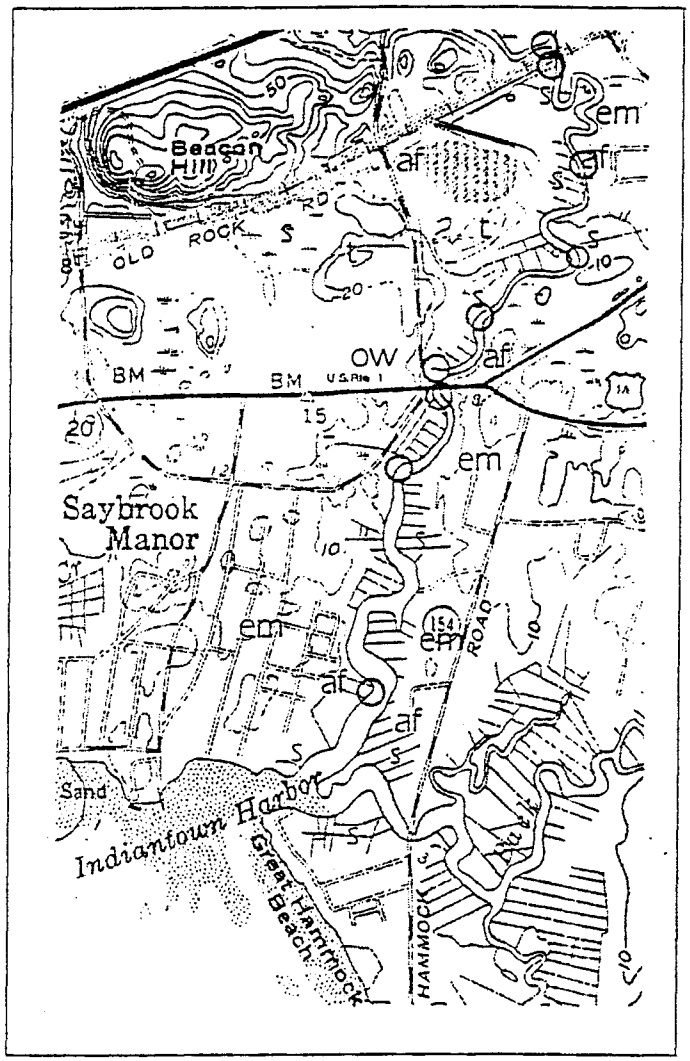

Figure 3.6: U.S.G.S. Surficial Mapping.

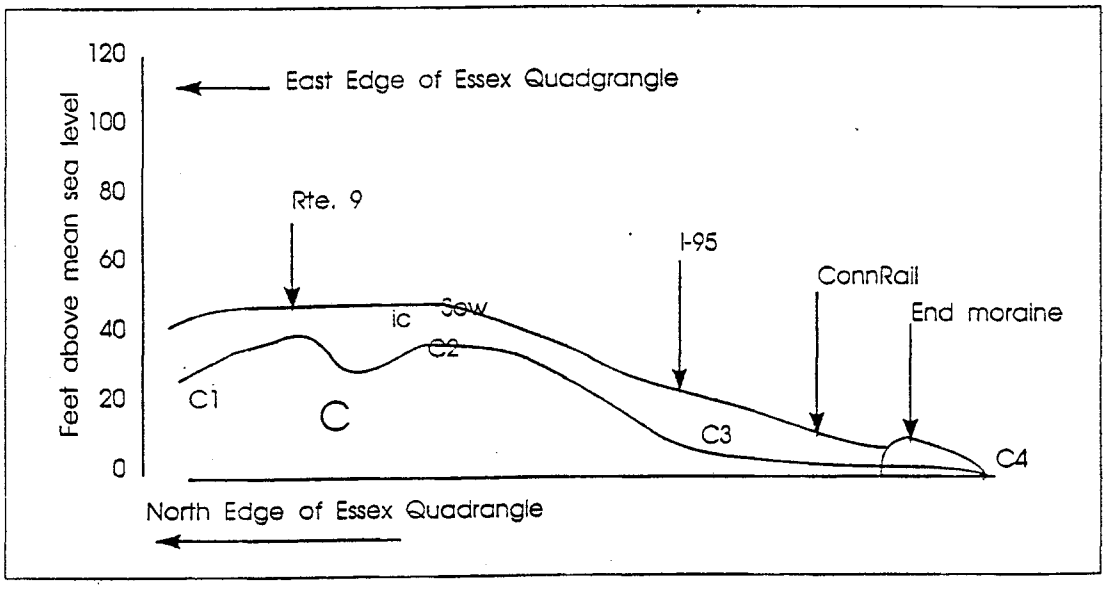

Figure 3.7: Cross-section Showing Bedrock and Surficial Deposits(from Flint, 1972).

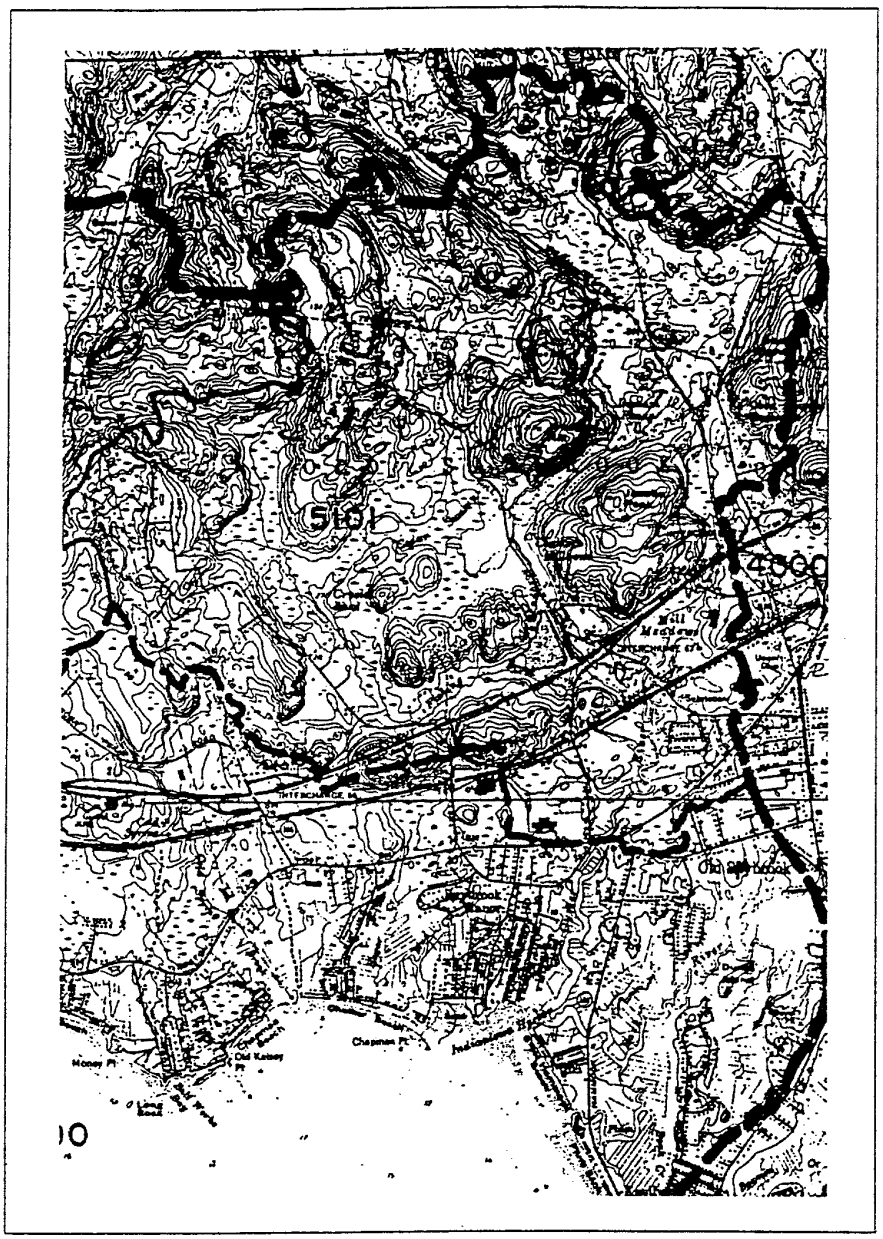

Figure 3.8: Drainage Basins (State of Conn. Drainage Basin Atlas, 1982).

Figure 3.9: Digitized Topography Used in the Computer Simulation.

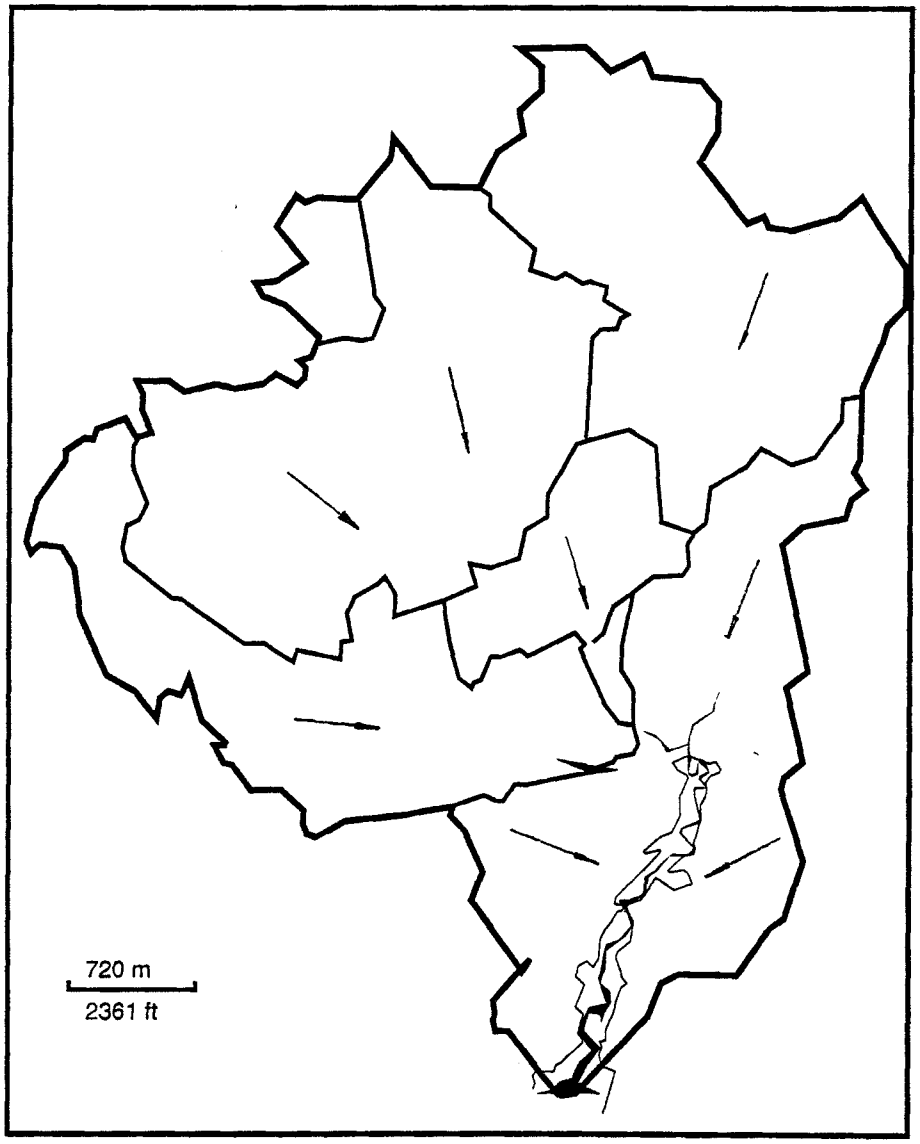

Figure 3.10: Basin Convergences.

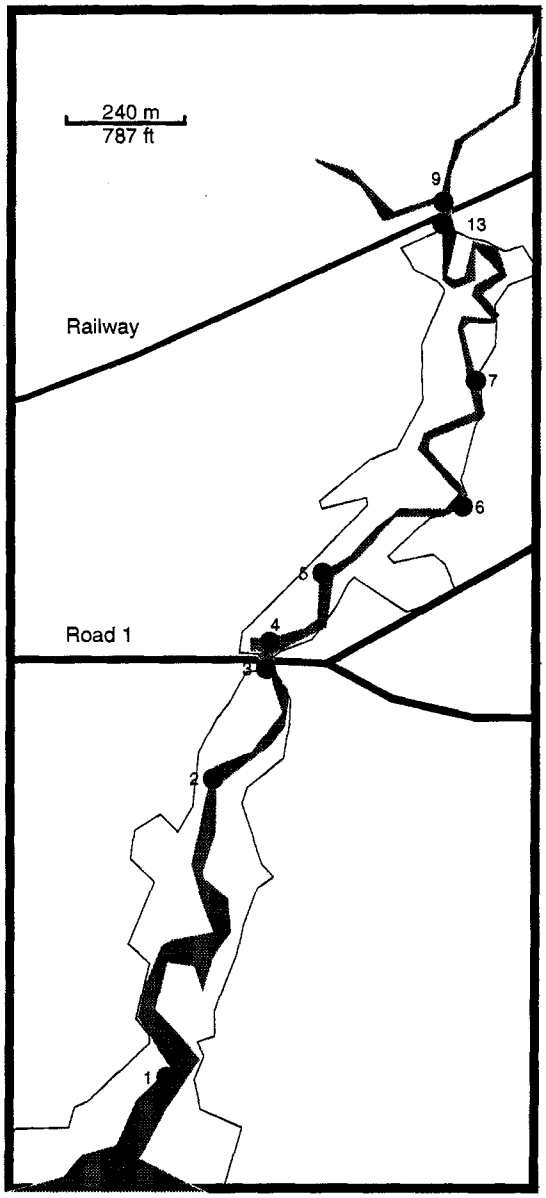

Figure 3.11: Locations of Tide Staff.

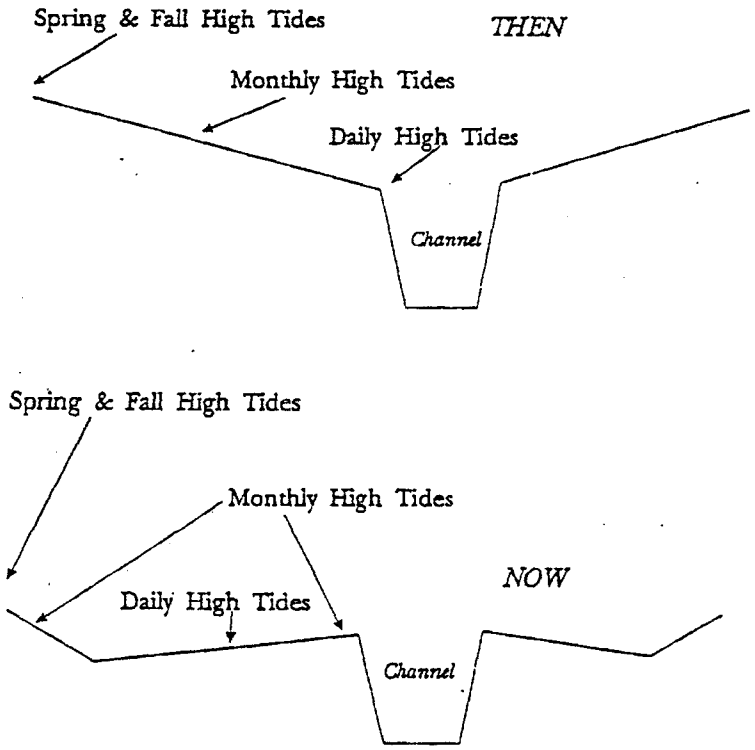

Figure 3.12: Schematic Cross-sections of Salt Marsh Channels.

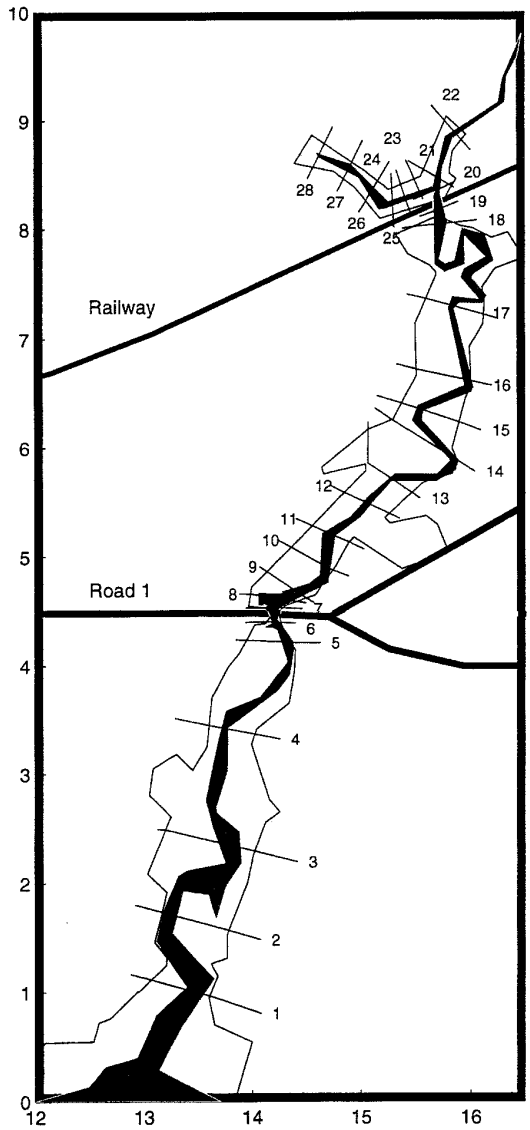

Figure 3.13: Locations of Cross-sections for Model Calculation.

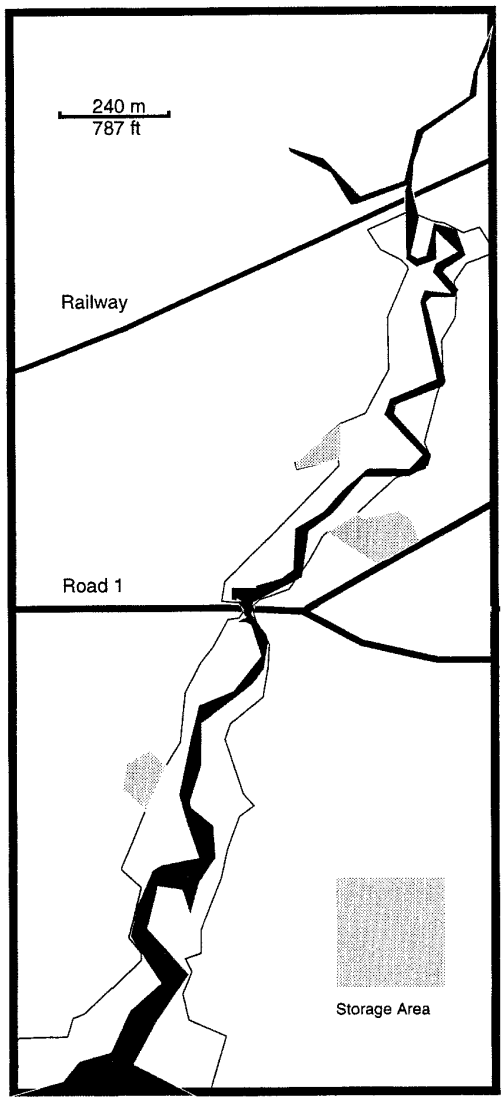

Figure 3.14: System Storage Areas.

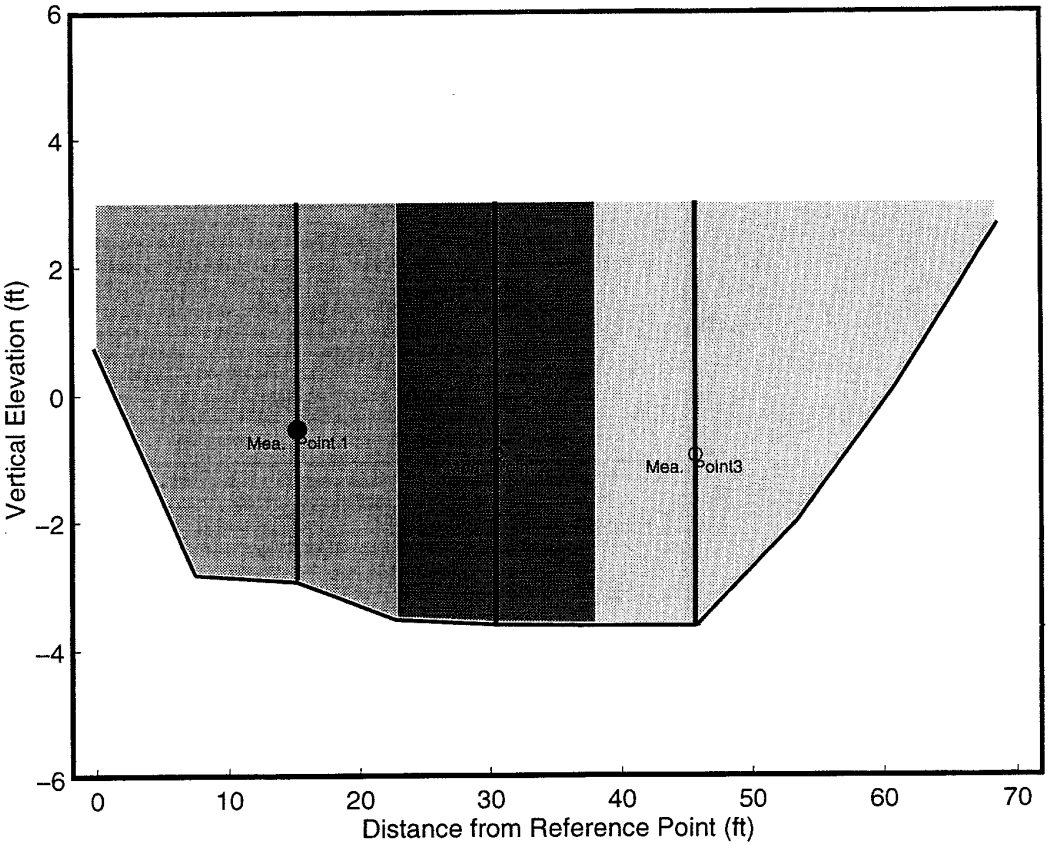

Figure 3.15: Current Measurements at the Rte. 1 Bridge Section.

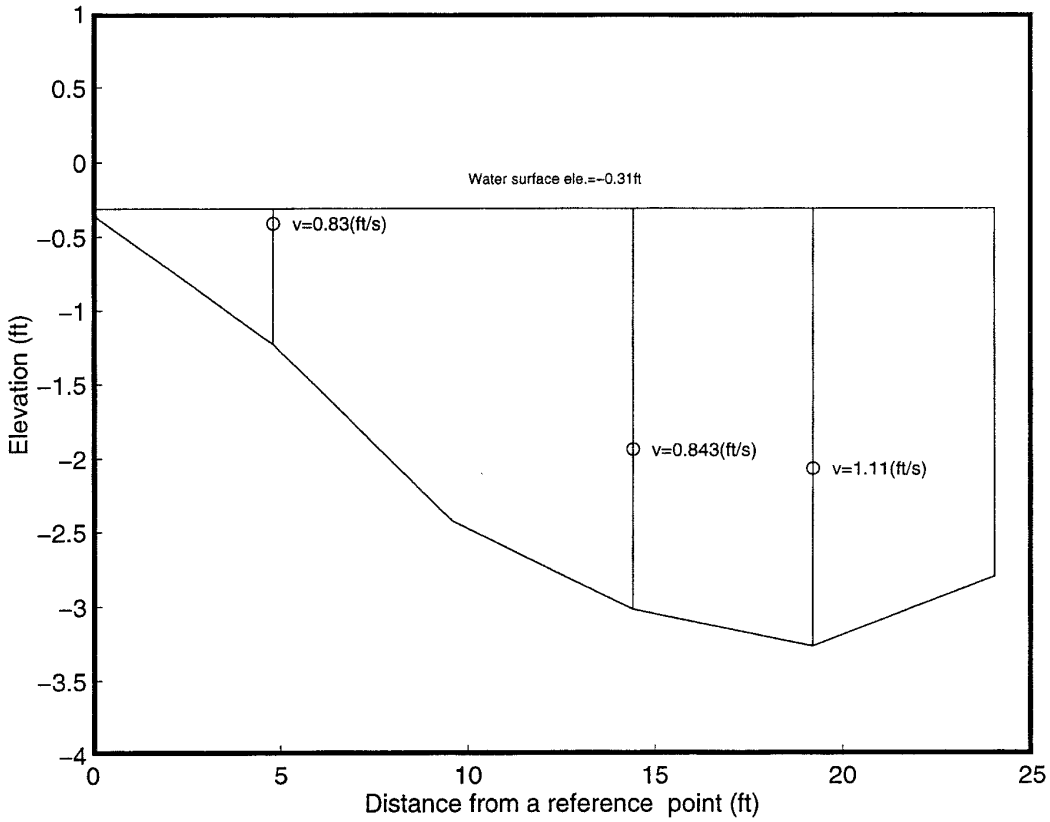

Figure 3.16: Current Measurements at the ConnRail Bridge Section.

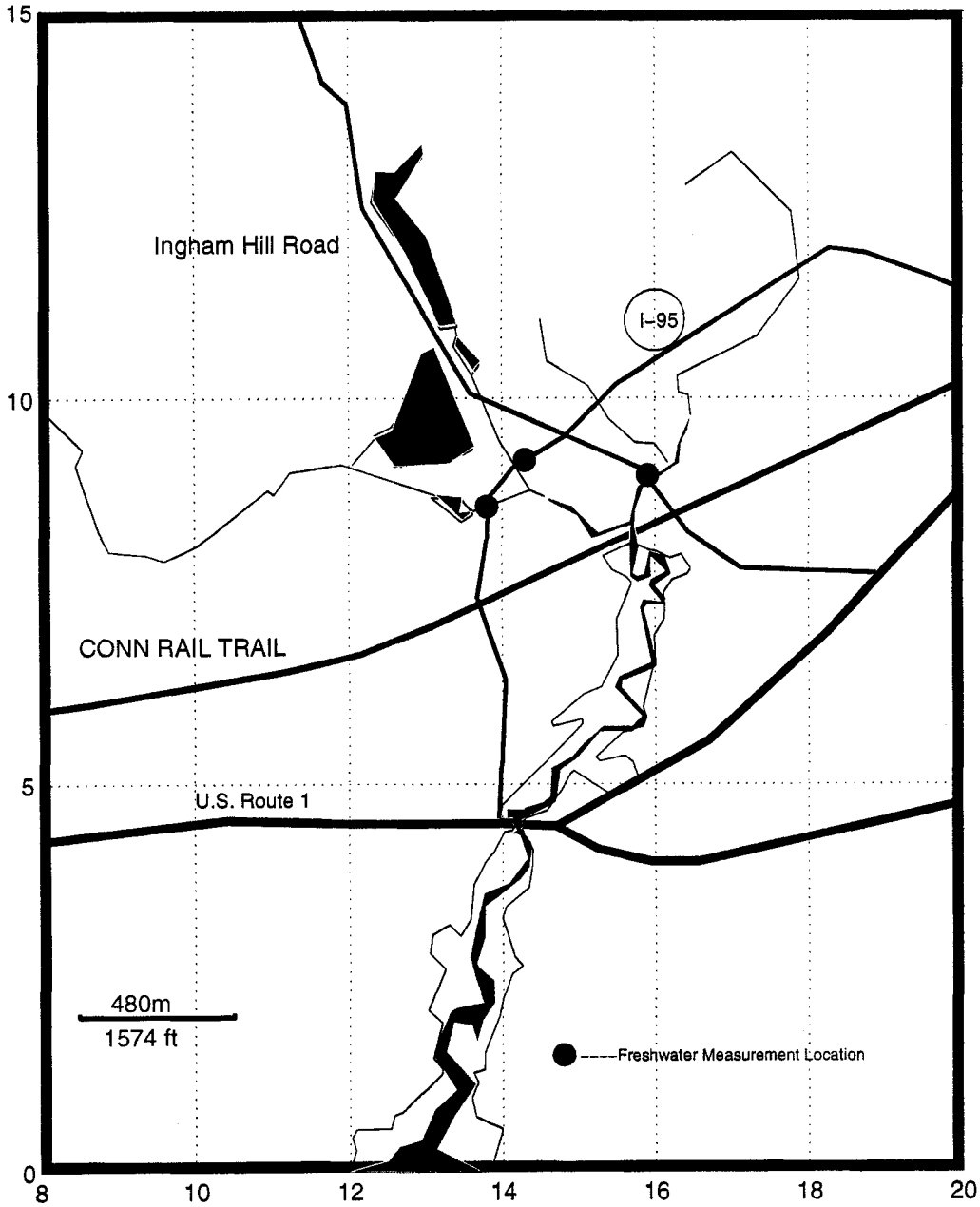

Figure 3.17: Locations For Fresh-Water Runoff Measurements.

4. Model Calibration and Simulation

The diurnal tidal flow in the Oyster River and its salt marsh at Old Saybrook, Connecticut, was used for calibrating this model. The physical characteristics of the river-marsh system have been discussed in detail in the previous chapter. The main channel roughness coefficient, n_c, and the overbank roughness coefficient, n_s (assuming $n_s = n_l = n_r$), are the primary calibration parameters. The calibration procedure involves selecting the values of these parameters to be used in the model calibration and comparing the calculated results with field measurements of water surface elevations and profiles along the main channel and with the discharges at selected locations throughout a tidal cycle. Normally, transition losses are significant only in the vicinity of bridges, culverts, and other hydraulic controls and locations, where strong changes in channel geometry occur. Therefore, the transition loss is considered as a secondary calibration parameter and has an insignificant global effect on the river-marsh system. A sensitivity analysis to determine the effect of the transition loss coefficient is described in the next section.

4.1 Transition Loss Coefficient

The transition-loss coefficient K_e is an emprical parameter that critically depends on channel configuration and the presence of hydraulic structures on the channel. Suggested values for this coefficient as given by the U. S. Army Corps of Engineers are shown in Table 4.1.

Table 4.1: Suggested Values for K_e.

K_e	Contraction	Expansion
Gradual Transition	0.1	0.3
Bridge Sections	0.3	0.5
Abrupt Transitions	0.6	0.8

These values were used on the basis of the sensitivity analysis. Figure 4.1 shows the effect of K_e on the discharge over a tidal cycle at the U.S. Route 1 Bridge and the water surface profile along the Oyster River. The calculated results were obtained using the measured water surface elevations of May 16-17, 1995 at cross sections 1 and 20 as the boundary conditions. A four-fold increase in the magnitude of K_e results only in a 4 % decrease in the difference of maximum and minimum discharge, and practically no change in the water surface profile along the river throughout the tidal cycle. This insignificant effect can be explained by the following:

(1) Both the Route 1 bridge and the railway bridge are single-span bridges without piers, and the openings are nearly as wide as the channel itself. Therefore, a gradual transition always exists under the no overbank flow condition.

(2) When overbank flow occurs, some contraction or expension takes place near the bridges due to the bridge abutments. However, the overbank flow is very shallow and the flow is mostly confined within the main channel.

(3) Under normal tidal conditions, the flow velocity along the river is not great enough

to cause significant transition losses. In extreme events, however, the transition losses near the bridges may require more careful consideration.

4.2 Manning's Roughness Coefficient for the Main Channel

The Oyster River is a small river, and its configuration is mainly molded by the tidal flow. It is reasonable to assume that bottom conditions and hence the roughness coefficient in the main channel are nearly the same along the reach through the marsh up to the railroad bridge. At this time, without knowing the vegetation distribution in the marsh and lacking a direct method to determine Manning's n for that vegetation (work in progress), at this point a constant value for n_c is therefore assumed for the whole reach. A series of model calculations were conducted for different values of Manning's n_c and n_s. Three sets of calculated results for n_c=0.014, 0.028 and 0.056 are shown in Figures 4.3 to 4.5 for the discharges and water surface elevations at section 6 on the downstream side of U.S. Route 1 bridge. The water surface profiles during flood and ebb tide are given in Figures 4.5 and 4.6. Again, the water surface elevation data at sections 1 and 20 of May 16-17, 1995 were used as the forcing boundary conditions.

The results indicate the following:

(1) $n_c = 0.028$ provided the best comparison between the calculated results and field measured data (detailed comparisons of the results will be presented in the next section);

(2) the effect of n_c on the discharge is quite significant. A decrease in the value of n_c

causes a rapid increase in the magnitude of discharge;

(3) the water surface elevation is much less sensitive to the change in n_c as compared with the discharge;

(4) the asymmetric effect of n_c on water surface elevation between the flood and ebb tides is evident throughout the tidal cycle. A small value of n_c facilitates the draining of water in the river; and,

(5) when $n_c = 0.014$, the water surface elevation profile along the river is not smooth. This is due to the fact that when the discharge becomes larger for smaller roughness, the adjustment of kinetic energy change between sections becomes more sensitive. A shorter nodal distance should have been used in the calculation.

4.3 Manning's Roughness Coefficient for Overbank Regions

With the same conditions for n_c above, three sets of calculated results for n_s=0.0275, 0.055 and 0.110 are shown in Figures 4.7 to 4.10. The effect of the roughness coefficient, n_s, on tidal flow in the Oyster River site is quite limited. The reason for this is that the flow is mostly confined within the main channel and the water depth in the overbank region is very small. Marsh vegetation significantly increases the magnitude of n_s, however. This roughness coefficient has a direct effect on the spreading and draining of lateral flow on the marsh, and only a secondary effect on the longitudinal flow through the variable cross sections of overland regions. Comparisons and discussions of the calculated results and field measured data for n_s=0.055 are presented in the following section.

4.4 Calibration Results

Using the results of the sensitivity analysis of K_e and the calculated values of n_c and n_s, the appropriate values of these parameters for the Oyster River can be summarized as shown in Table 4.2.

Table 4.2: Calibrated Parameters.

K_e for contraction	0.1 for gradual transition 0.3 for bridge sections
K_e for expansion	0.3 for gradual transition 0.5 for bridge sections
n_c	0.028
n_s	0.055

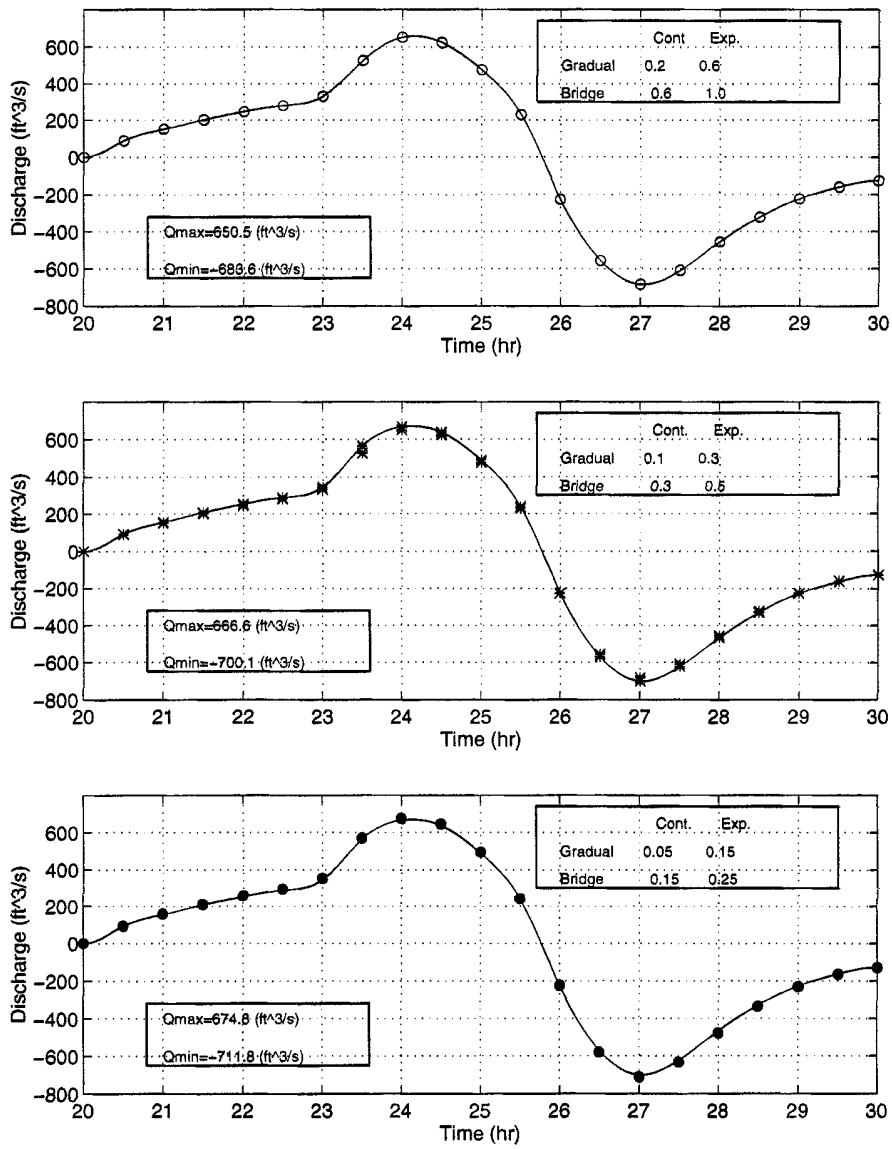

Figure 4.1: Influence of K_e on Discharge Process.

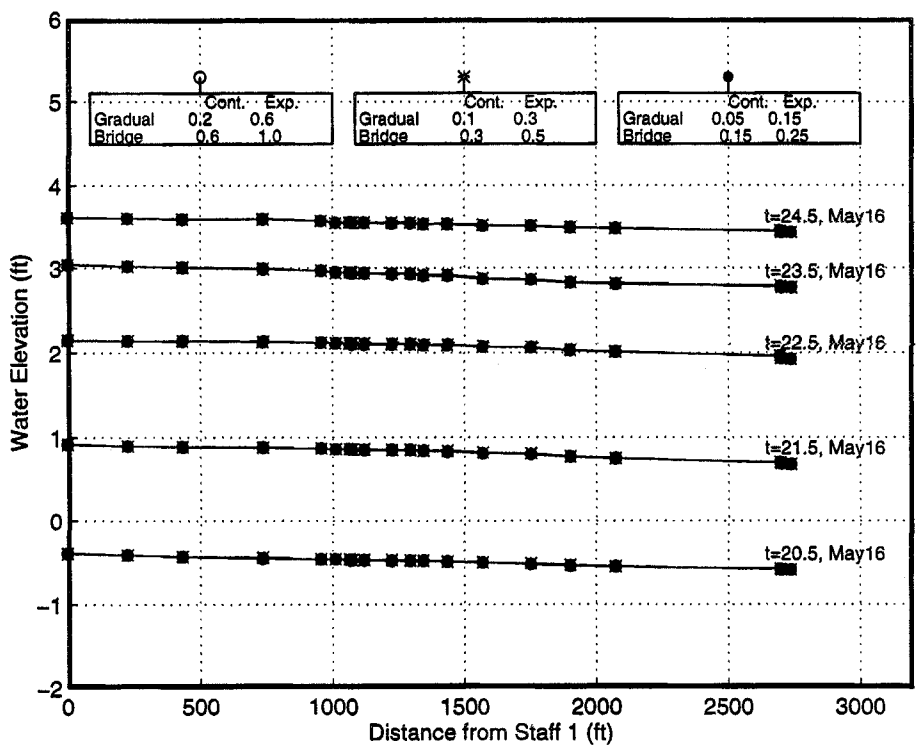

Figure 4.2: Influence of K_e on Water Elevation Distribution.

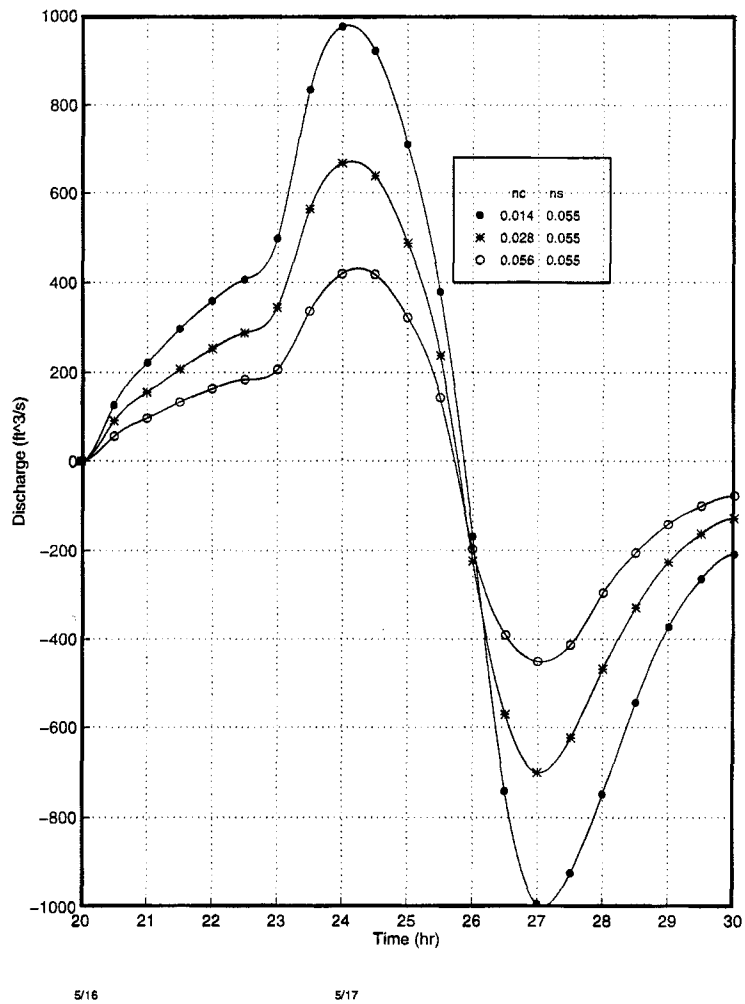

Figure 4.3: Influence of n_c on Discharge at Section 6 near Rte 1 Bridge

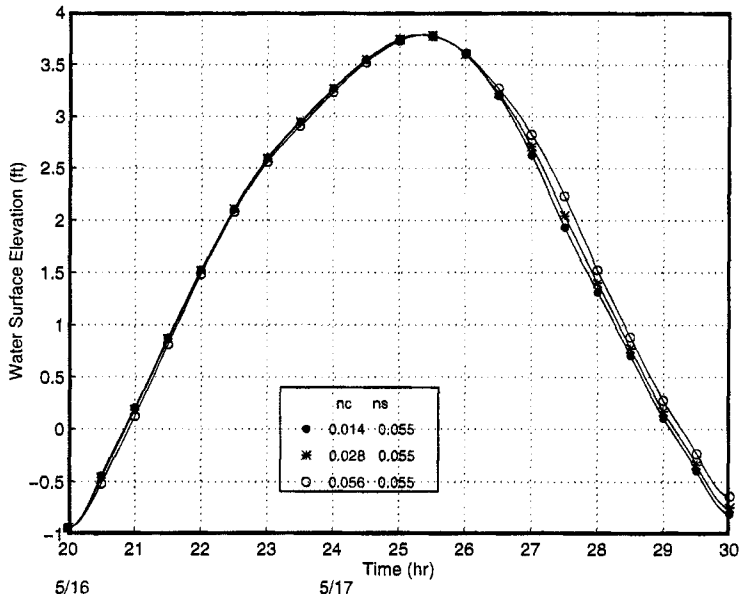

Figure 4.4: Influence of n_c on Water Surface Elevation at Section 6 near Rte 1 Bridge

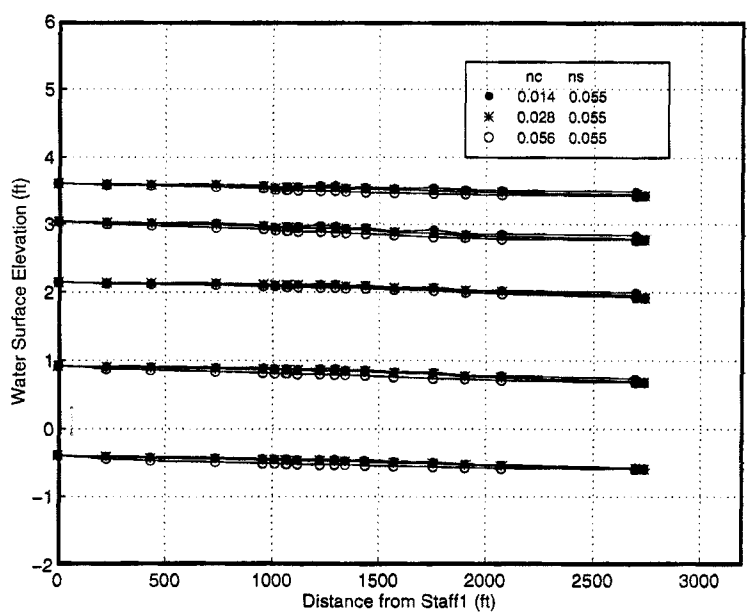

Figure 4.5: Influence of n_c on Water Surface Elevation profile During Flood Tide

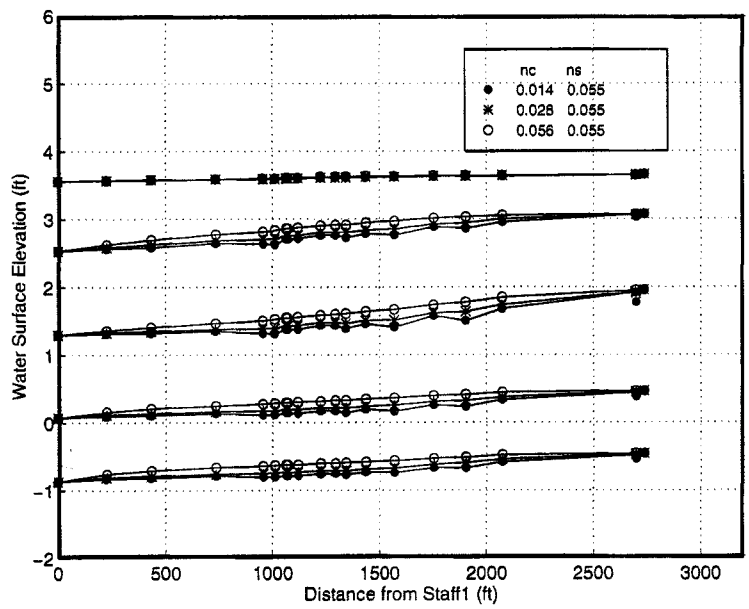

Figure 4.6: Influence of n_c on Water Surface Elevation profile During Ebb Tide

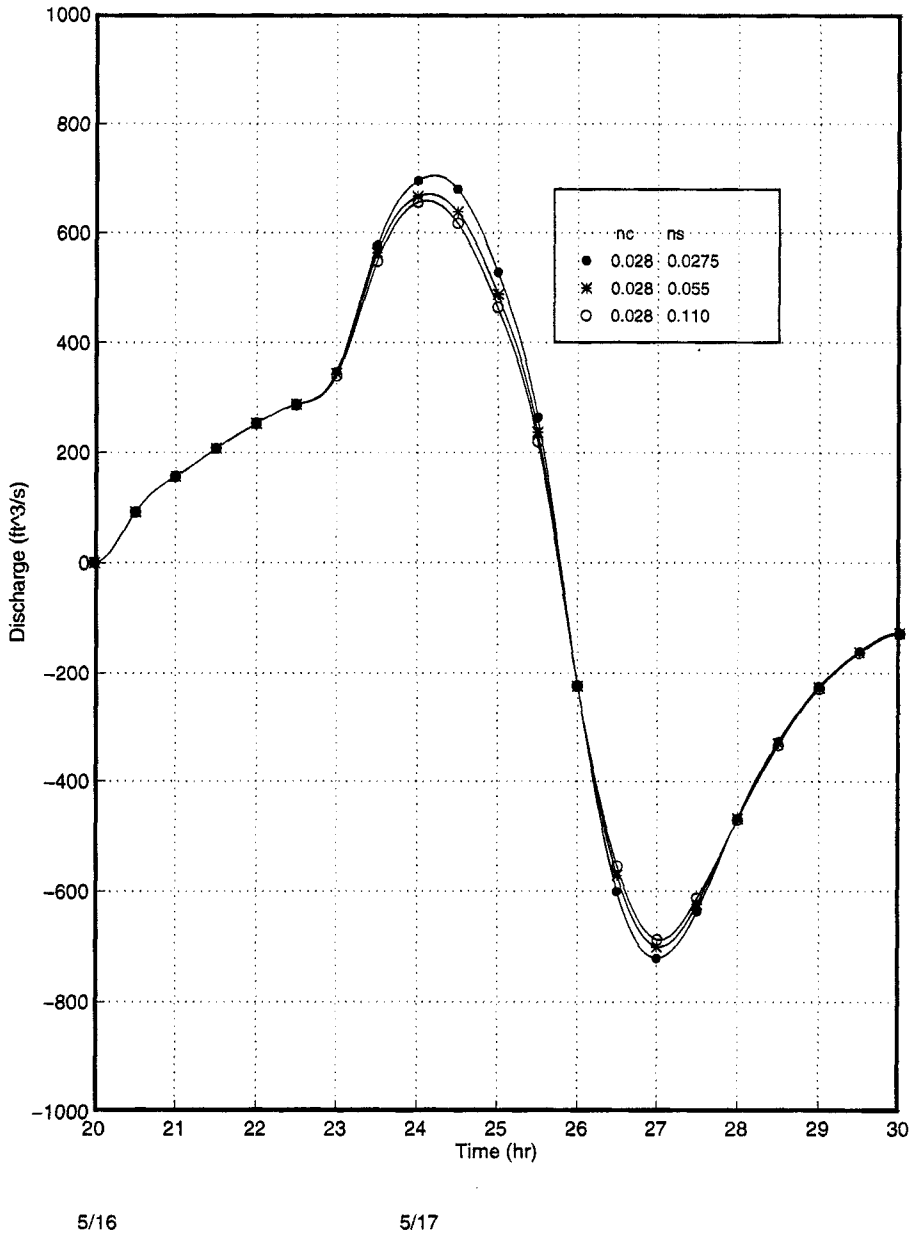

Figure 4.7: Influence of n_s on Discharge at the Section 6 near Rte 1 Bridge

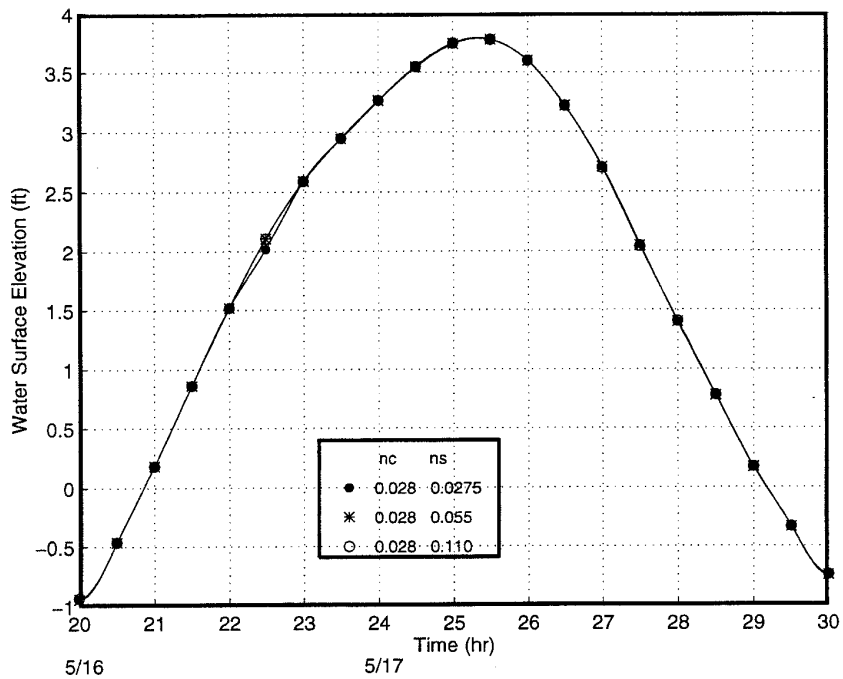

Figure 4.8: Influence of n_s on Water Surface Elevation at Section 6 near Rte 1 Bridge

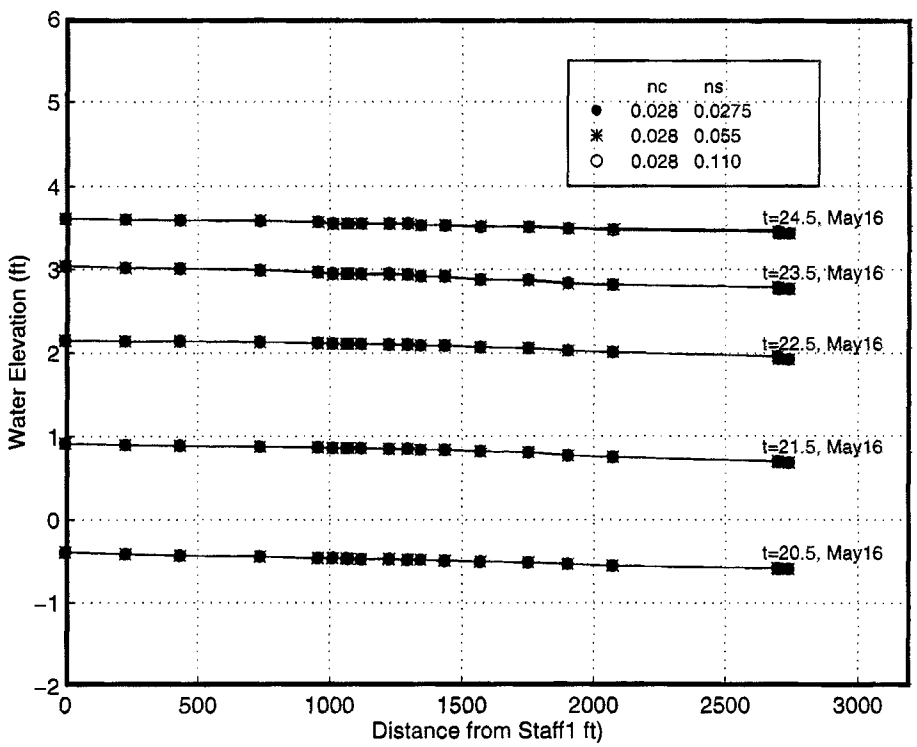

Figure 4.9: Influence of n_s on Water Surface Elevation profile During Flood Tide

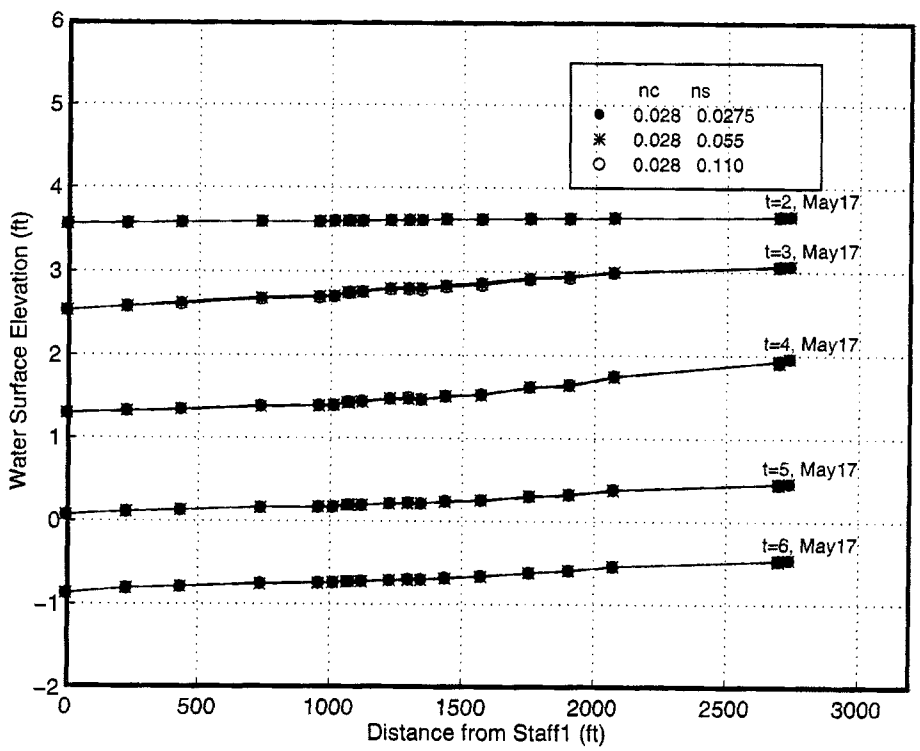

Figure 4.10: Influence of n_s on Water Surface Elevation profile During Ebb Tide

4.5 Comparisons of Simulation Results With Measured Data

The measured data includes the stage and discharge acquired from four runs of field measurements conducted on October 26, 1994, December 1, 1994, April 19, 1995, and May 15, 1995 (see Table 3.2). The overland flow in the first two runs was very limited and tidal flow was mostly confined within the main channel. The last two runs were conducted during spring high tides with sufficient overland flows for testing the pseudo-2D hydrodynamic model. The maximum overland depth in the first two runs is 0-0.2 ft as compared with 0.8-1.3 ft in the last two runs. As discussed in the previous section, the calibrations of Manning's roughness coefficients are based on the first run. The calibrated parameters given in Table 4.2 were used for simulation of the tidal flow in the subsequent three runs. The simulation results together with the calibration results are presented in this section.

The first run results of measured data and simulation are shown in Figures 4.11 to 4.17, over two tidal cycles. The agreement of the water surface elevations on staffs 2, 3, 5 and 7 is very good throughout the tidal cycles at these locations. The discrepancy in the water surface profiles could have been caused by inaccurate determination of staff datums, or disturbances to the staffs, because the tidal amplitudes at these locations are in good agreement.

Similar comparisons of the results were carried out for the second run as shown in Figures 4.18 to 4.22. In this case, the calculated water surface profiles are also in good agreement with the measured ones.

The comparison of the water surface elevations at staff 7 of the third run at the spring high tide is depicted in Figure 4.23. The water surface elevations at staff 6 and the discharge through U.S. Route 1 Bridge are depicted in Figure 4.24. Both results show reasonable agreement.

The fourth run results are shown in Figures 4.25 to 4.27. The water surface elevations at staffs 4 to 7, located downstream and upstream of U.S. Route 1 Bridge respectively, and at staff 6 near the bridge are all in good agreement. The discharge for this run is in better agreement than for the third run.

These results indicate that using the calibrated parameters, the model performed reasonably well for the tidal flow at the Oyster River site.

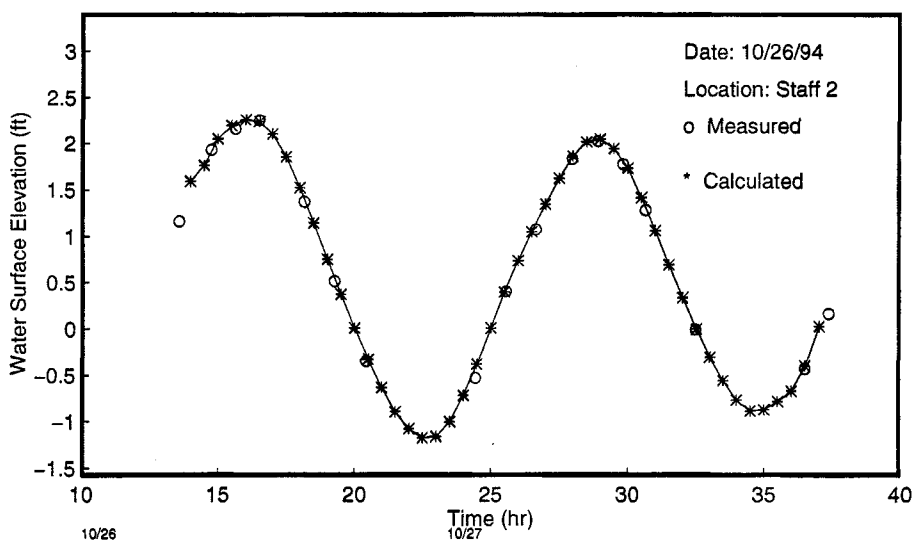

Figure 4.11: Comparison of Water Elevation at Staff 2.

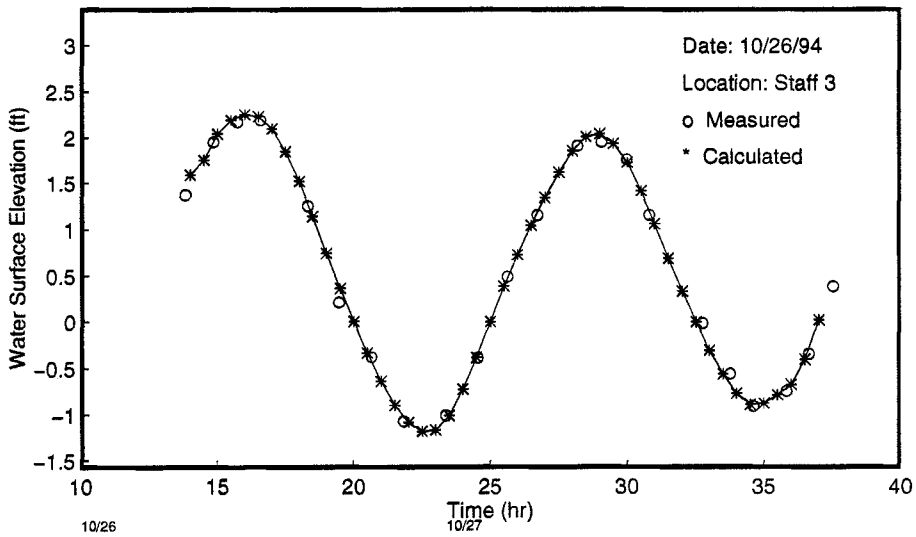

Figure 4.12: Comparision of Water Elevation at Staff 3.

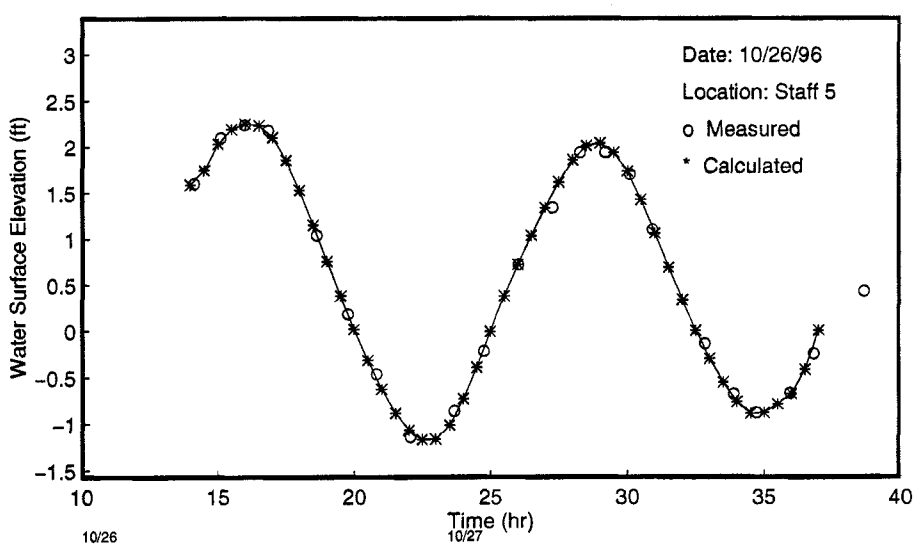

Figure 4.13: Comparision of Water Elevation at Staff 5.

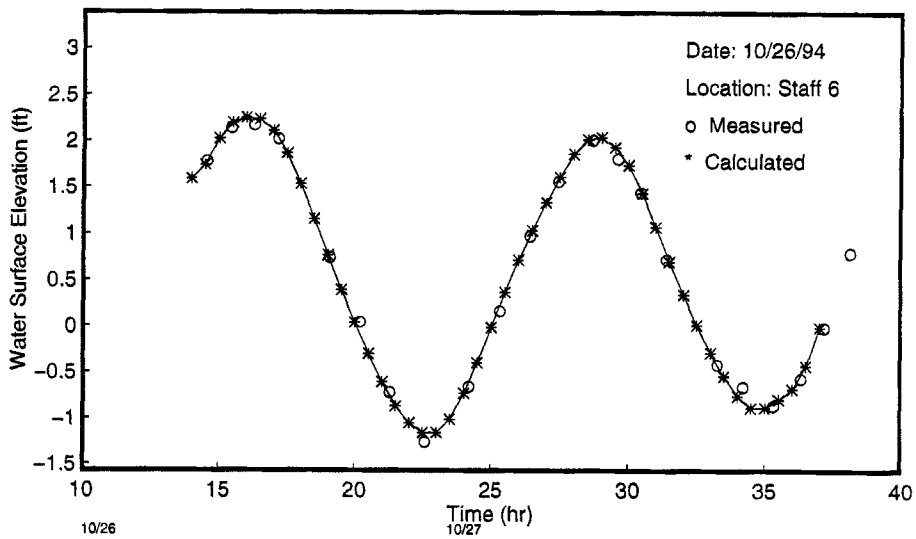

Figure 4.14: Comparision of Water Elevation at Staff 6.

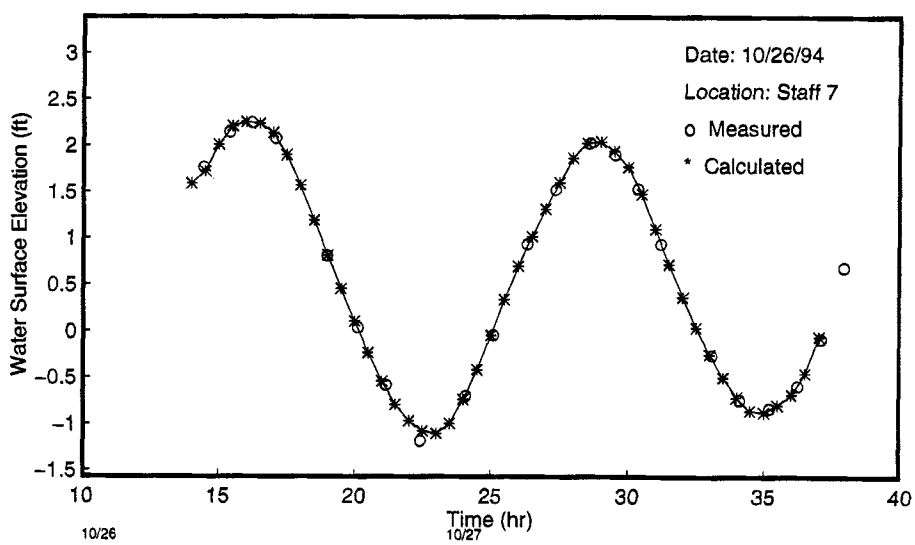

Figure 4.15: Comparision of Water Elevation at Staff 7.

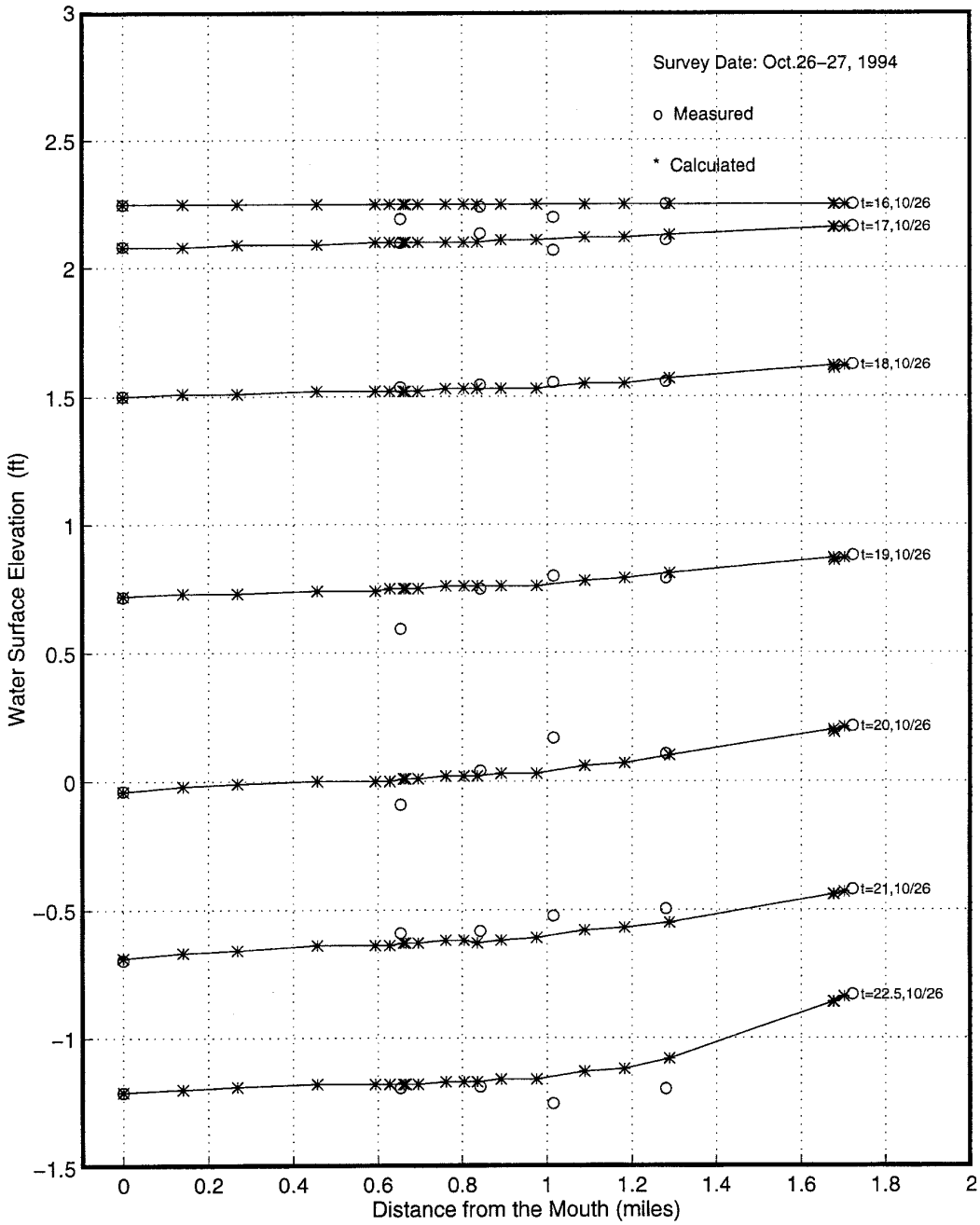

Figure 4.16: Comparision of Water Elevation During Ebb Tide.

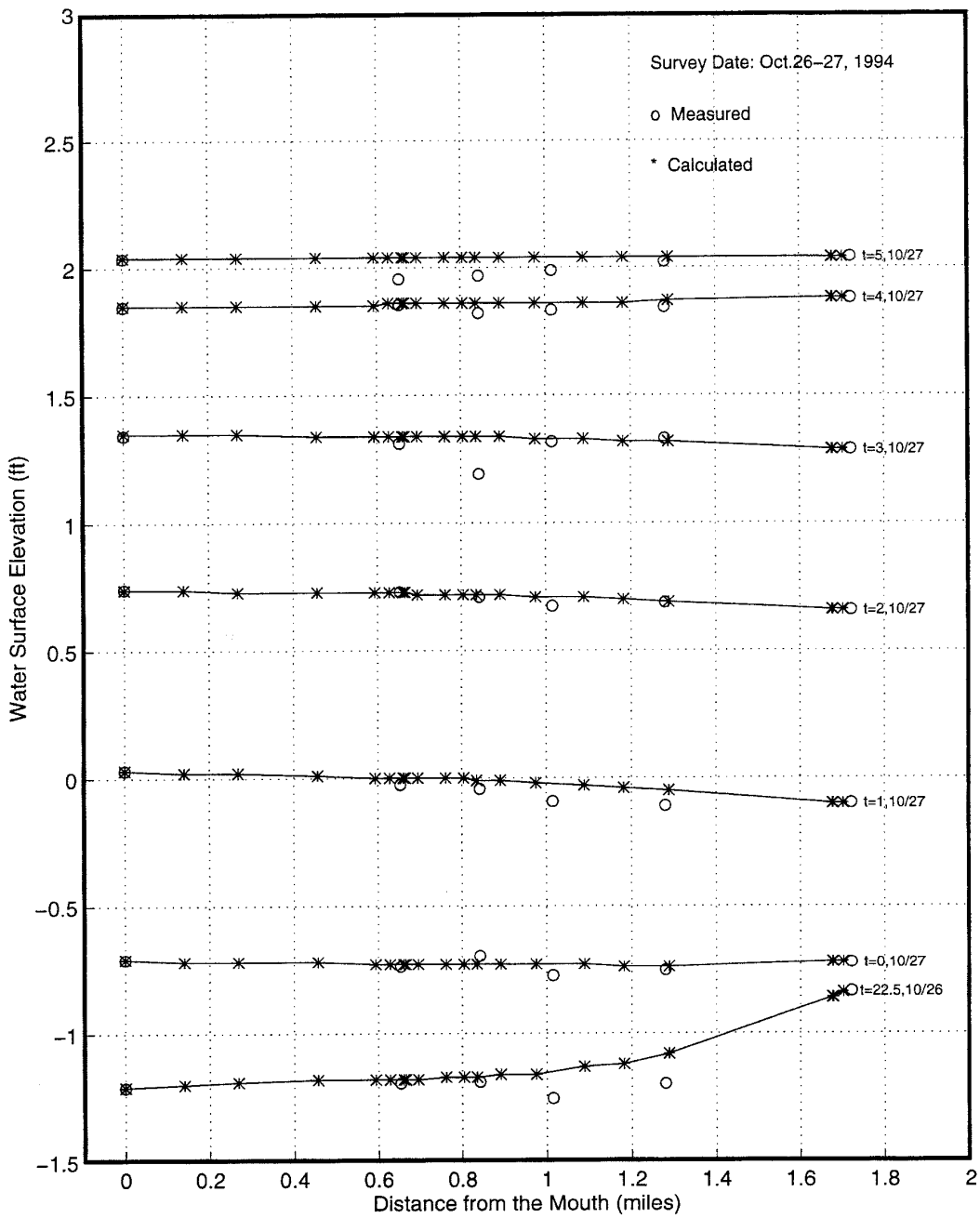

Figure 4.17: Comparision of Water Elevation During Flood Tide.

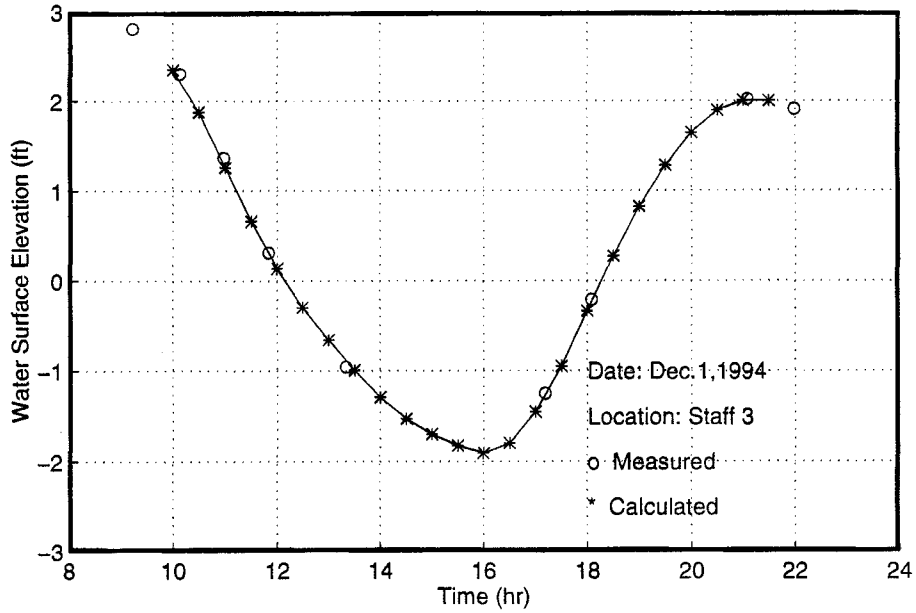

Figure 4.18: Comparision of Water Elevation at Staff 3.

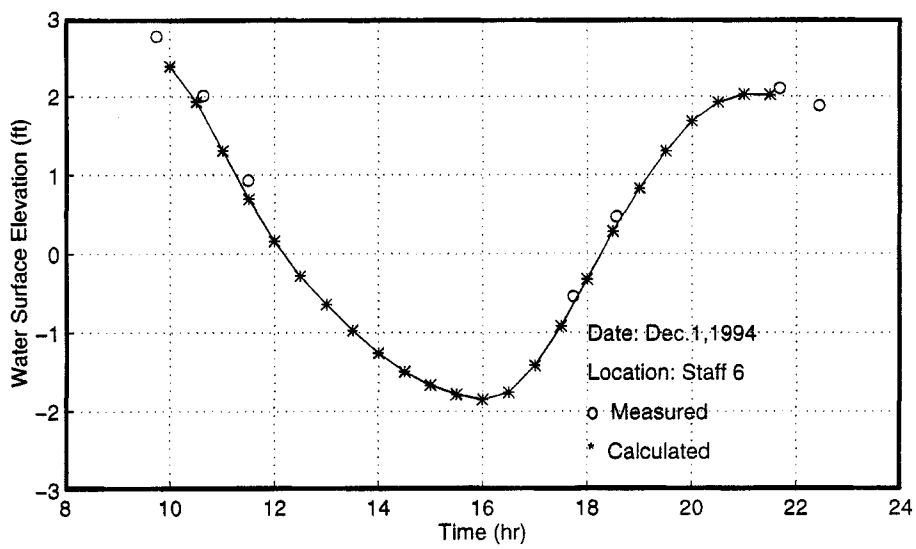

Figure 4.19: Comparision of Water Elevation at Staff 6.

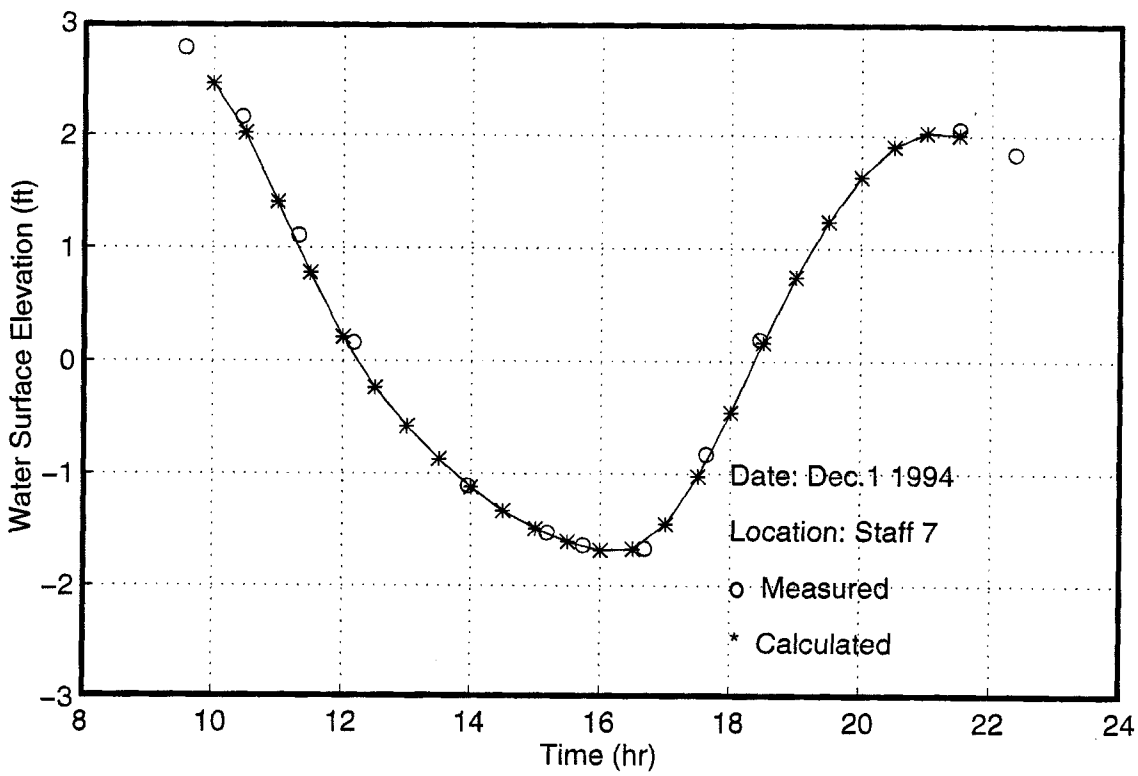

Figure 4.20: Comparision of Water Elevation at Staff 7.

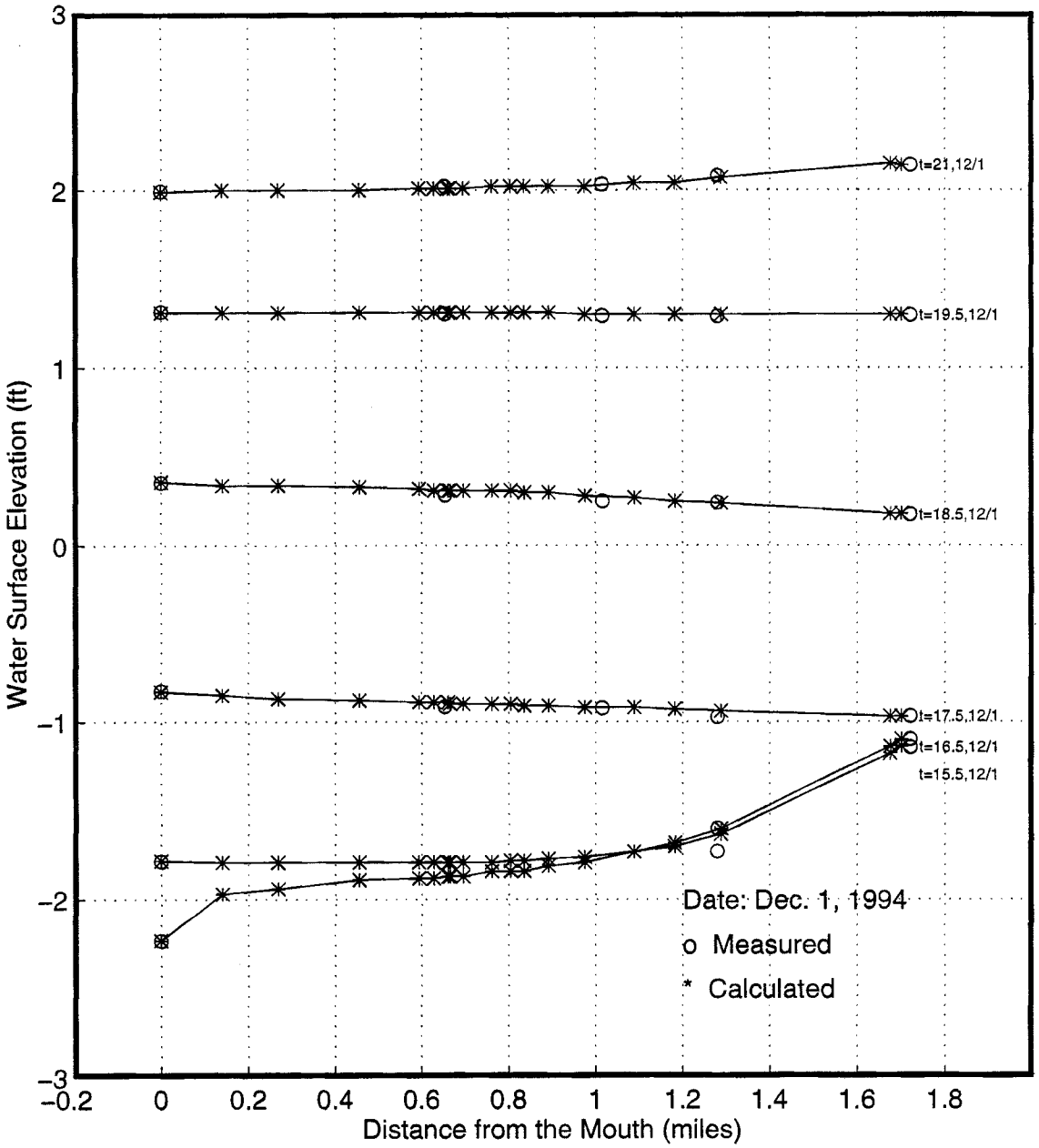

Figure 4.21: Comparision of Water Elevation Distribution During Flood Tide.

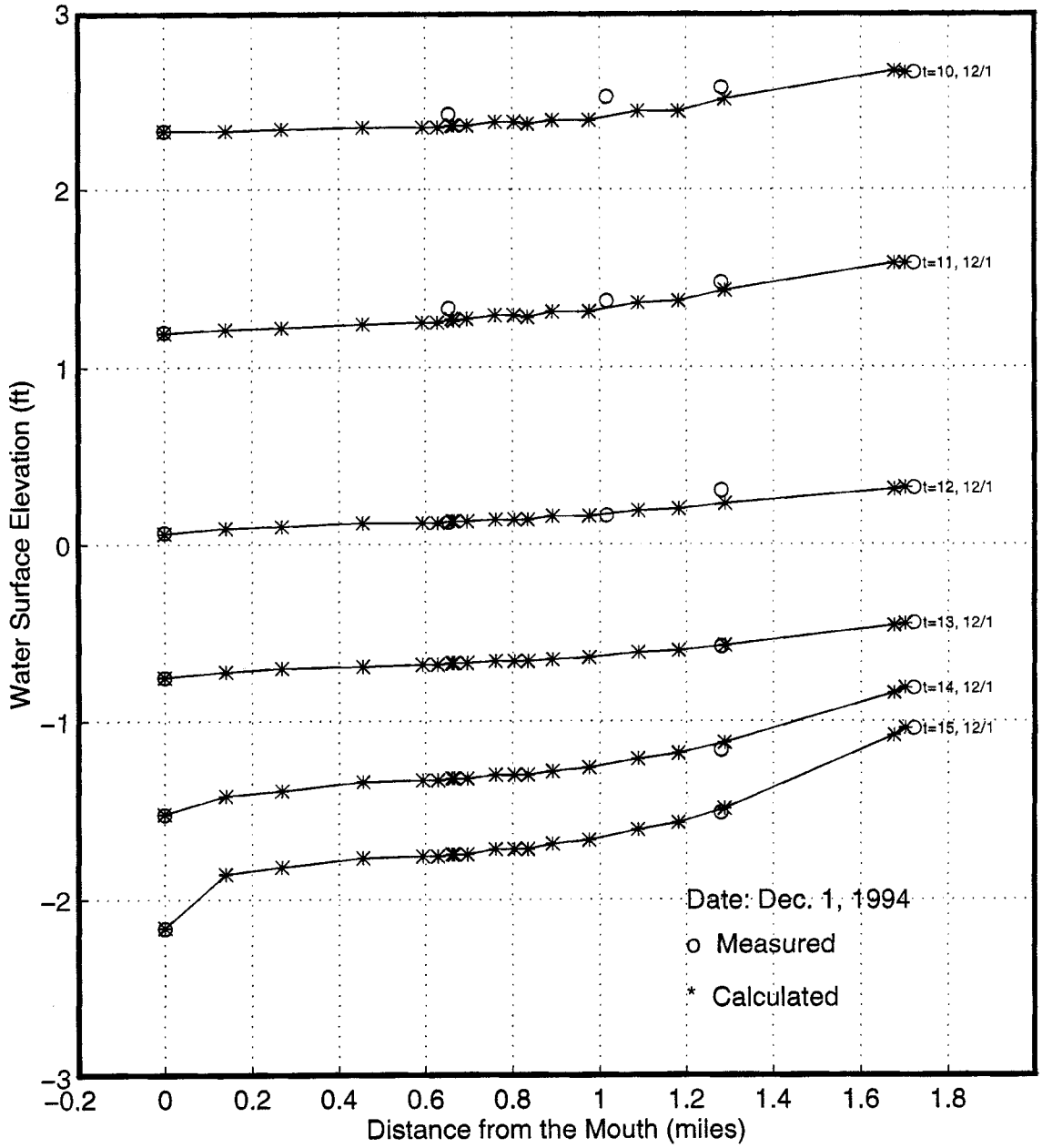

Figure 4.22: Comparision of Water Elevation Distribution During Ebb Tide.

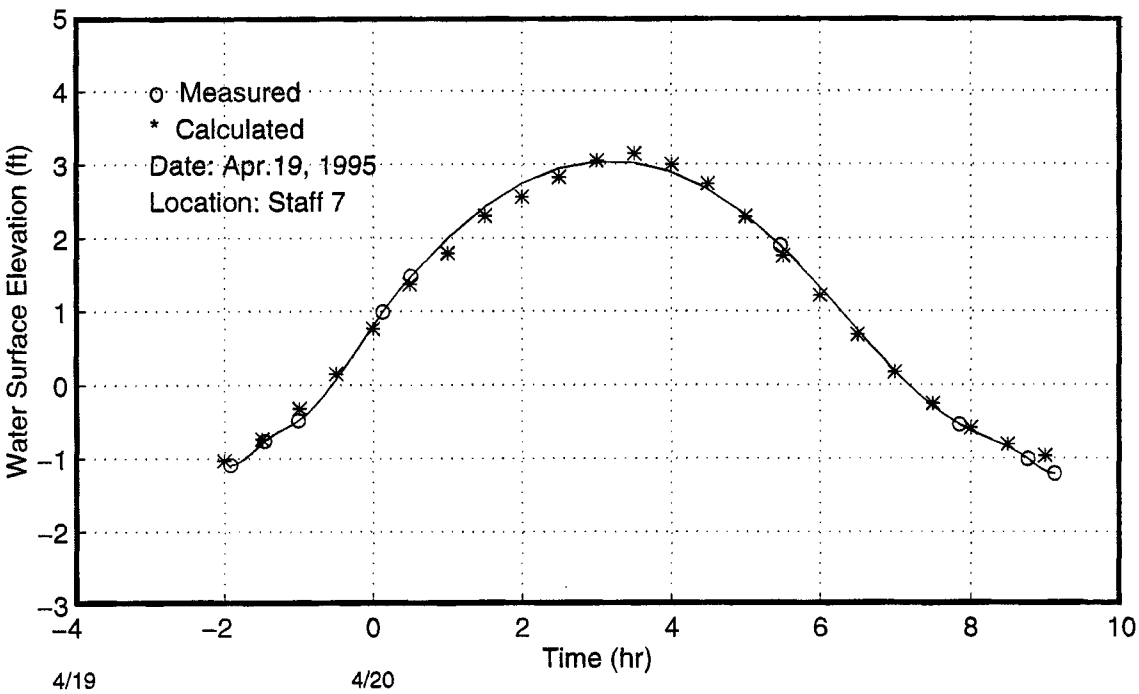

Figure 4.23: Comparision of Water Elevation at Staff 7.

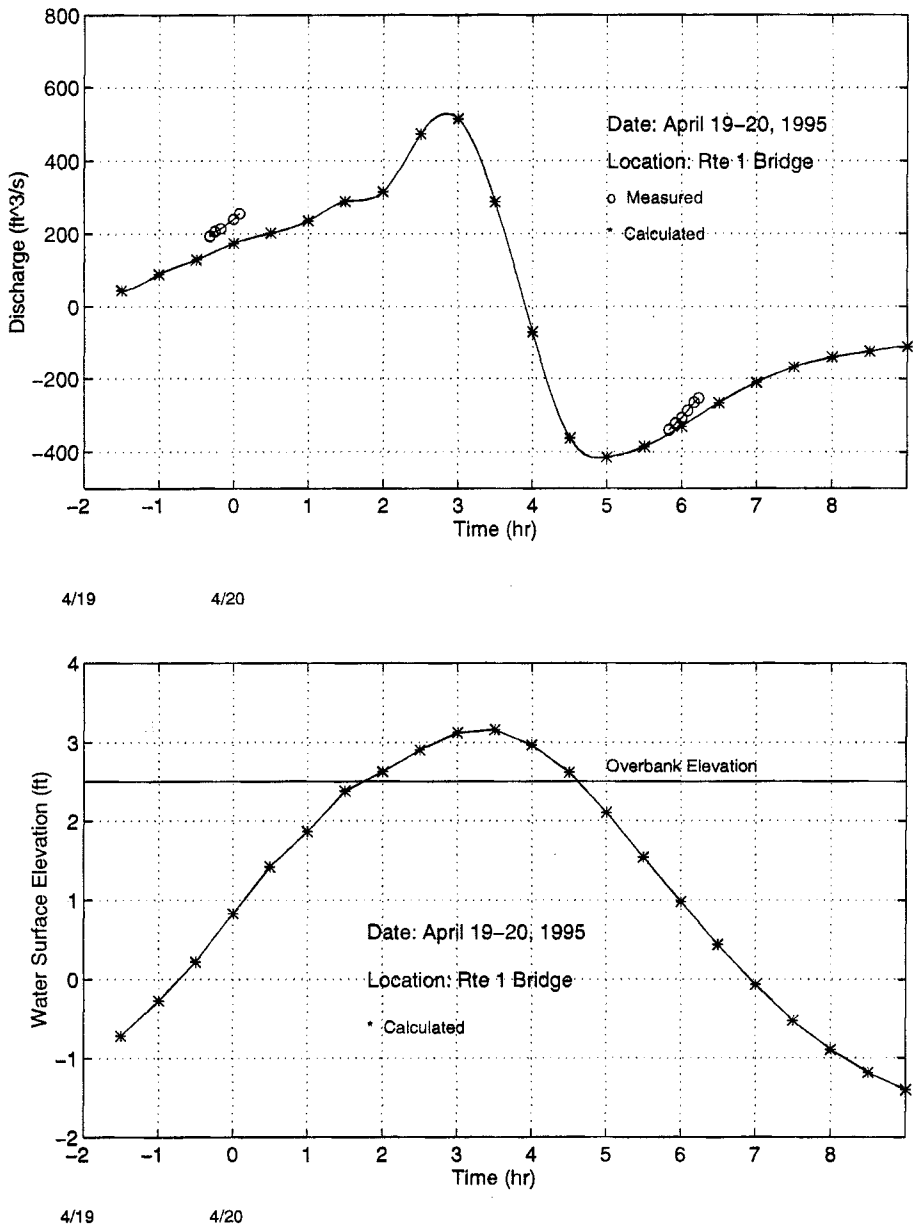

Figure 4.24: Comparision of Discharge and Water Elevation at Section 6.

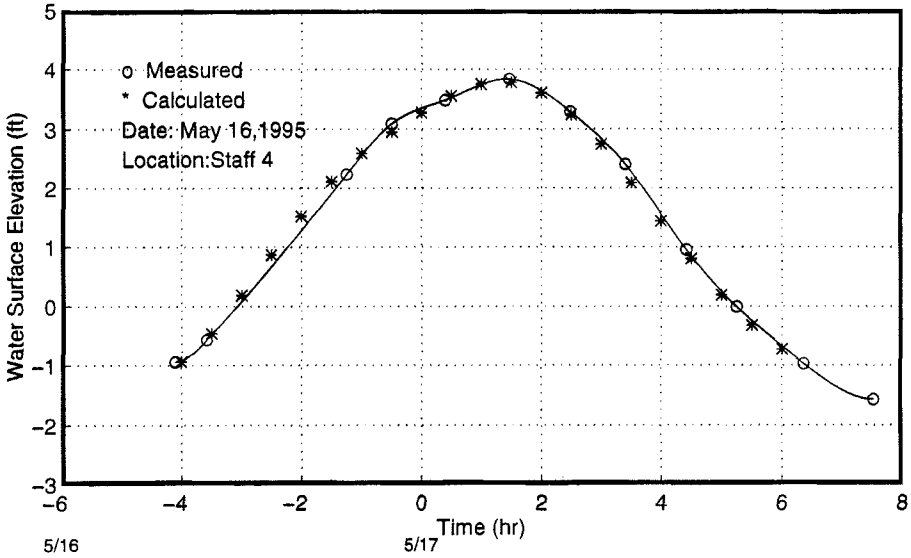

Figure 4.25: Comparision of Water Elevation at Staff 4.

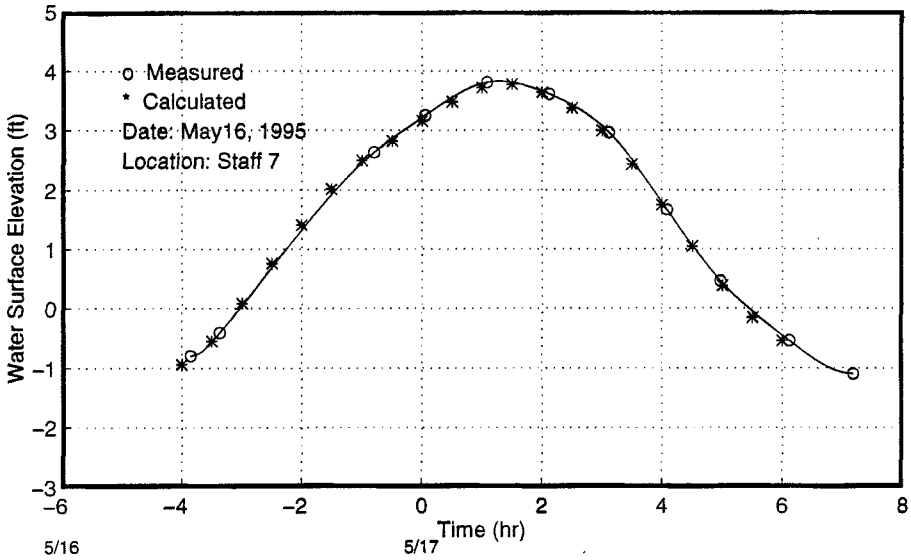

Figure 4.26: Comparision of Water Elevation at Staff 7.

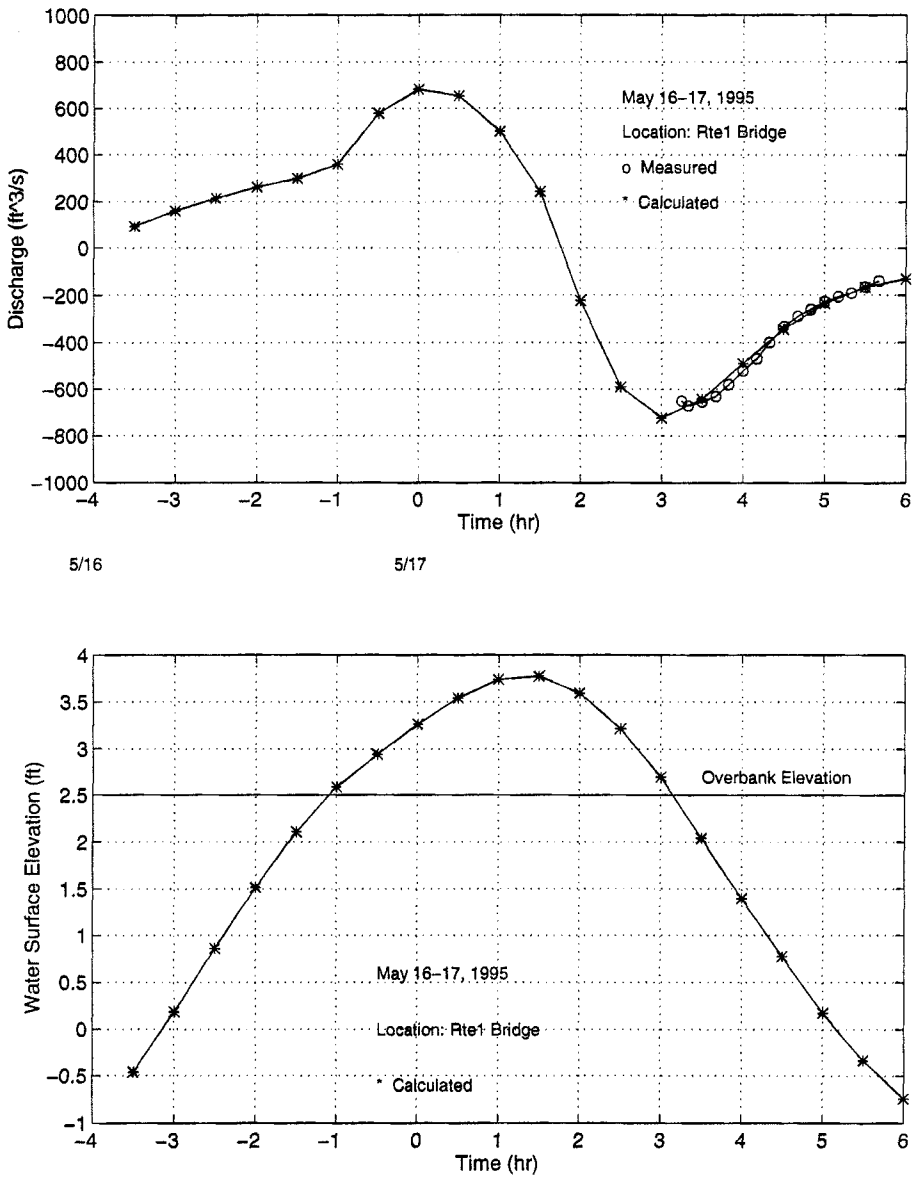

Figure 4.27: Comparision of Discharge and Water Elevation at Section 6.

5. Model Applications

The calibration and validation of the pseudo-2D hydrodynamic model have been carried out with field data obtained from the Oyster River as described in the preceeding sections. The model has performed reasonably well in view of the agreement between the calculated results and field data. In the following sections, further analyses of the model results from the Oyster River will be presented to indicate that the model can provide the essential hydrodynamic data and the two-dimentional flow field for a coastal river-marsh system. In addition, the results of an assessment of the impact of the U.S. Route 1 Bridge on the tidal flow will be carried out.

5.1 The Effect of Overbank Flow

The effect of overband flow on the Oyster River-Marsh system may be studied by model simulation using the water surface elevations observed at the mouth (Section 1) and at the railroad bridge (Section 20) as boundary conditions (see Figure 3.13) for the four runs listed in Table 3.2. Tidal stages and discharges were calculated for all sections at each time step throughout a tidal cycle. The first two runs had no overland flows. The last two runs had significant overland flow with a maximum depth in excess of 1.3 feet. Figure 5.1 shows the relationship between discharge and time of the four runs at the Route 1 Bridge. Since overband flow occurs only with high tidal amplitude at the mouth of the river, the maximum discharge is significantly larger than that without overband flow. An asymmetric behavior exists in the discharge during flood and ebb tides. In particular, the rapid rise in the discharge during flood

tide indicates that there is a sudden increase of flow area due to overland flow on the marsh; however, during ebb tide the recession is smooth.

A larger effect can be achieved with a simulation by blocking the overland flow with vertical walls at the banks of the main channel, and thus the flow of the Spring high tide of May 15-16 , 1995 can be confined within the main channel. Figures 5.2 and 5.3 show the calculated results at the Route 1 Bridge and the railroad bridge, respectively. The simulation was done by using the observed tidal stages at the mouth of the Oyster River in the fourth run (Table 3.2). In this case, a no-flow condition was imposed upstream of the railroad bridge by extending the computational domain as shown in Figure 3.13. There is practically no difference in the tidal amplitude throughout the tidal cycle at both locations. The asymmetric behavior of the discharge curves with overland flow is similar to that discussed in the previous example. Small time lags in stage and discharge are indicated at both locations, more at the railroad bridge than at the Route 1 Bridge. A significant reduction of discharge is evident when the flow is confined within the main channel. The time lags can be obtained from the enlarged plot of water surface elevations at the mouth of the river, the Route 1 Bridge, and the railroad bridge as shown in Figure 5.4. The marsh tends to increase the time lag both at the Route 1 Bridge and at the railroad bridge. The time lag at the railroad bridge is approximately 10 minutes in the Oyster River for the Spring high tide.

5.2 Tidal Flow in the Oyster River-Marsh System

The pseudo-2D hydrodynamic model can provide the two-dimensional flow field for

a coastal river-marsh system. The model calculates the water surface elevations, longitudinal velocity and transverse velocity at all nodal points along the main channel and over the marsh at each time step. Therefore, the results can provide local depths of submergence and velocity over the marsh, the propagation of flood front over the marsh during flood tide and receding water surface during ebb tide, and the interchange of the water between the main channel and the marsh. An analysis of the calculated results for Spring high tide of May 15-16, 1995 at the railroad bridge at the Oyster River is presented in Figures 5.5 through 5.13.

(a) Overland Flow

In Figure 5.5, the water surface elevation or the depth distributions over a section of marsh on the western side of the channel at every half hour are shown for flood tide and ebb tide periods. At the beginning of the flood tide, a flood front propagates toward the outer boundary of the marsh. It indicates that in this marsh the entire marsh surface will be covered by water within a period of much less than 0.5 hour. Due to the no-flow condition imposed on the outer boundary, the water surface rises rapidly, which was observed previously in the discharge curve in Figure 5.1(d). A receding front is absent during the ebb tide, however, and the water surface will decrease slowly over the marsh. When the water surface drops below the critical depth at the edge of the bank, it creates a control section there, and the overland flow is now treated as lateral inflow into the main channel. This condition may persist long after this time, until the marsh surface becomes dry.

The transverse propagation of tidal fronts over the marsh is depicted in Figure 5.6 at three time stepsuntil the whole marsh was flooded. The velocity distributions during the flood and ebb tides are shown in Figures 5.7 and 5.8, respectively. The velocity vectors are derived from the longitudinal and transverse velocities at the nodal points.

(b) Water Interchange Between Main Channel and Marsh

The transverse flow rate, velocity and water depth at the same junction between the western overbank and the main channel during the Spring tide is plotted in Figure 5.9 for the overland flow period. The Q-T plot indicates that the volumes of inflow and outflow are nearly equal because detention, evaporation and seepage are not accounted for in the model. The drainage velocity is substantially higher than the flooding velocity, indicating a strong tidal flushing on the marsh. This asymmetrical behavior may have some implication for salinity and nutrient transport between the main channel and the marsh for a substantial part of the tidal cycle.

(c) Transverse Velocity and Longitudinal Velocity Over the Marsh

The distributions of longitudinal and transverse velocity over the same western marsh area throughout the tidal cycle are shown in Figure 5.10. The transverse velocity is almost the same order of magnitude as that of the longitudinal velocity, which indicates divergent angles of the stream-lines as water spreads over the marsh.

(d) Comparison of Longitudinal Velocity in Main Channel and Marsh

A comparison of the longitudinal velocity at maximum discharge during flood and ebb

tides between the main channel and the marsh is shown in Figure 5.11. The magnitude of velocity indicates that the tidal flow in the Oyster River system is dominated by longitudinal flow in the main channel. However, the magnitude of transverse velocity shown in both Figures 5.10 and 5.11 implies the two-dimensional characteristics of tidal flow over the marsh. Similar characteristics are exhibited in Figures 5.12 and 5.13 for flow rate and cross sectional area.

5.3 The Effect of Bridge Crossings

There are two bridge crossings on the Oyster River. The railroad bridge at the upstream end of the river is located at the north boundary of the major portion of the marsh under study; therefore, it has little effect on the system (see Figure 3.3). The U.S. Route 1 Bridge crosses at the mid reach of the river and is located so to divide the marsh into halves. The present bridge was constructed in 1970 with a major modification of the channel configuration by cutting off a bend of the river, and both the present and former crossing configuration will be used in the study in the following sections.

(a) The Effect of the Route 1 Bridge on the Modified Channel

The bridge and abutment were removed in this study. This is a single-span bridge of 82.66 feet. The effect on the tidal flow is primarily due to the west abutment, which extends into the modified channel about 200 feet, while the east abument is more or less in alignment with the bank. Comparisons of the tidal flow for the spring tide of May 19-20, 1995 are given in Figures 5.14-5.16. There is no measurable effect on the

local tidal stage at the bridge and water surface profiles during flood and ebb tide, and only a small increase in the magnitude if the peak discharges at the abutment are removed. These results are expected because the extrusion of the south abutment is small.

(b) The Effect of Reduced Bridge Opening

In order to show the sensitivity of the bridge opening, the existing opening was reduced by one half. The comparison of water surface profiles is shown in Figure 5.17 for the spring tide of 1995 during peak flows of flood and ebb tides. There is little effect downstream of the bridge; however, the effect on the upstream tidal stage is significant, with a nearly 0.3 feet drop in the water surface elevation downstream of the bridge during ebb tide. The effect is even more pronounced when the forcing tidal amplitude is increased as shown in Figures 5.18 and 5.19.

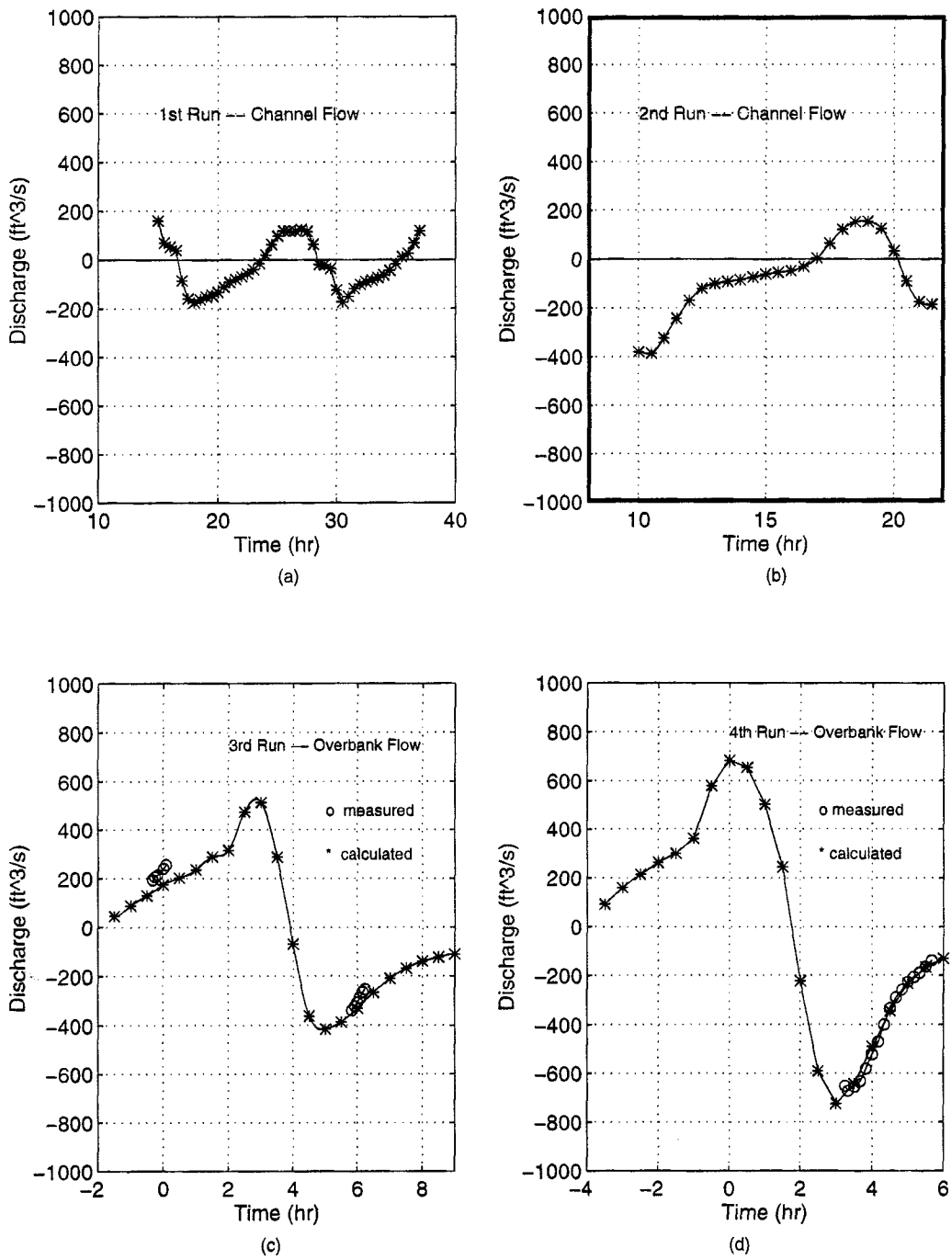

Figure 5.1: Q-T Relation at Rte. 1 Bridge (Section 6).

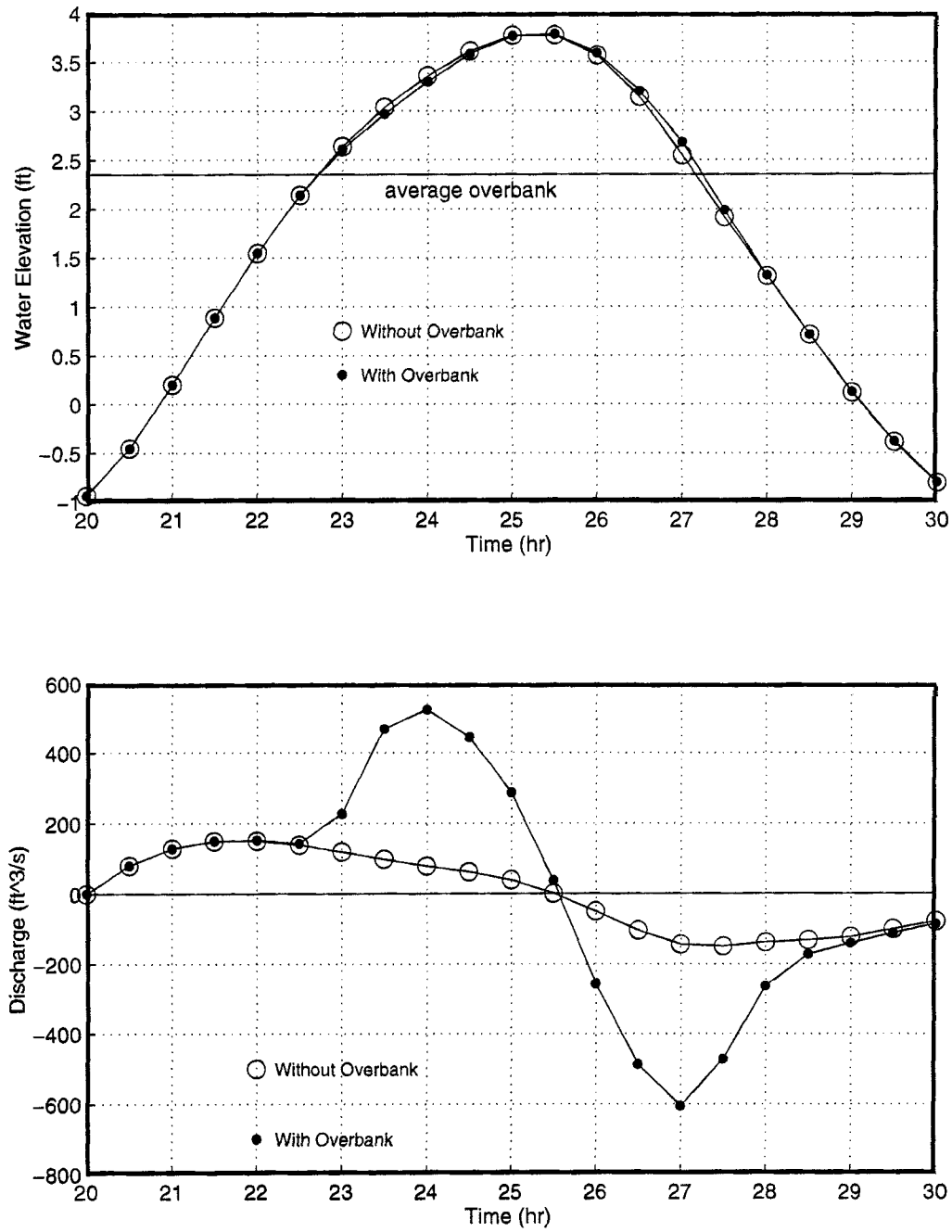

Figure 5.2: Water Surface Elevation and Discharge at Rte. 1 Bridge (Section 6).

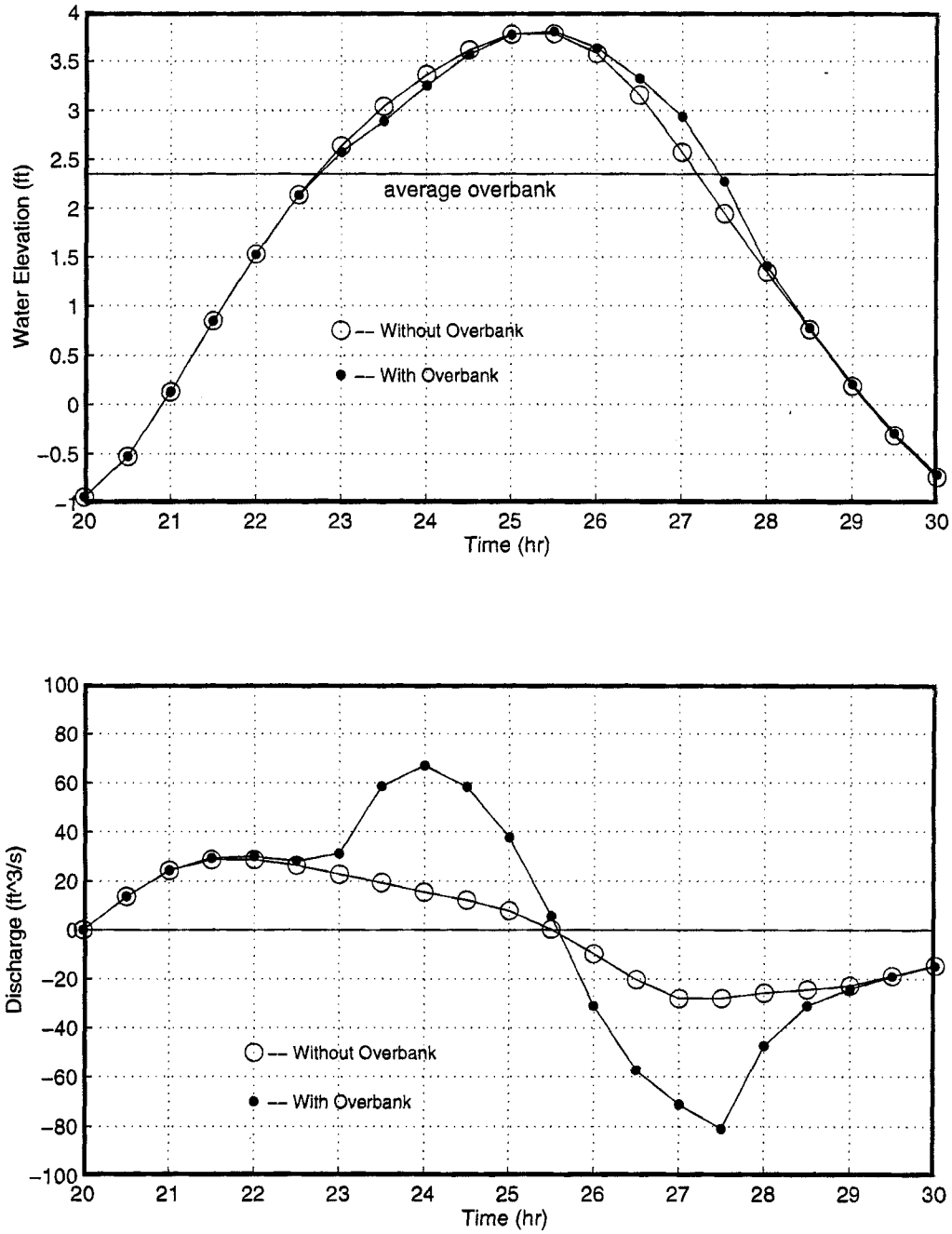

Figure 5.3: Water Surface Elevation and Discharge at R.R. Bridge (Section 20).

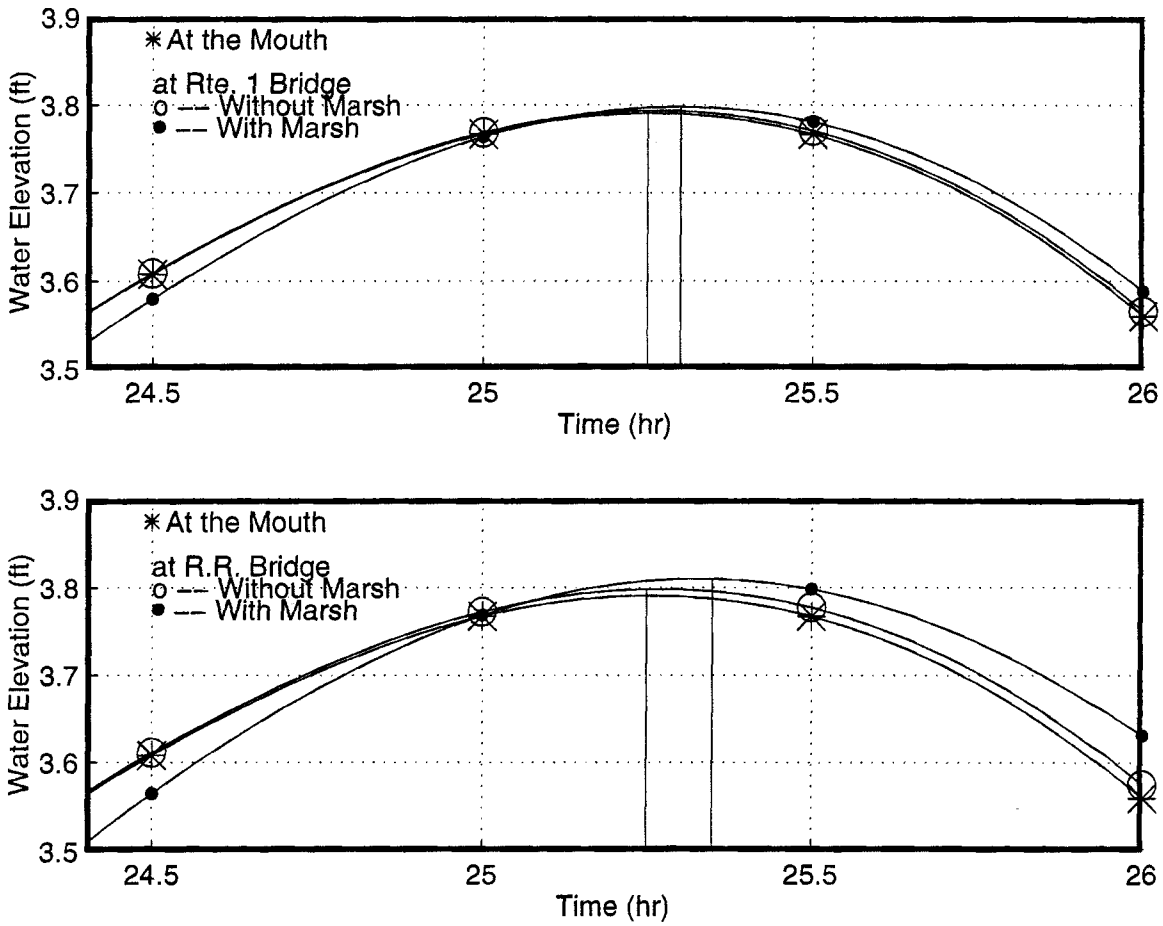

Figure 5.4: Time Lag Analysis.

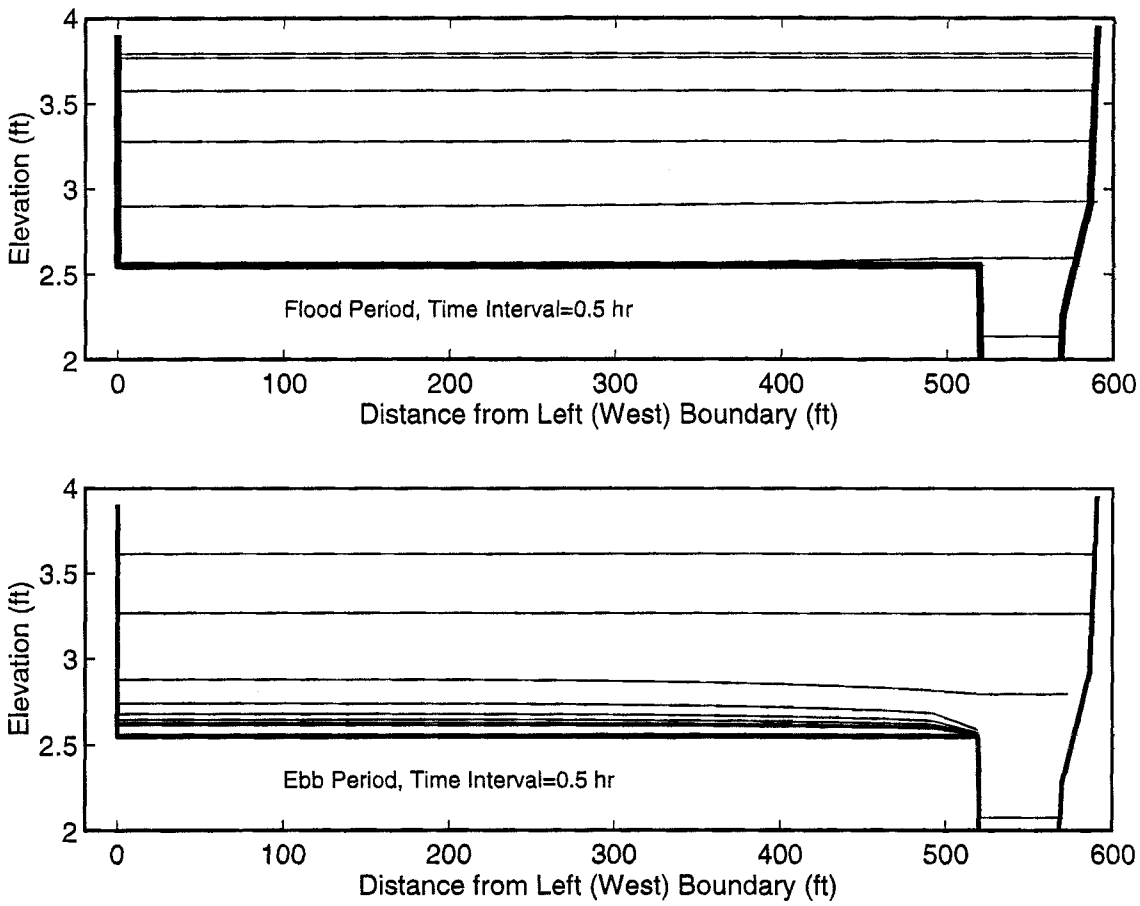

Figure 5.5: Transverse Propagation of Water Surface at Section 14.

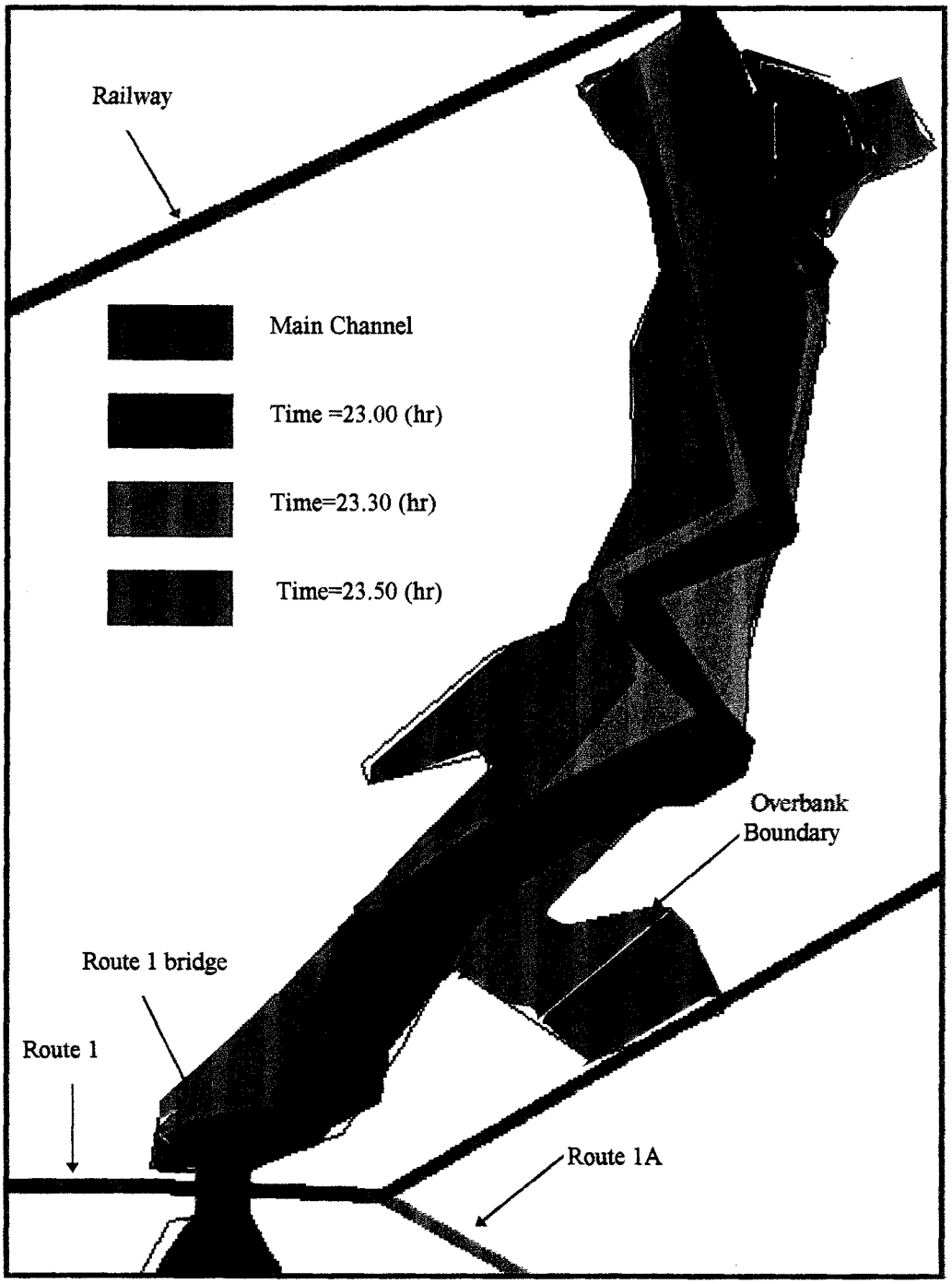

Figure 5.6: Transverse Propagation of Tidal Fronts Over the Marsh.

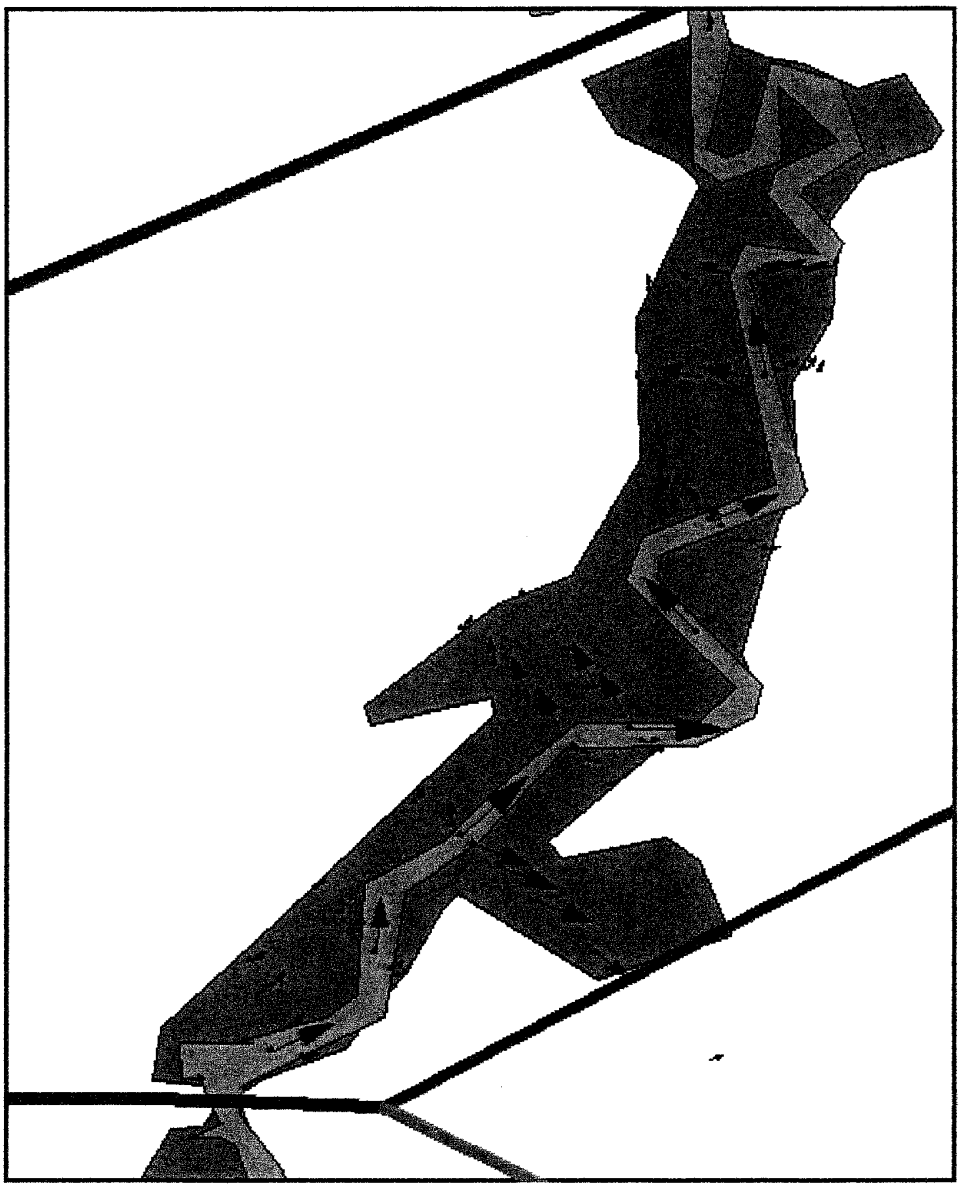

Figure 5.7: Velocity Distribution During Flood Tide Over the Marsh.

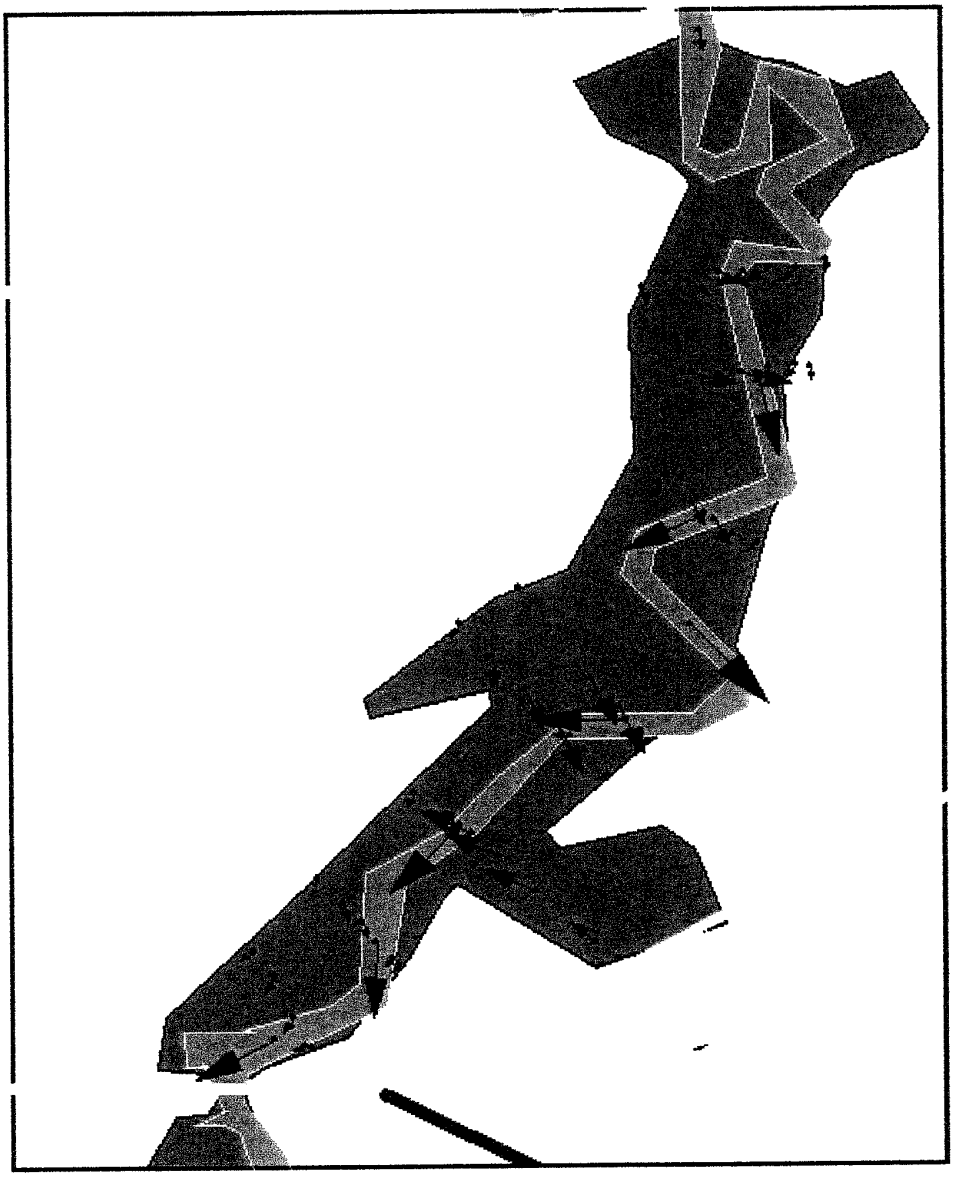

Figure 5.8: Velocity Distribution During Ebb Tide Over the Marsh.

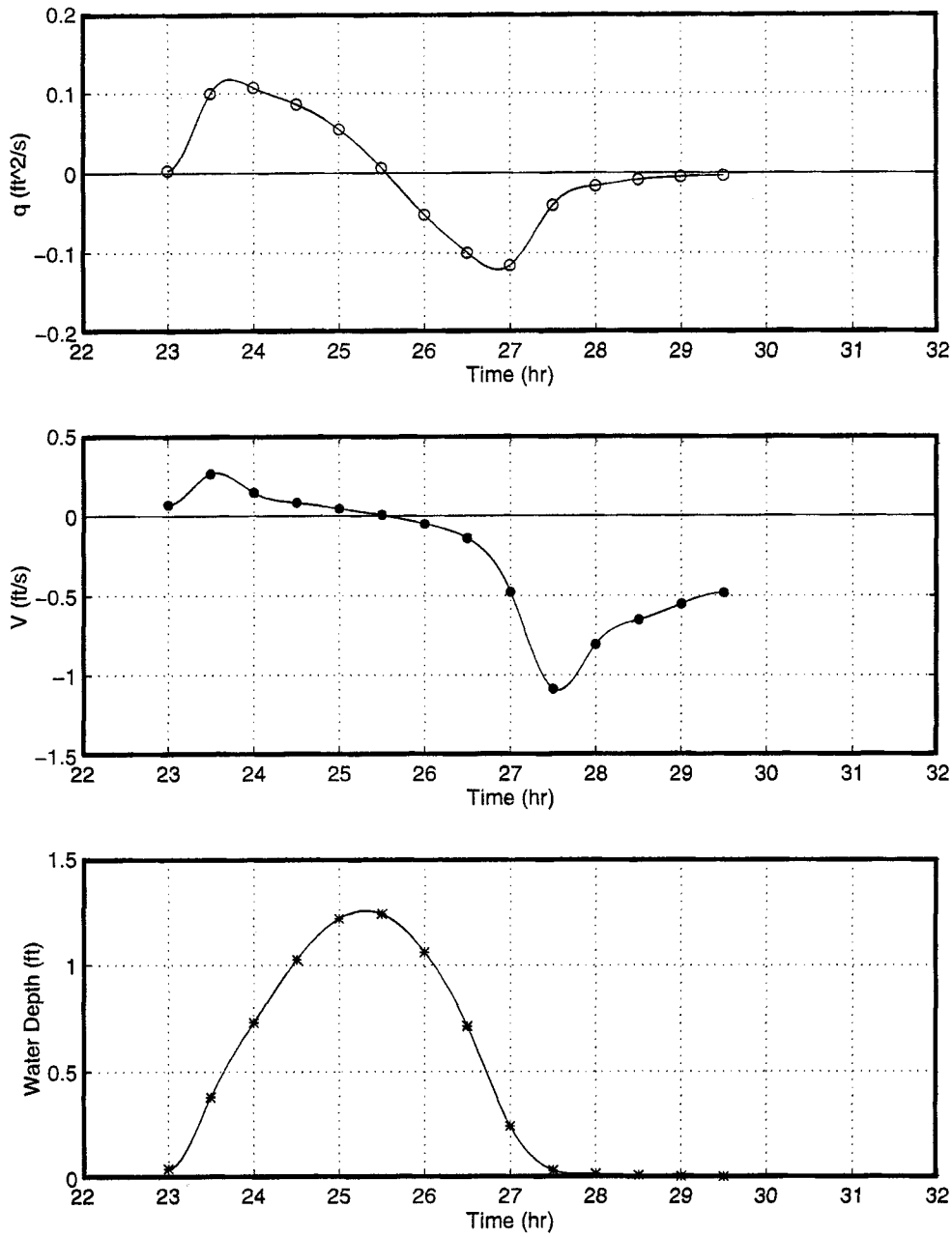

Figure 5.9: Water Exchange between Main Channel and Left Marsh at Section 14.

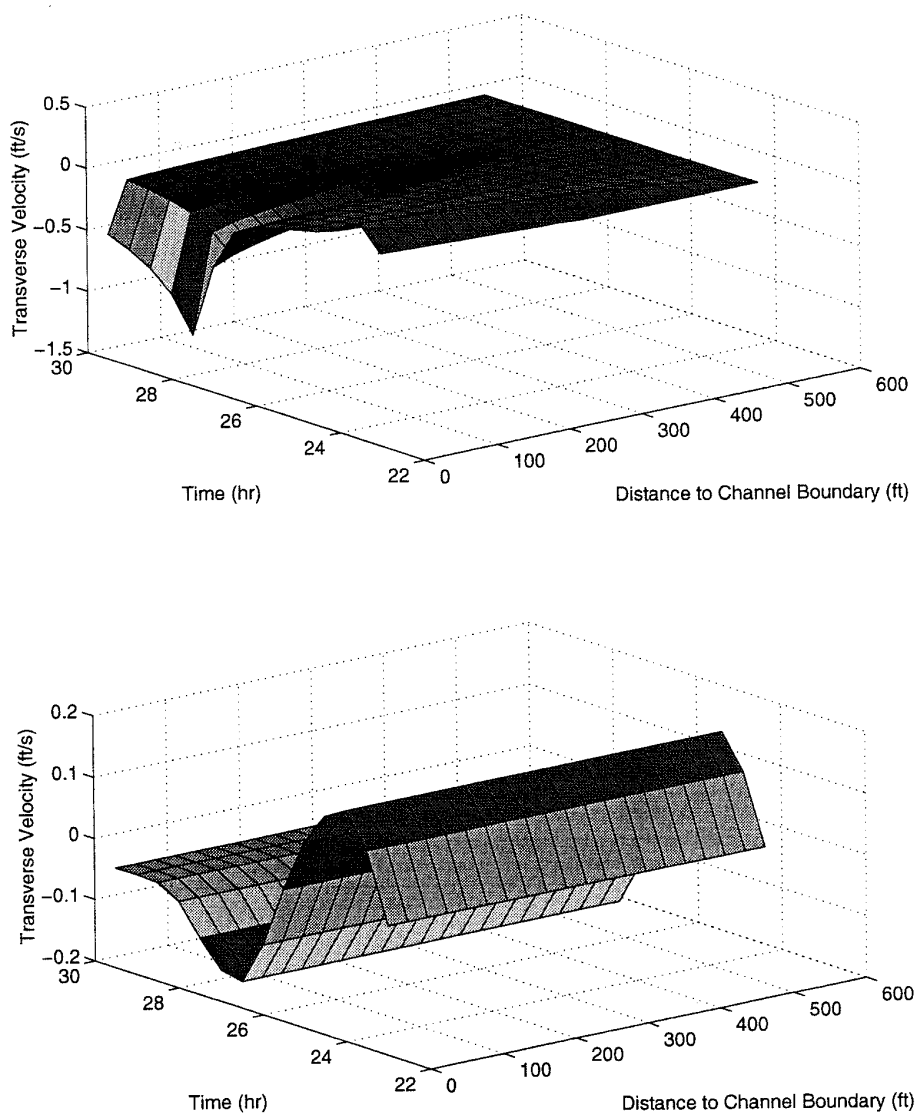

Figure 5.10: Comparison of Longitudinal and Transverse Velocity at Left Marsh at Section 14.

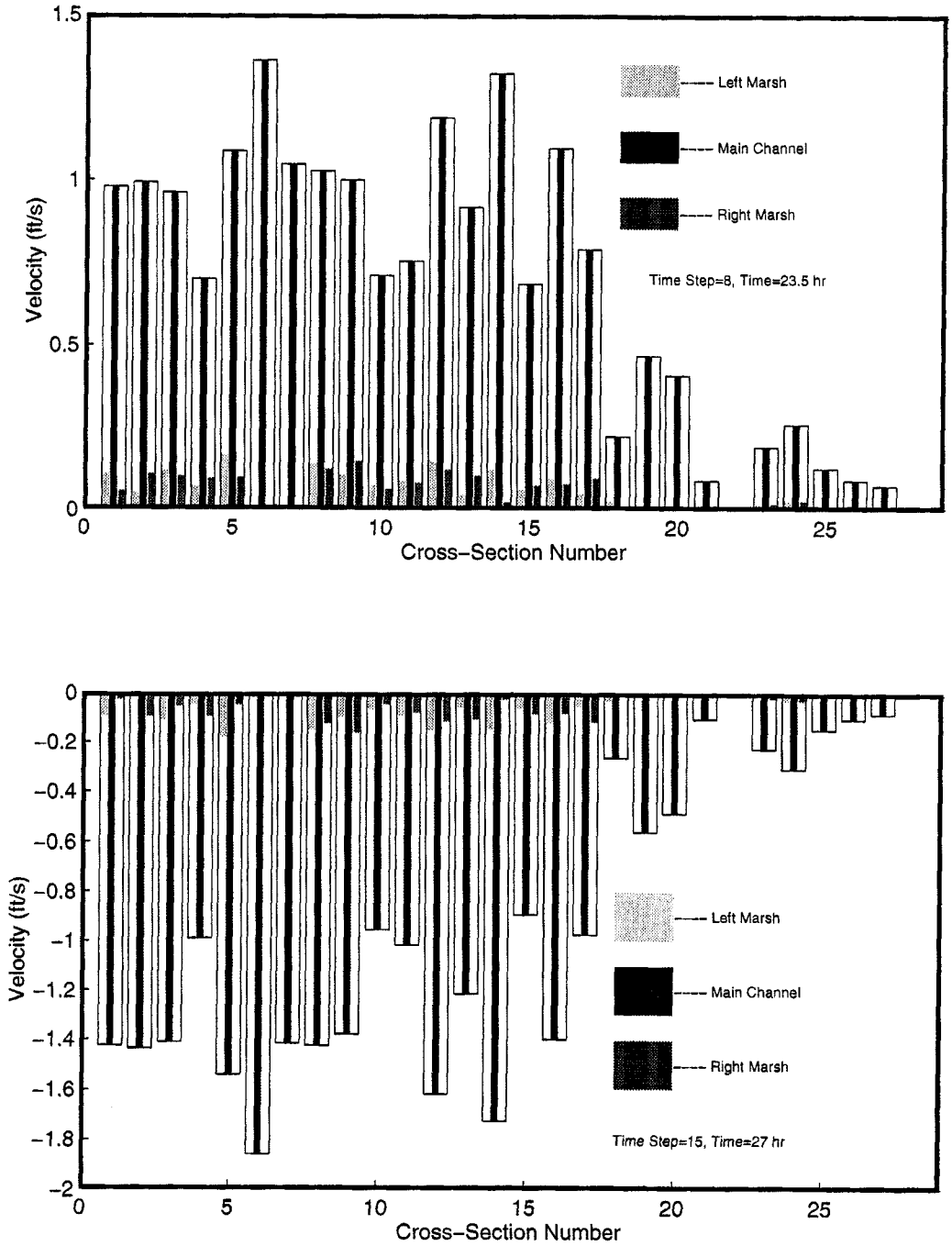

Figure 5.11: Comparision of Longitudinal Velocity in Main Channel and Overbank Region.

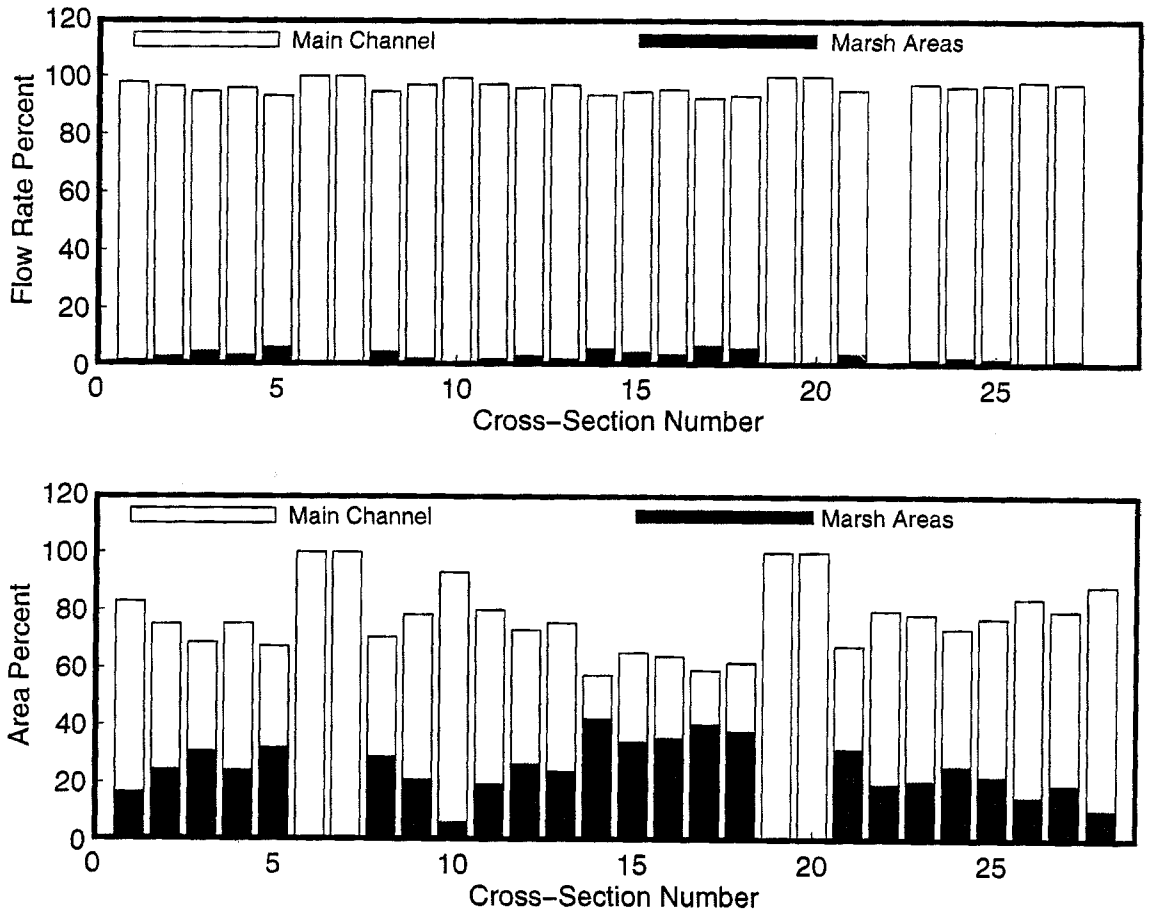

Figure 5.12: Comparision of Discharge in Main Channel and Overbank Region.

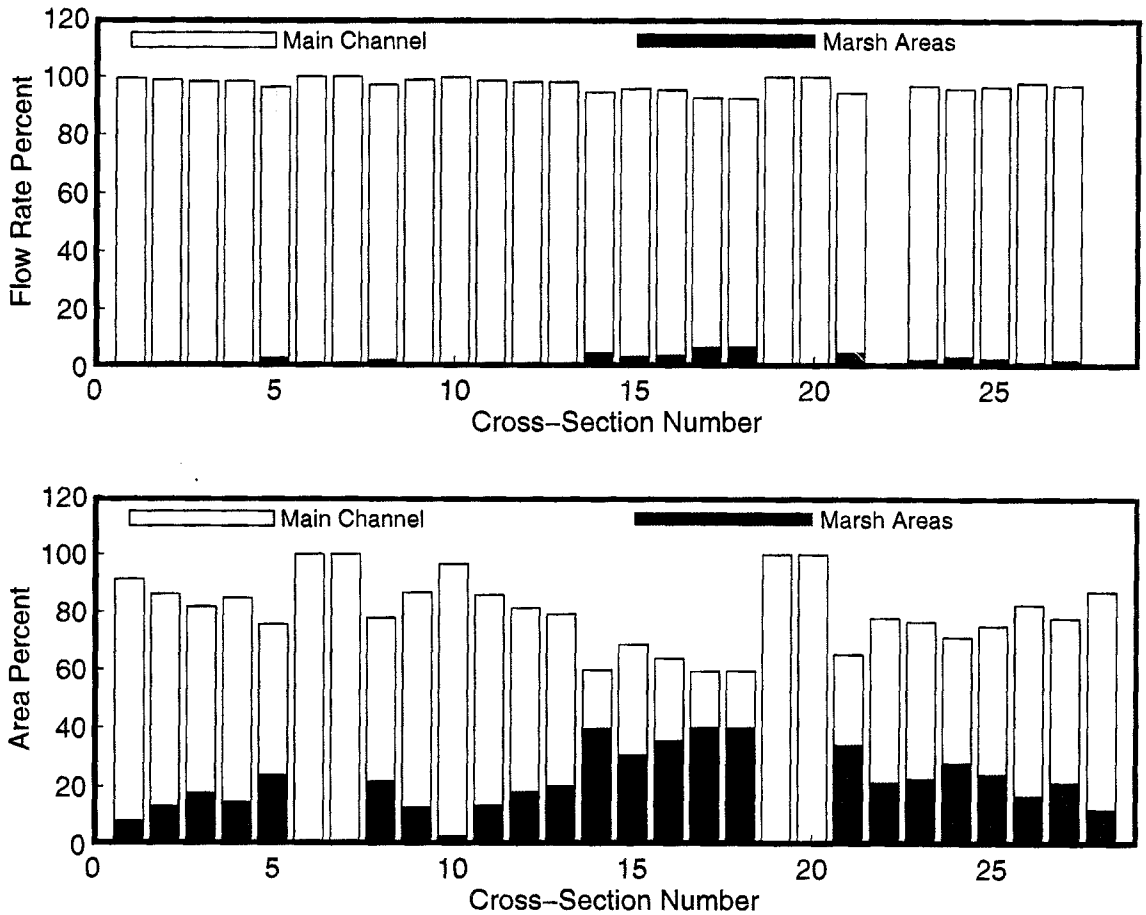

Figure 5.13: Comparision of Discharge in Main Channel and Overbank Region.

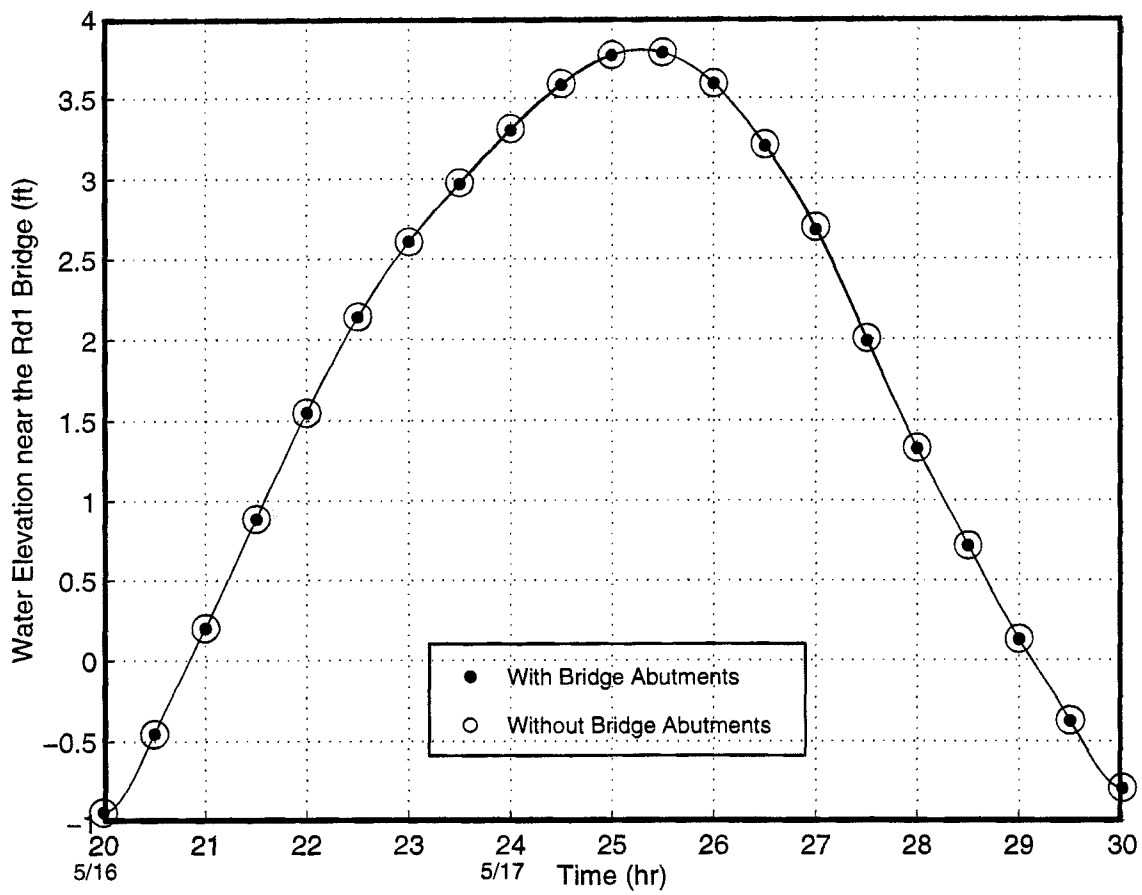

Figure 5.14: Comparison of Water Elevations at Rte 1 Bridge (Section 6).

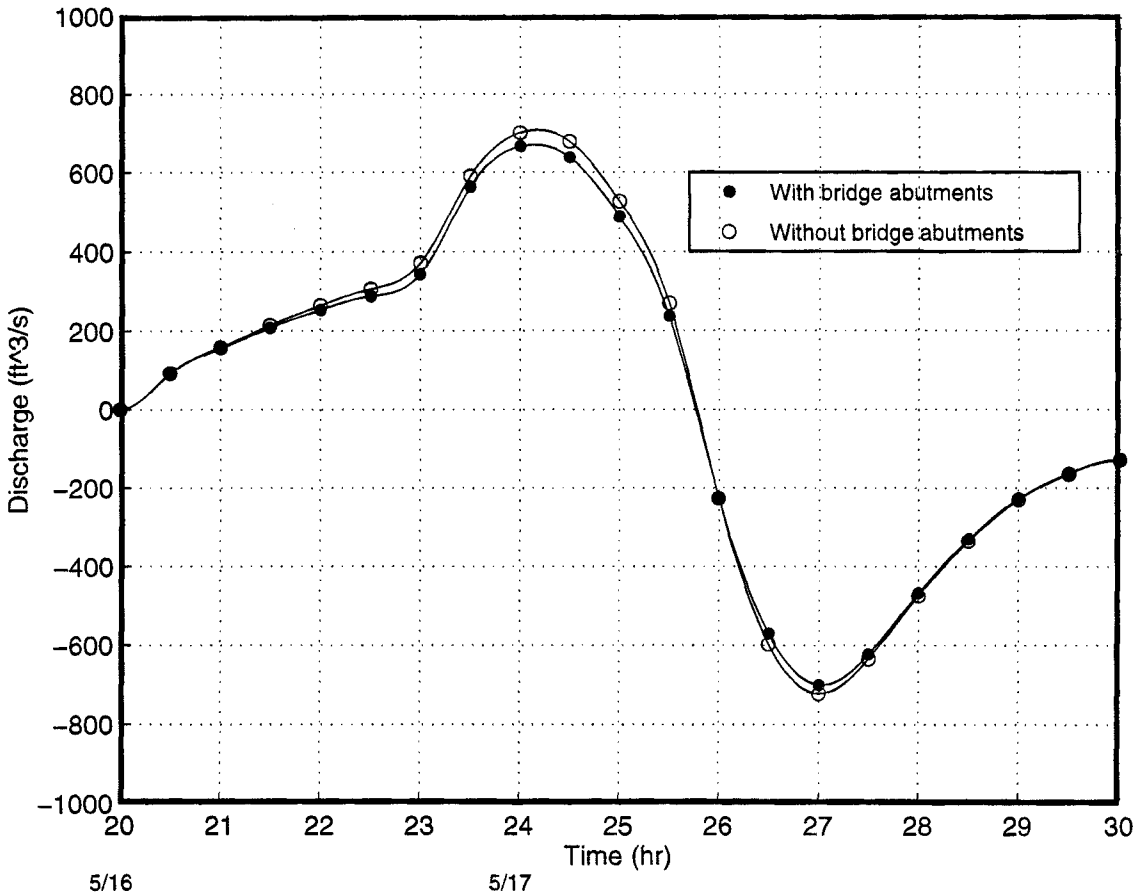

Figure 5.15: Comparison of Discharge at Rte 1 Bridge (Section 6).

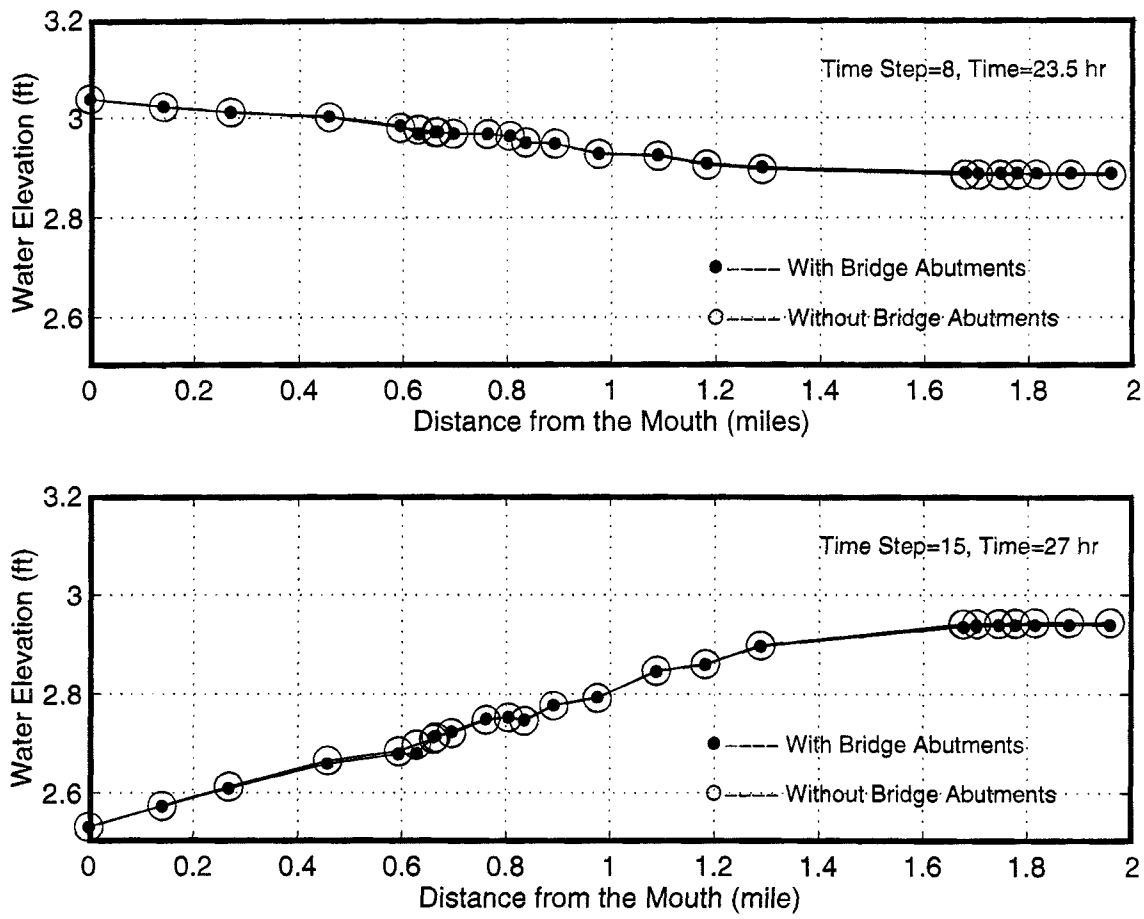

Figure 5.16: Comparison of Longitudinal Water Elevation Distributions.

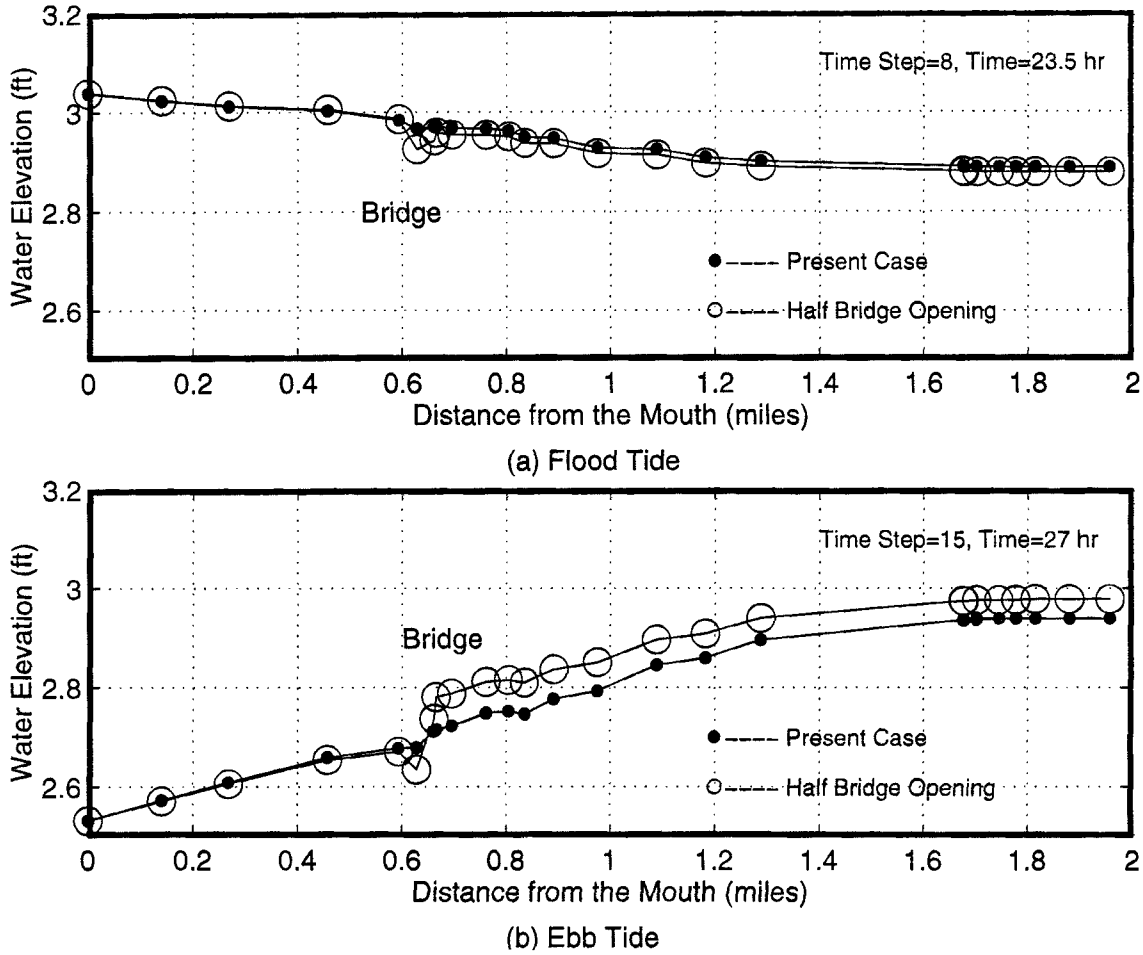

Figure 5.17: Influence of Bridge Opening on Tidal Flow.

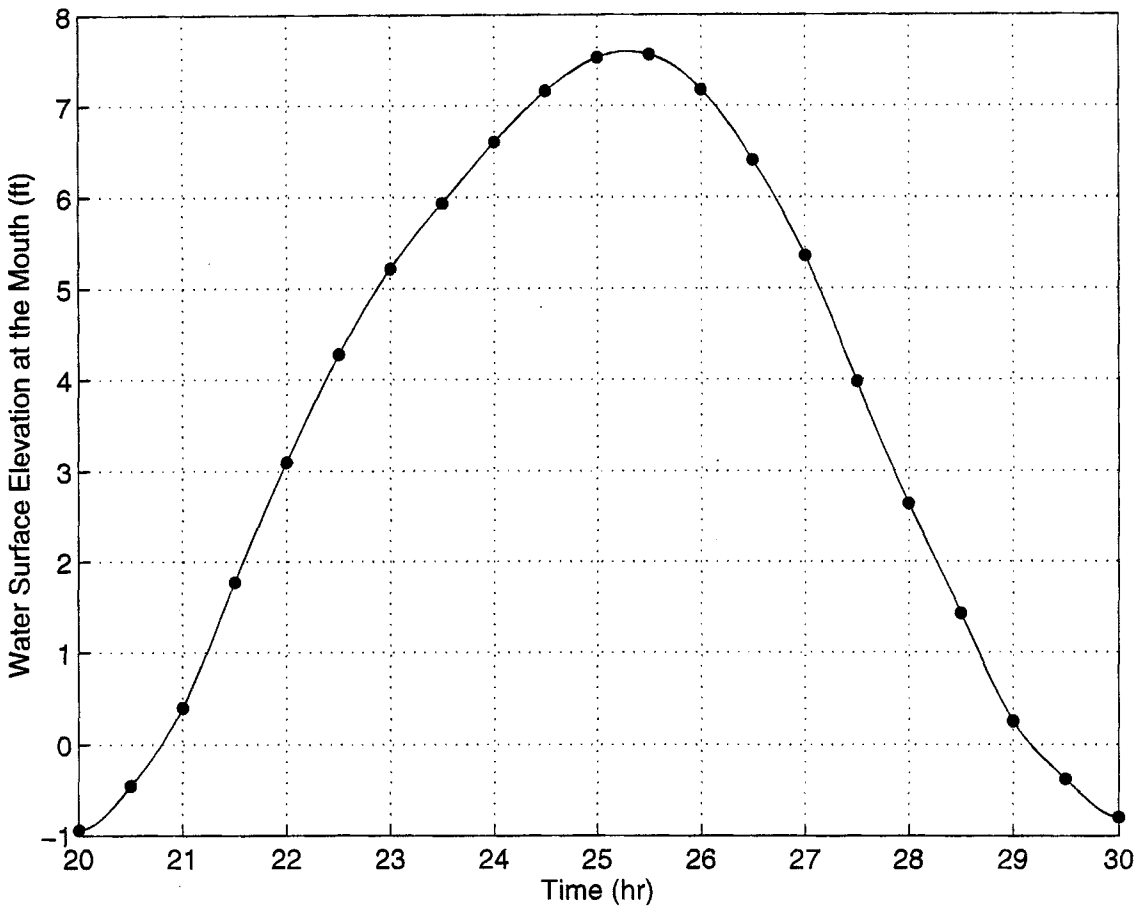

Figure 5.18: Water Surface Elevation Near the River Mouth for the Spring High Tide in 1995.

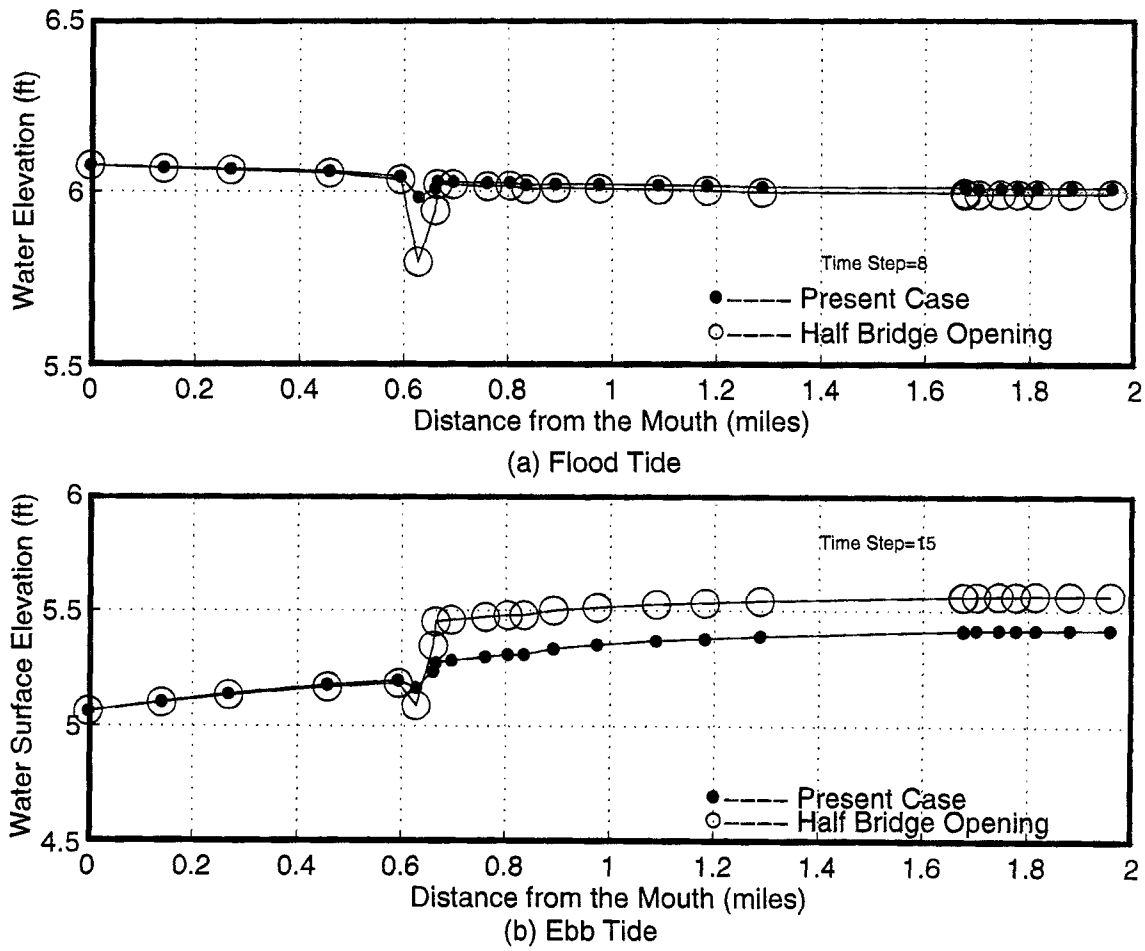

Figure 5.19: Influence of Bridge on Tidal Flow.

5.4 The Impact of the U.S. Route 1 Bridge

The model was applied to studying the impact of the construction of the present U.S. Rte. 1 Bridge in 1970-1972 on tidal flushing in the Oyster River-Marsh system. That construction involved a realignment of the river channel near the previous bridge (constructed in 1935) and an increase in the span of the bridge, as shown in Figure 5.20.

A comparison of the flow regimes in the Oyster River-Marsh system before and after construction of the present Rte. 1 Bridge has been made. Calculations were carried out under the same bounbary conditions of the spring high tides of May 15-16, 1995 as described previously. It is assumed that the construction of the present bridge Rte. 1 Bridge only caused the topographic changes between Sections 6 and 8, which have been estimated according to the 1970's construction plan as shown in Figure 5.20, while the present cross sections given in Appendix A were used for all other sections. Figures 5.21-5.23 show previous cross sections 6, 7, and 8. The same transition loss coefficient was used for both cases, since the numerical tests have shown that a five-fold change of transition loss coefficient (0.1-0.5) plays little role in the calculated results.

The longitudinal water level elevations along the river at different times of the tidal cycle are compared in Figures 5.24-5.27. There are practically no changes between the mouth of the river and the bridge. Because the 1972 bridge was widened and the river reach between Sections 5-9 straightened, water flows more smoothly through

the present bridge. Although changes upstream of the bridge are small, the 1972 bridge does provide a smooth transition in the vincinity of the bridge and improve tidal flushing of the marsh. From Figures 5.28 and 5.29, which compare both water levels and flow rates at Section 6, the Rte. 1 Bridge, and Section 16, near the Railroad Bridge, respectively, it is found that the maximum differences for water level and flow rate at these two sections are approximately 0.25 ft and $25 ft^3/s$, respectively for either the flood or the ebb period. Figures 5.31 and 5.32 also indicate the improvement of tidal flow rate over the whole tidal cycle throughout the marsh.

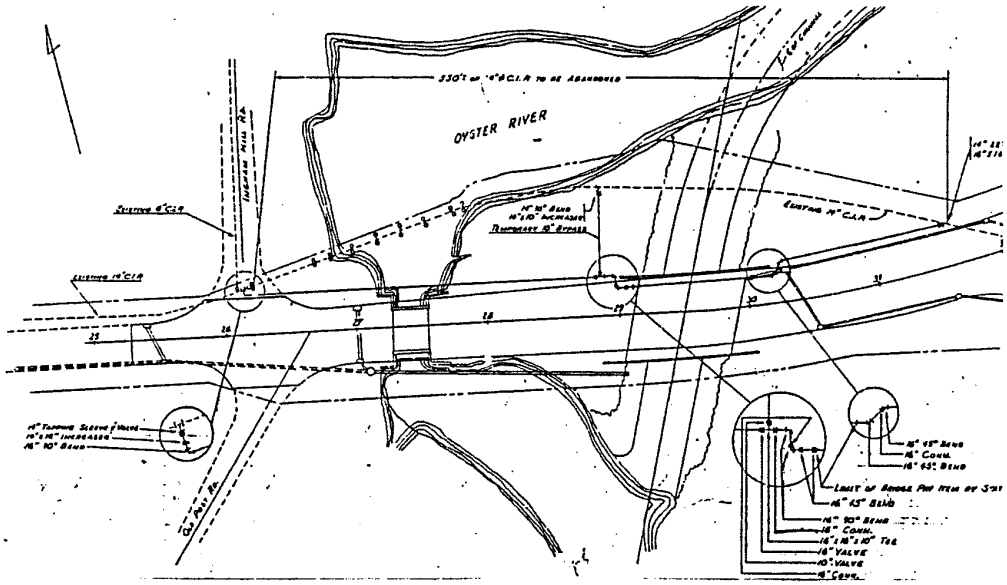

Figure 5.20: 1935 and 1972 Sites of U.S. Rte. 1 Bridge.

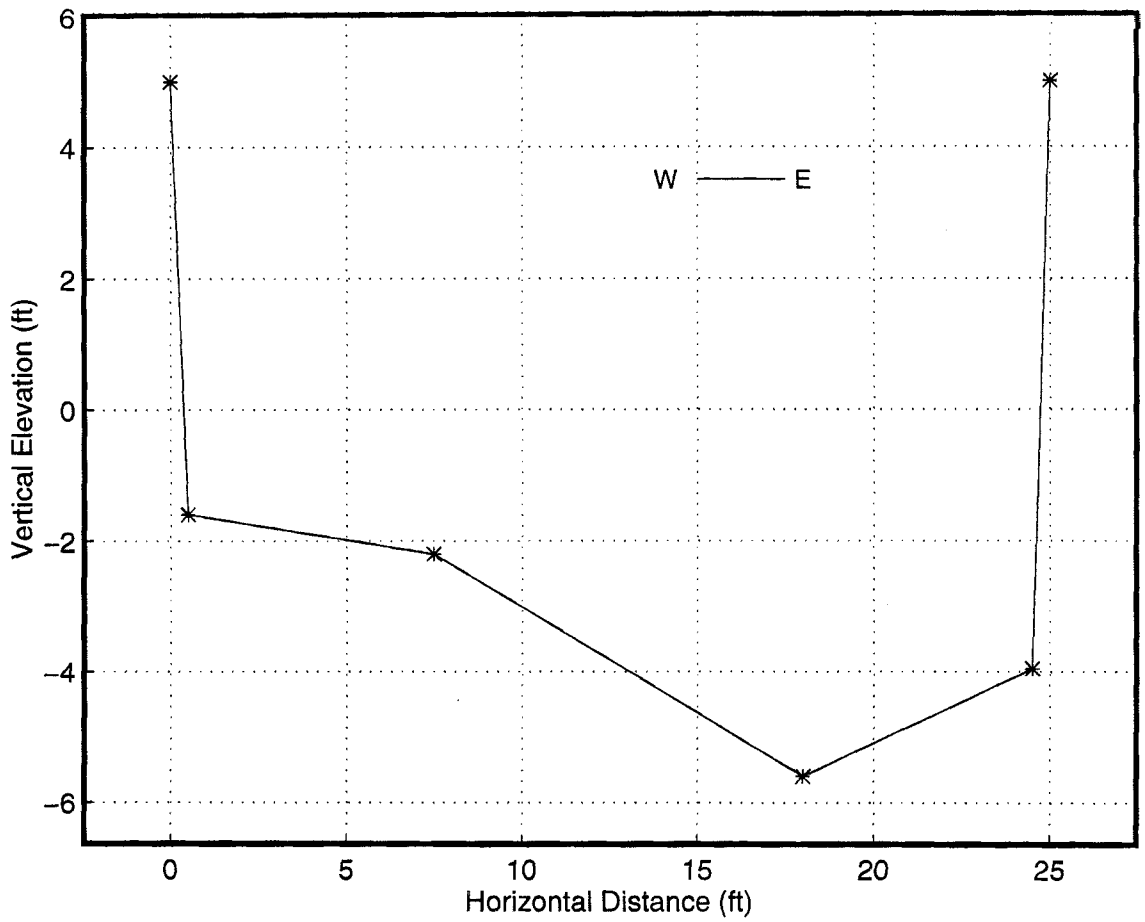

Figure 5.21: Previous Cross Section 6.

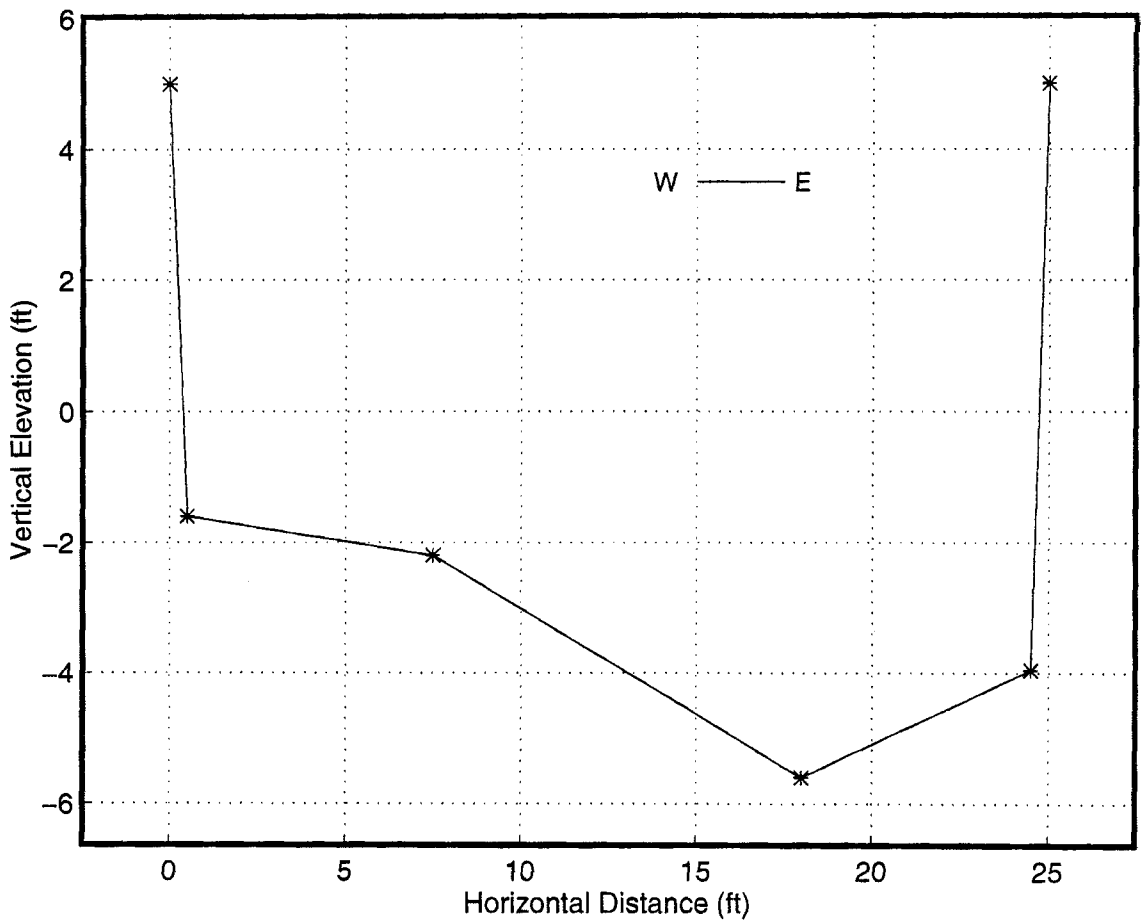

Figure 5.22: Previous Cross Section 7.

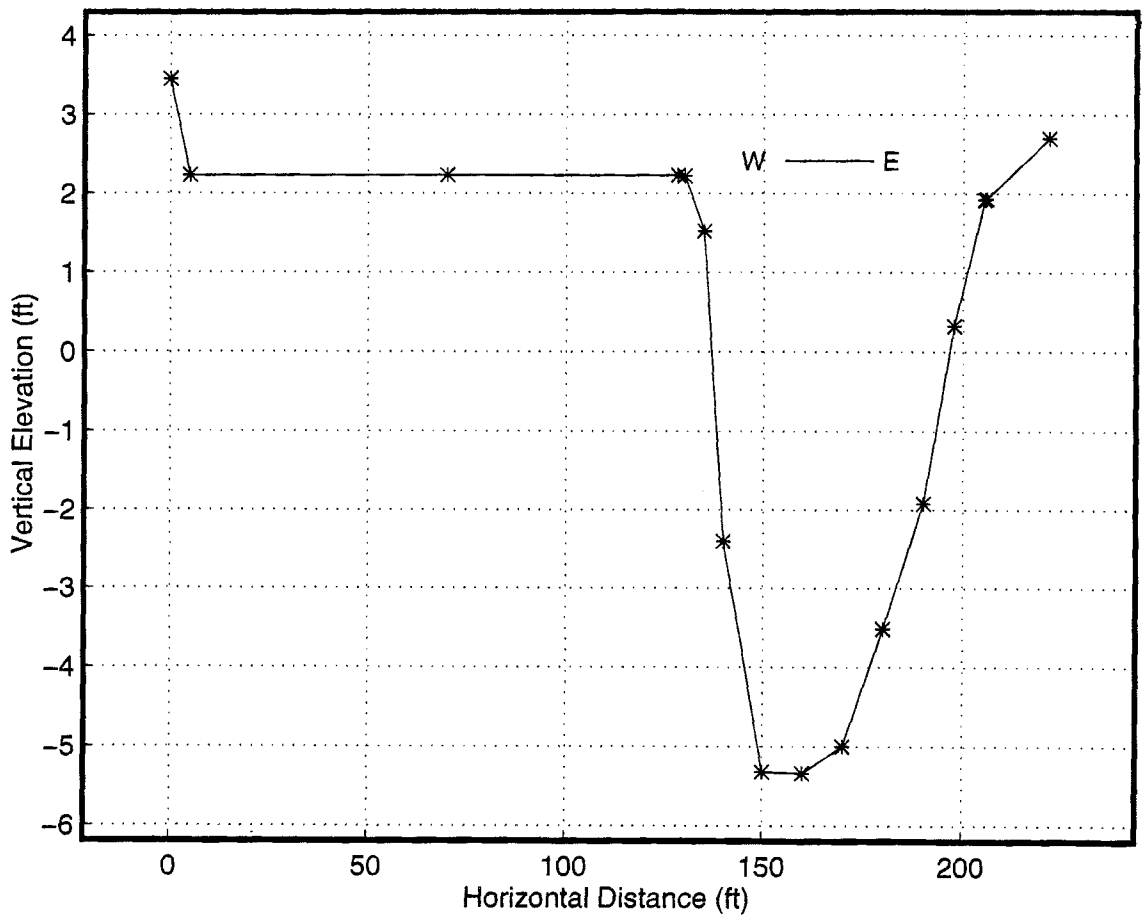

Figure 5.23: Previous Cross Section 8.

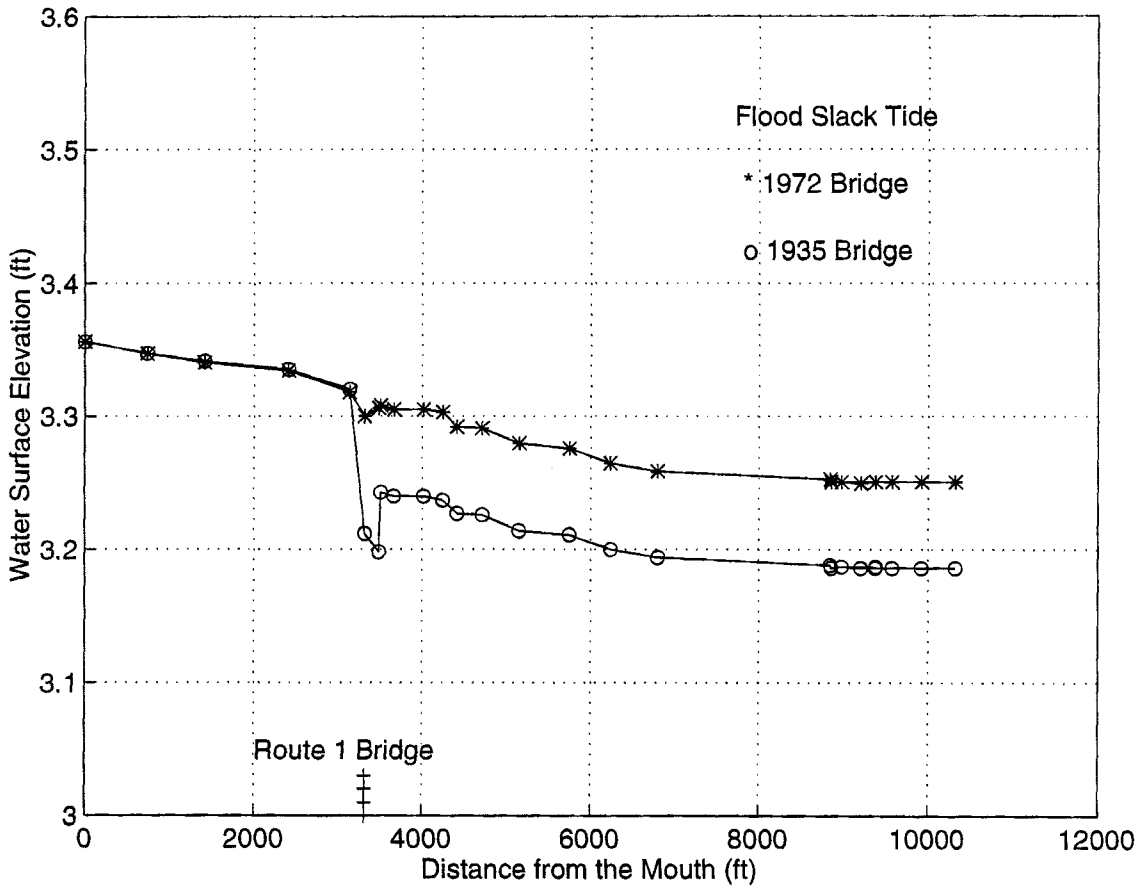

Figure 5.24: Water Surface Profiles for Spring Tide at 22:30 on May 15, 1995.

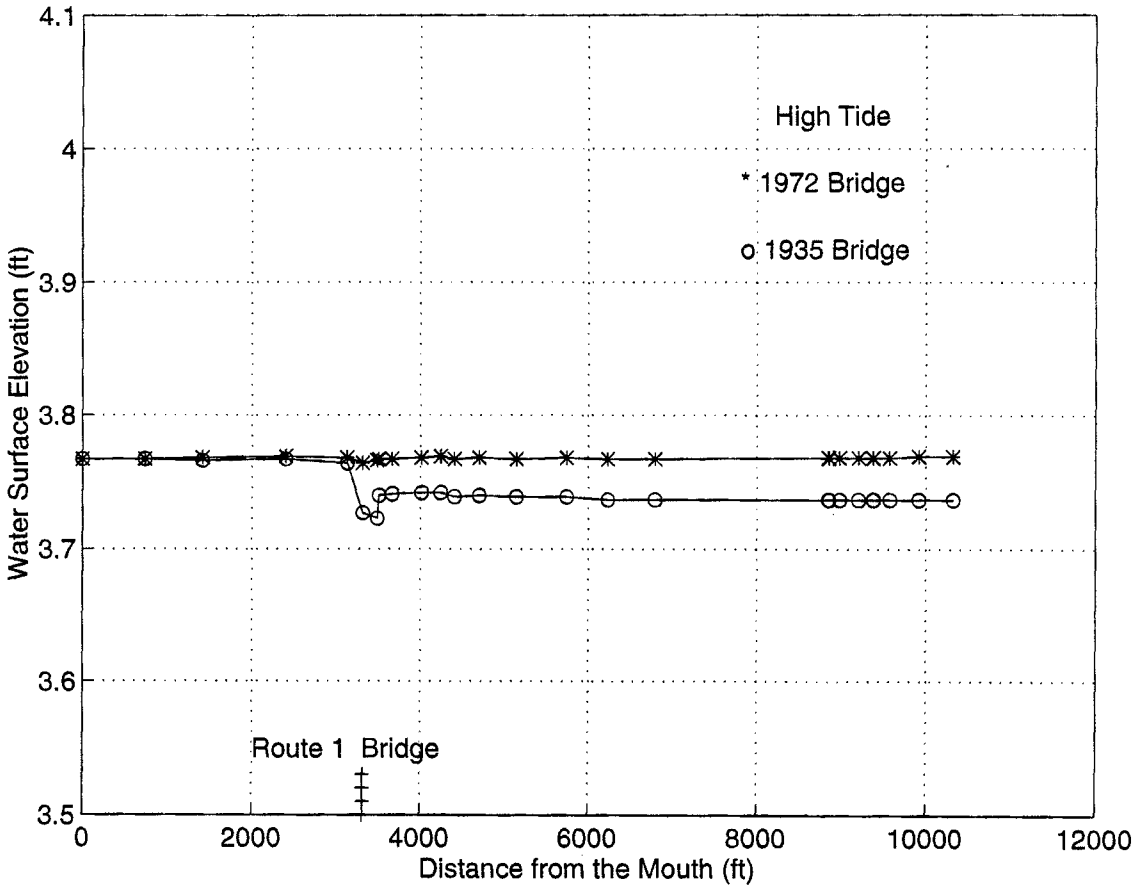

Figure 5.25: Water Surface Profiles for Spring Tide at 1:30 on May 16, 1995.

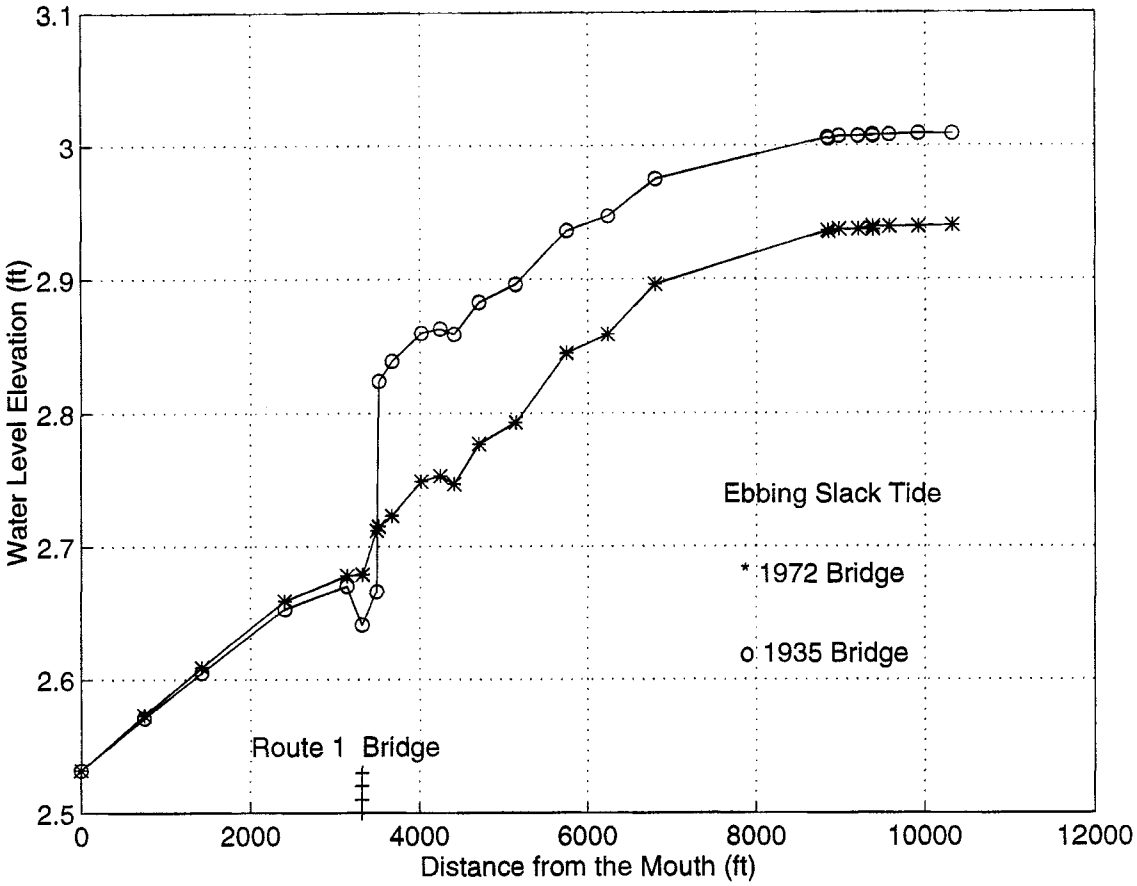

Figure 5.26: Water Surface Profiles for Spring Tide at 3:30 on May 16, 1995.

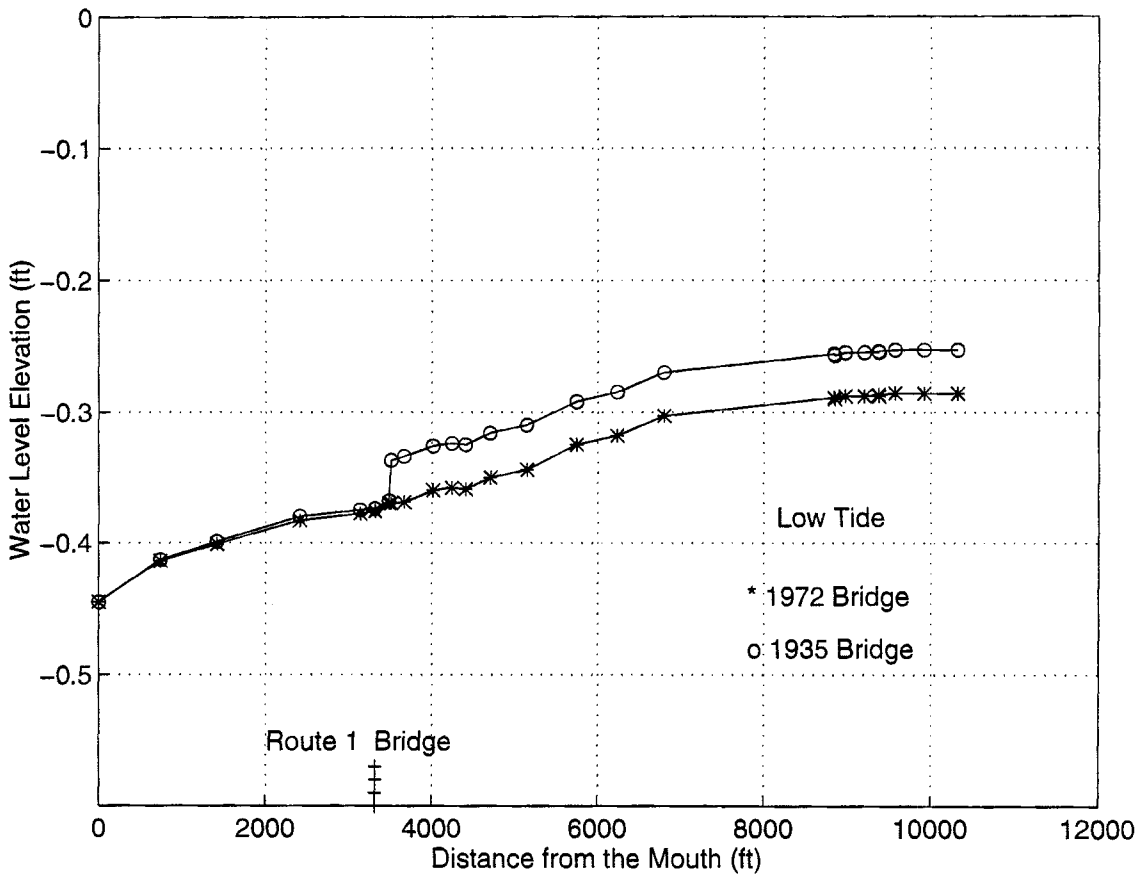

Figure 5.27: Water Surface Profiles for Spring Tide at 6:00 on May 16, 1995.

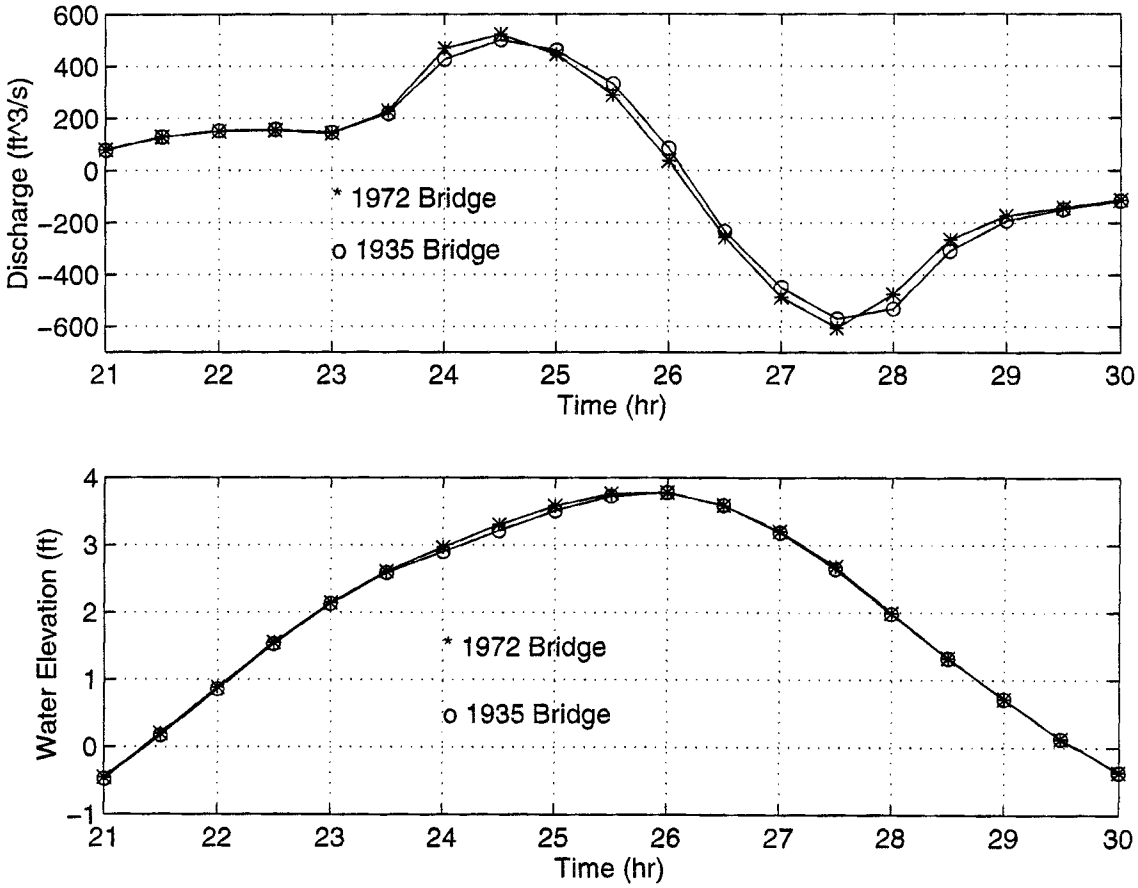

Figure 5.28: Discharge and Elevation at Rte. 1 Bridge for Spring Tide on May15-16, 1995.

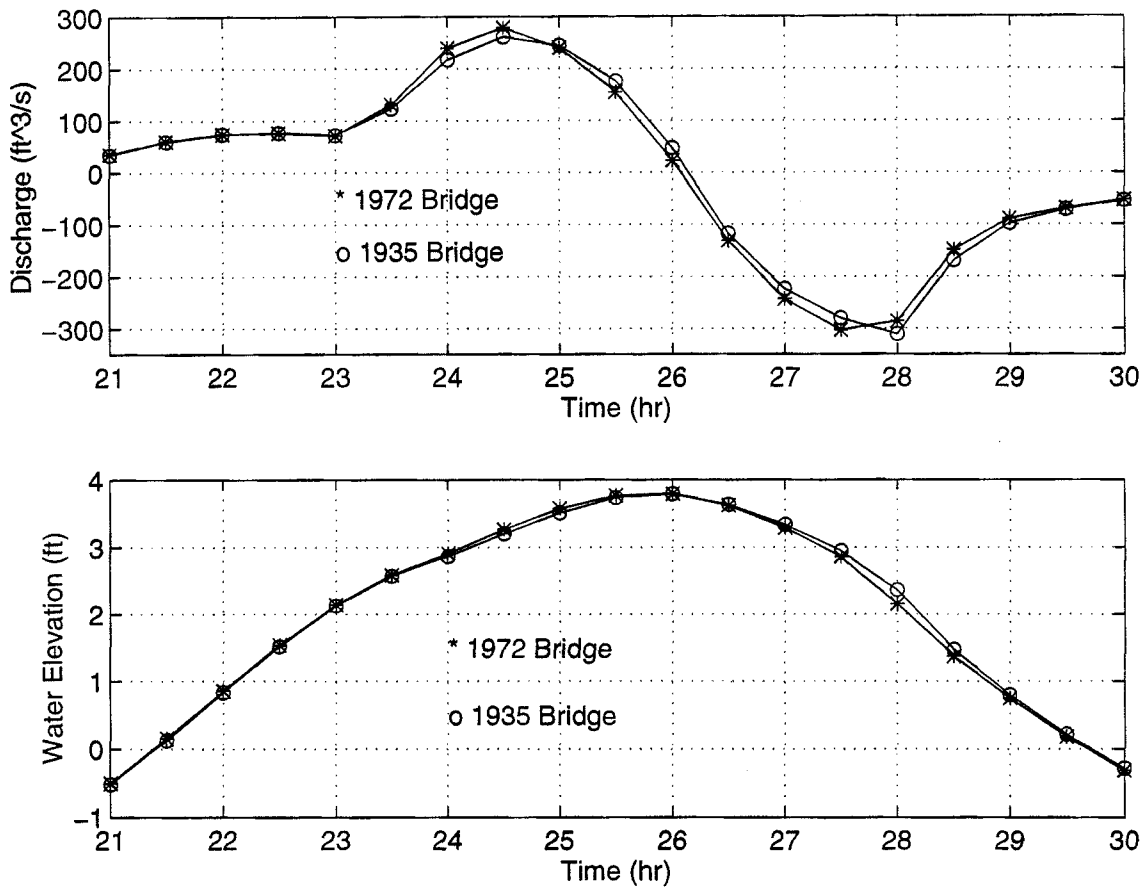

Figure 5.29: Discharge and Elevation at Railroad Bridge for Spring Tide on May 15-16, 1995.

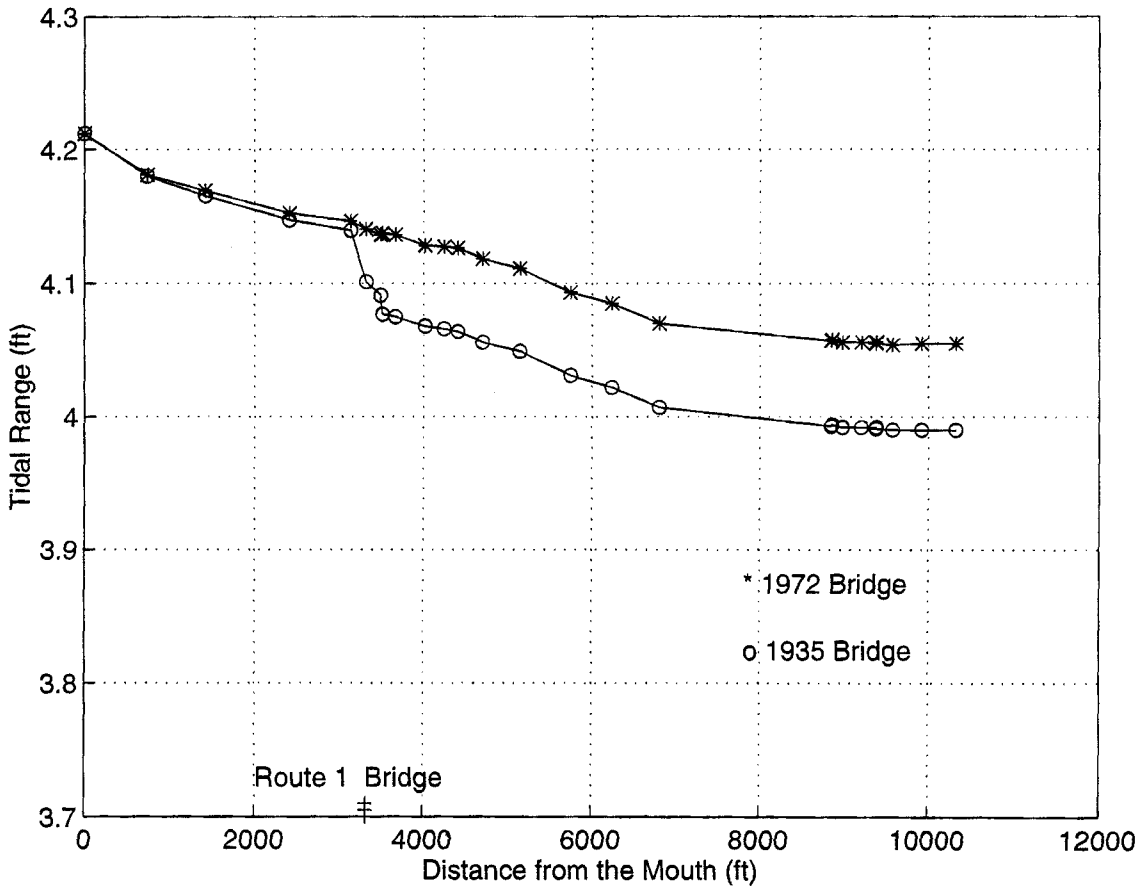

Figure 5.30: Tidal Range for Spring Tide on May 15-16, 1995.

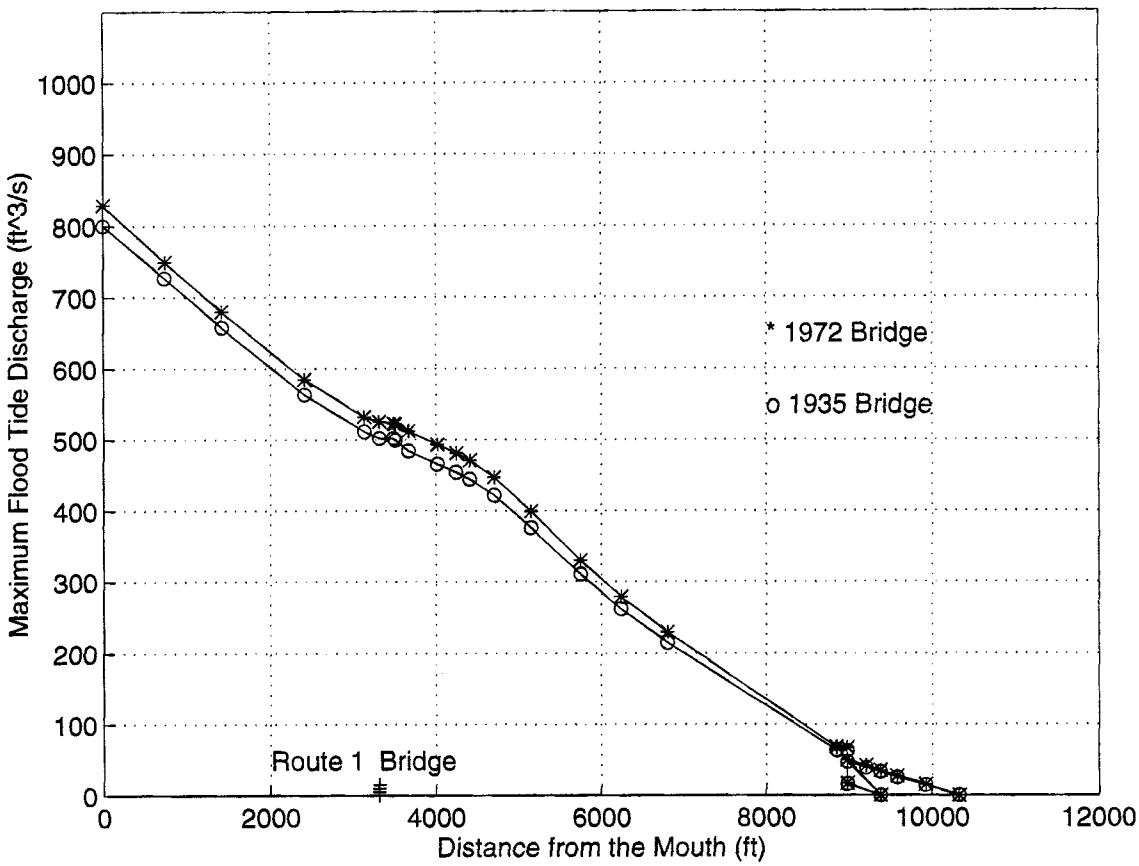

Figure 5.31: Maximum Flood Tide Discharge for Spring Tide on May 15-16, 1995.

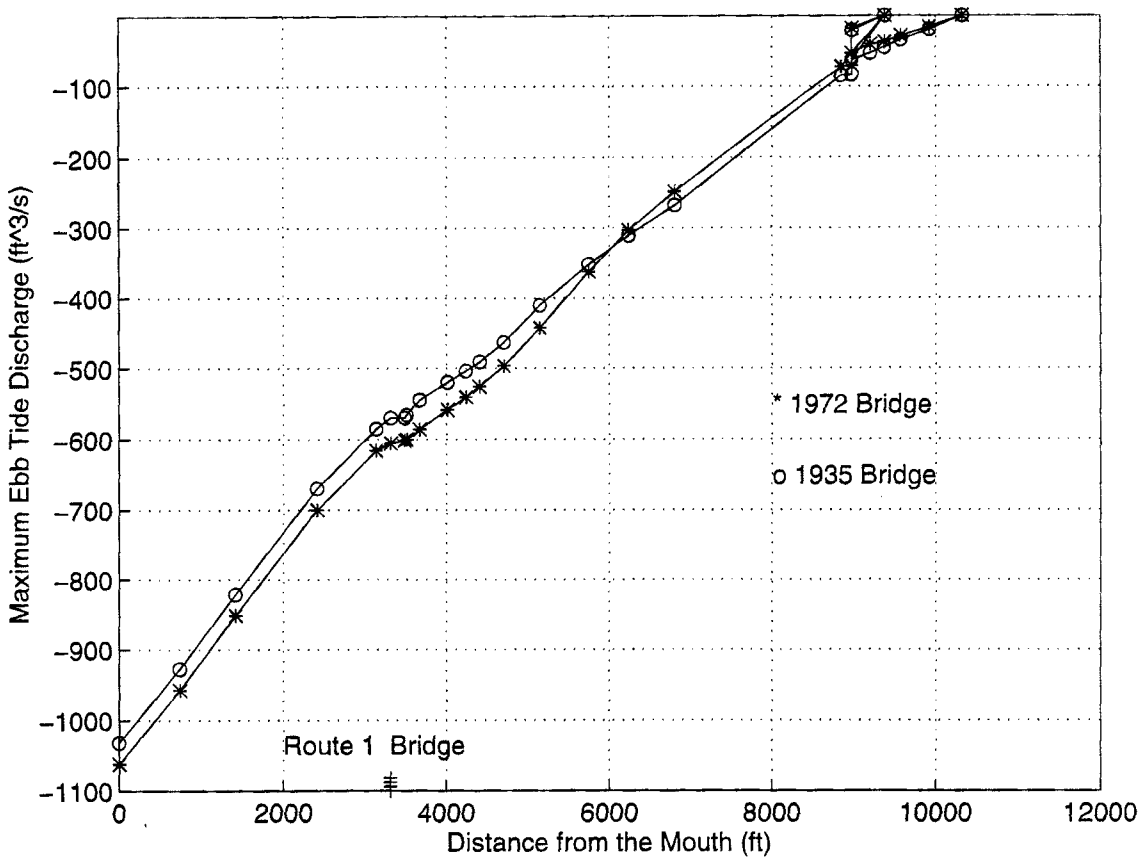

Figure 5.32: Maximum Ebb Tide Discharge for Spring Tide on May 15-16, 1995.

6. Summary and Conclusions

(1) A Pseudo-2D hydrodynamic model has been developed for a coastal river and marsh system, a tidal river meandering through expansive salt marshes. The model is based on the one-dimensional Saint-Vennant equations for longitudinal flow along the main channel and marshes, and is coupled interactively to another one-dimensional flow over the marsh surface in the transverse direction. Computational results can provide the water depth and current distribution over the entire marsh for assessment of environmental impacts of tidal flushing due to the construction of highway structures such as culverts, bridges, causeways, etc.

(2) A research site is located at the Oyster River, Old Saybrook, Connecticut. The survey work at the site provided the topographic and channel cross-section data for the Oyster River and its salt marsh for model calibration, validation, and simulation. In addition, the cover-type map for different salt-marsh vegetation types has been constructed. The map will be useful for estimating roughness coefficients for model simulation and for correlating tidal flow regions to marsh vegetation.

(3) Tidal stage and current measurements were conducted at this site for small tidal amplitudes without overland flow, and for spring high tides with significant overland flow.

(4) The model was calibrated for the parameters of energy dissipation coefficients and Manning's roughness coefficients by using stage and current data acquired at the Oyster River. Model validation was accomplished by comparing calculated tidal

stages and discharges with those acquired in four series of field measurements.

(5) The simulation results of the spring tide of 1995 were analyzed to demonstrate that the model can provide water depth and current distributions over the marsh and water interchange between the main channel and the marsh. The data can be used for quantitative assessment of environmental impacts due to construction of highway structures.

(6) The model has been used to conduct a sensitivity study of the U.S. Route 1 Bridge including the effect of the abutment and the size of the bridge opening on tidal flushing. Comparisons of tidal stages and discharges before and after bridge reconstruction were also made to assess the impacts of the bridge construction and the main channel realignment in 1970-1972 on tidal flushing.

References

Amein, M., and N. C. Kraus, 1991. Dynlet1: Dynamic Implicit Numerical Model of One Dimensional Tidal Flow Through Inlets. US Army Corps of Engineers, Tech. Rept. CERC-91-10.

Amein, M., and H. Chu, 1975. Implicit Numerical Modeling of Unsteady Flows. ASCE. Jour. of Hy. Division, Vol 101, No. HY6.

Bloom, A. L., and C. W. Ellis, Jr., 1965. Postglacial Stratigraphy and Morphology of Coastal Connecticut. State Geol. & Nat. Hist. Surv. Conn. Guidebk. No. 1, 10 pp.

Chapman, V. J., 1974. Salt Marshes and Salt Deserts of the World. Cramer, Lehre, 392 pp.

Cronon, W., 1983. Changes in the Land: Indiands, Colonists, and the Ecology of New England. Hill and Wang, N. Y. 241 pp.

De Leuw, Cather and Company, 1988. Marsh Impact Study, Old Saybrook, Connecticut, Prepared for Angus McDonald-Gary Sharpe & Associates. 43 pp.

Flint, R. F., 1972. Surficial Geology of the Essex Quadgrangle.

Hill, D. E., and A. E. Shearin, 1970. Tidal Marshes of Connecticut and Rhode Island. Conn. Agr. Exp. Sta. Bull. 709. 34 pp.

Hoggan, D. H., 1989. Computer-assisted Floodplain Hydrology and Hydraulics. McGraw-Hill Publishing Company.

Price J. S., and M-K. Woo, 1988. Studies of a Subarctic Coastal Marsh, II. Salinity. Journal of Hydrology, No 103, pp. 293-307.

Lefor, M. W., W. C. Kennard, and D. L. Civco, 1987. On the Relationship of Salt Marsh Plant Distributions to Tidal Levels in Connecticut, U. S. A. Envtl. Mgmnt. Vol. 11, pp. 61-68.

Lewandowski, J. A., R. J. Sobey, and P. Goodwin, 1993. A Hydrodynamic Model for a Tidal Wetland. Proceedings of the 1993 Conference on Hydraulic Engineering '93, Vol. 1, pp. 574-579.

Lundgren, Jr. L., 1994. The Bedrock Geology of the Essex Quadrangle. State Geol. & Nat. Hist. Surv. Conn., Quadgrangle Rept. No. 15.

Miller, W. R., and F. E. Egler, 1950. Vegetation of the Wequetequock Tidal Marshes, Connecticut. Ecol. Monogr. 20(2): pp. 142-172.

Mahmood, K., and V. Yevjevich, 1975. Unsteady Flow in Open Channel. Vols. I & II. Water Resources Publications, Fort Collins, Colo.

Niering, W. A., and R. S. Warren, 1977. Our Dynamic Tidal Marshes: Vegetation Change as Revealed by Peat Analysis. Conn. Arbor. Bull. 22.

Niering, W. A., and R. S. Warren, 1980. Vegetation Patterns and Processes in New England Salt Marshes. BioScience, 30(5): pp. 301-307.

Price, R. K., 1974. Comparison of Four Numerical Methods for Flood Routing. ASCE, Journal of the Hydraulics Division, Vol 100, No. HY7, pp. 879-899.

Tan, Weigang, 1992. Shallow Water Hydrodynamics–Mathematical Theory and Nu-

merical Solutions for Two-dimensional Systems of Shallow Water Equations. Elsevier Oceanography Series 65, Water and Power Press, Beijing. Elsevier, Amsterdam.

Tingsanchali, T., and N. L. Ackermann, 1976. Effects of Overbank Flow in Flood Computations. ASCE. Journal of the Hydraulics Division. Vol.112, HY7, pp. 1013-1025.

Appendix A—Cross Sections of the Oyster River

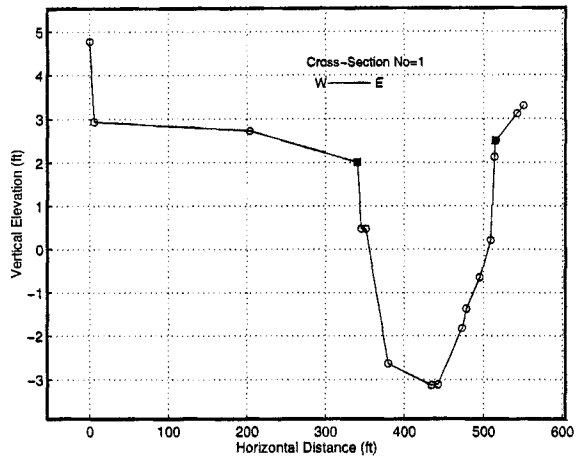

Figure A.1: Profile of Cross Section 1.

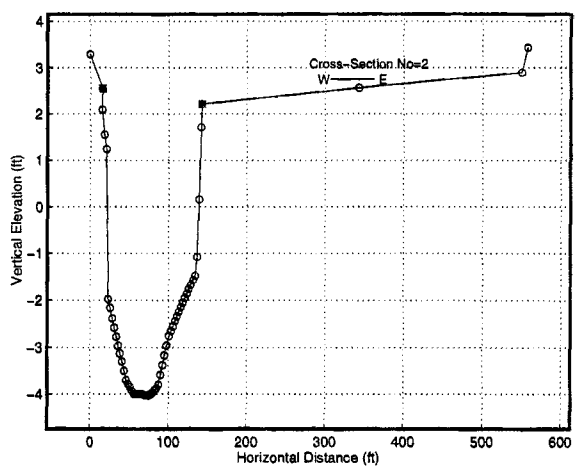

Figure A.2: Profile of Cross Section 2.

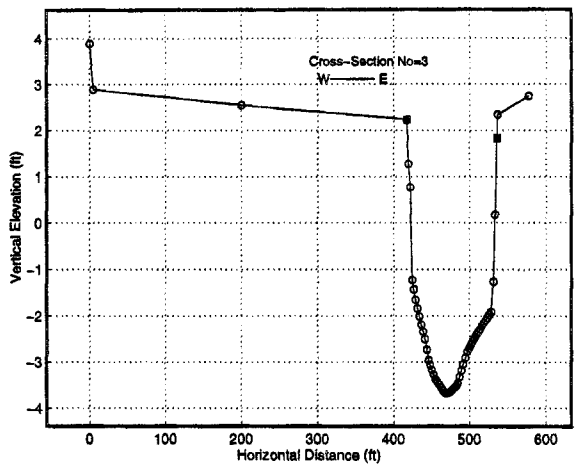

Figure A.3: Profile of Cross Section 3.

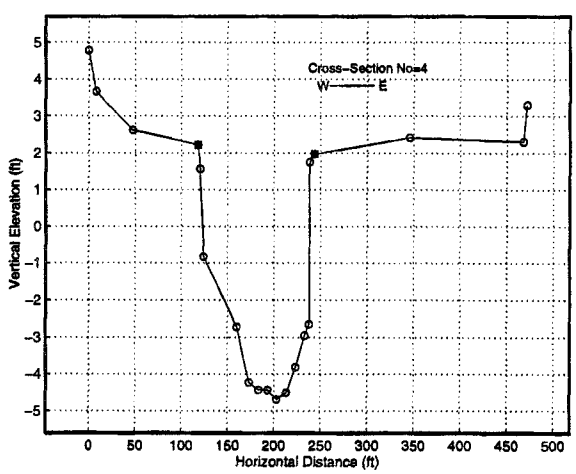

Figure A.4: Profile of Cross Section 4.

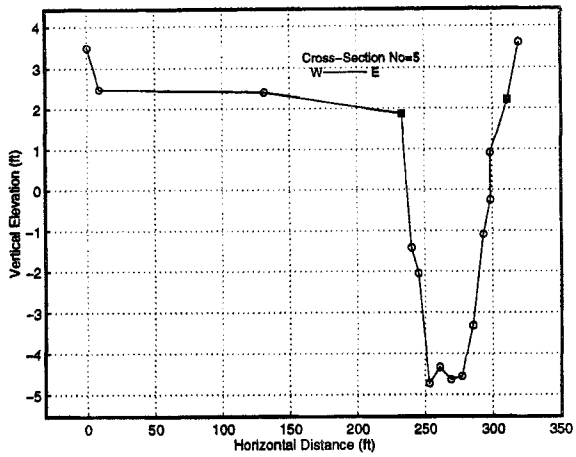

Figure A.5: Profile of Cross Section 5.

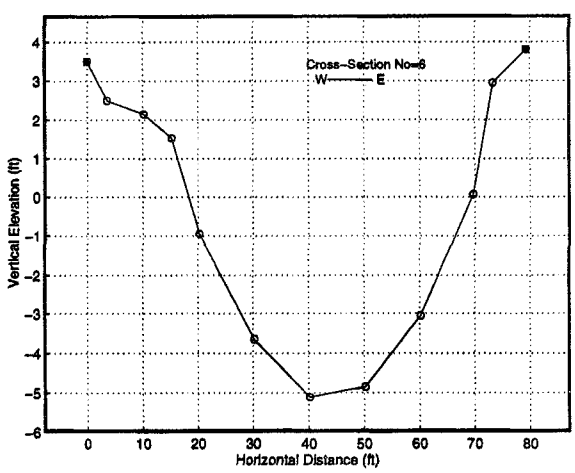

Figure A.6: Profile of Cross Section 6.

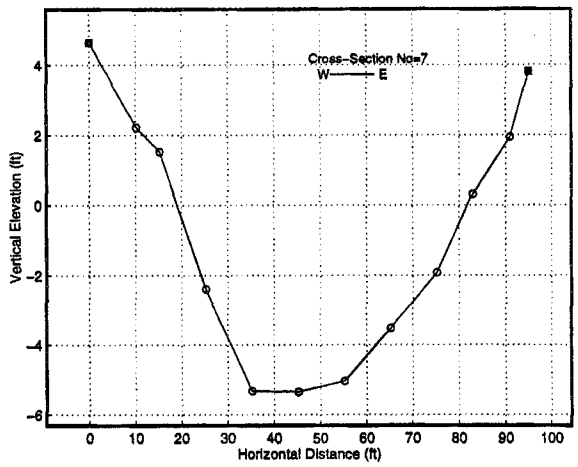

Figure A.7: Profile of Cross Section 7.

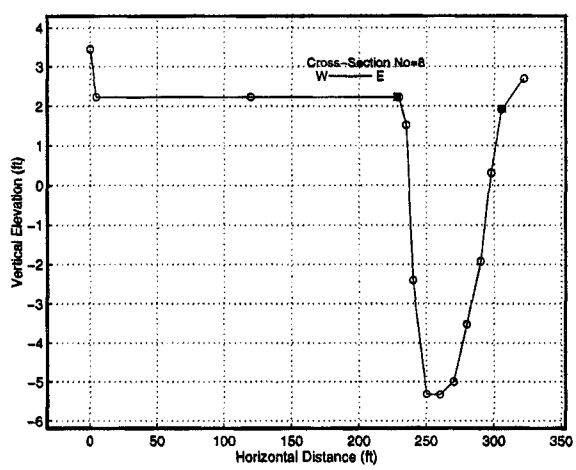

Figure A.8: Profile of Cross Section 8.

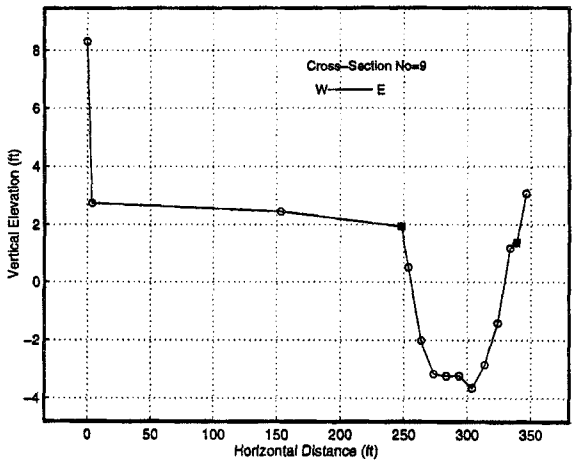

Figure A.9: Profile of Cross Section 9.

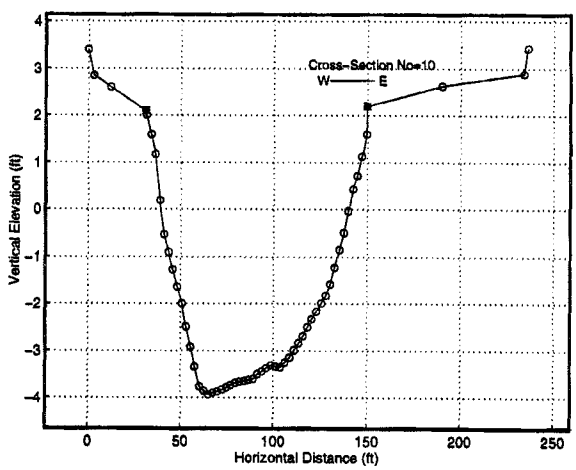

Figure A.10: Profile of Cross Section 10.

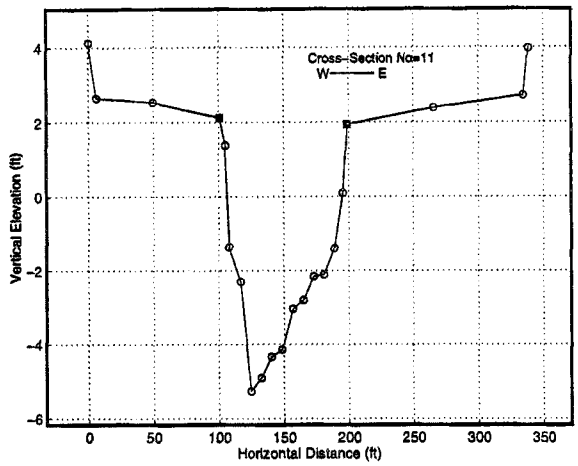

Figure A.11: Profile of Cross Section 11.

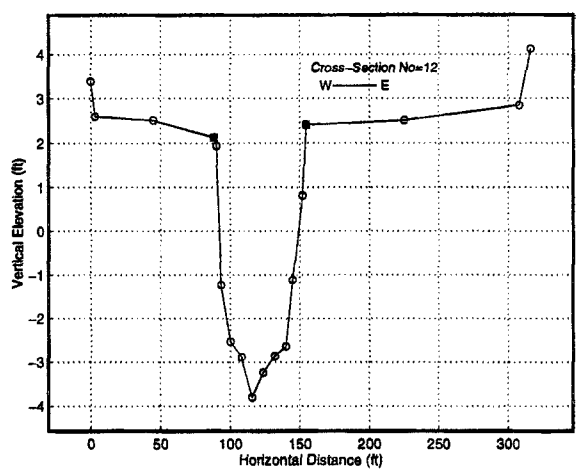

Figure A.12: Profile of Cross Section 12.

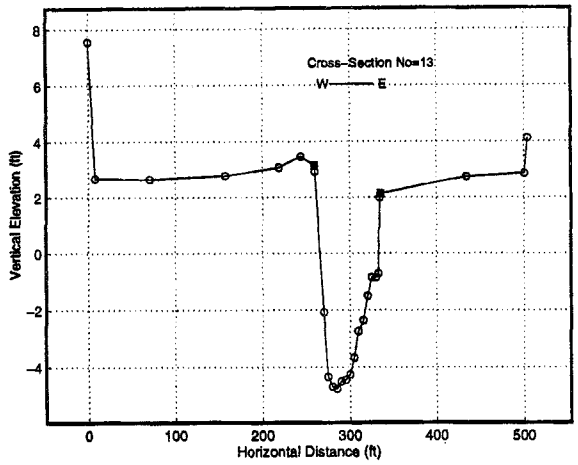

Figure A.13: Profile of Cross Section 13.

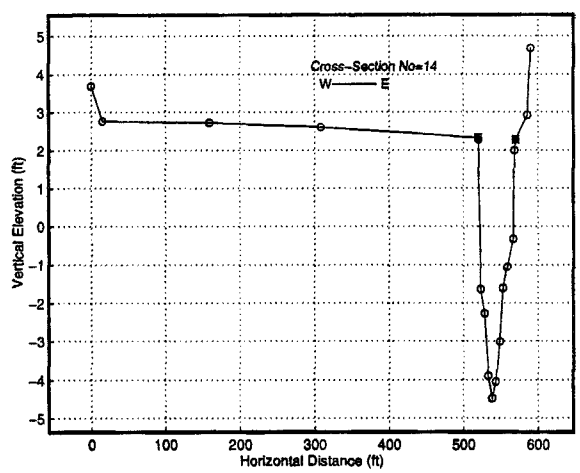

Figure A.14: Profile of Cross Section 14.

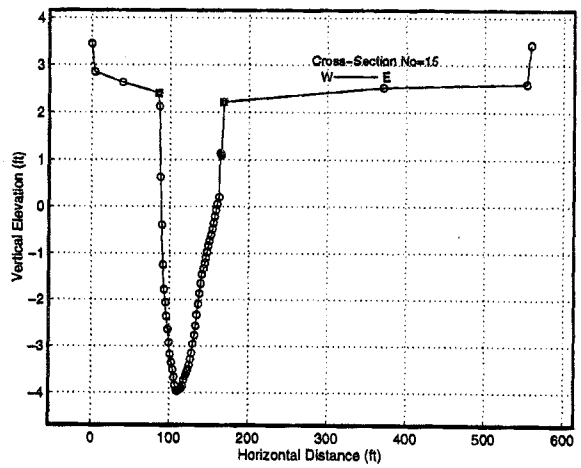

Figure A.15: Profile of Cross Section 15.

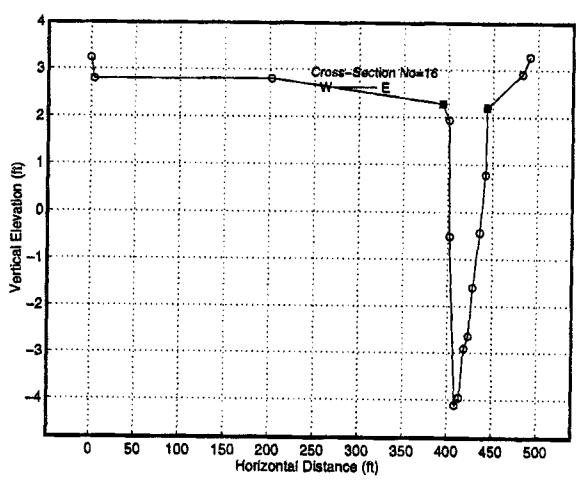

Figure A.16: Profile of Cross Section 16.

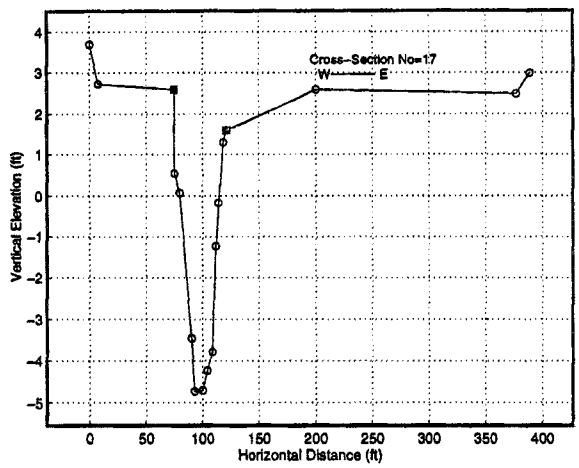

Figure A.17: Profile of Cross Section 17.

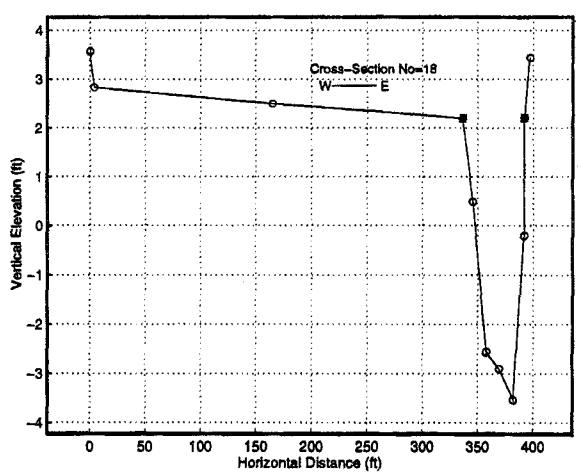

Figure A.18: Profile of Cross Section 18.

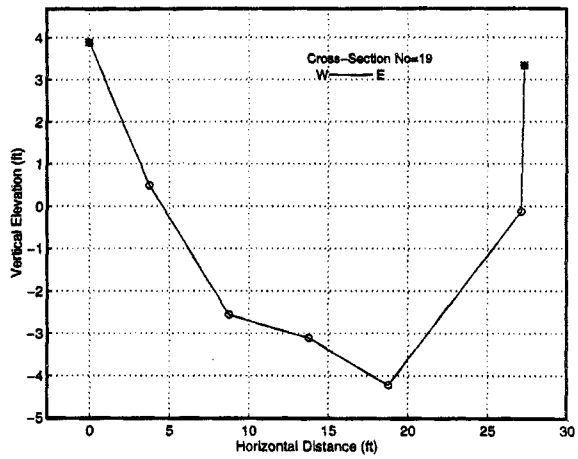

Figure A.19: Profile of Cross Section 19.

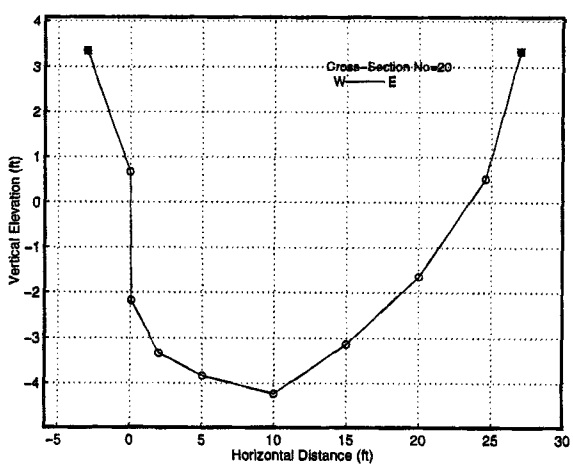

Figure A.20: Profile of Cross Section 20.

Appendix B — Tidal Stage and Current Data

Table B-1: Record of Tide Staff Readings (Run No. 1)

Date:Oct 26-27, 1994

No.	Staff Number	Time (EDST)	Reading (ft)	Elev. (ft)	No.	Staff Number	Time (EDST)	Reading (ft)	Elev. (ft)
1	1	10/26 13:22	3.87	1.03	29	1	15:34	5.04	2.2
2	2	13:36	11.39	1.26	30	2	15:38	12.39	2.16
3	R1BUS	13:45	14.30	1.70	31	R1BUS	15:53	13.33	2.67
4	R1BDS	13:47	17.06	1.44	32	R1BDS	15:51	16.18	2.32
5	3	13:50	4.98	1.37	33	3	15:44	5.78	2.17
6	11	13:52	3.78		34	11	15:47	4.57	
7	12	14:02	11.05		35	12	15:48	11.34	
8	4	14:02	11.05	1.50	36	4	15:54	11.81	2.26
9	5	14:09	3.66	1.60	37	5	15.59	4.30	2.24
10	13	14:20	11.92	1.584	38	13	16:09	12.50	2.164
11	RABUS	14:20	18.10	1.80	39	RABUS	16:07	17.50	2.49
12	RABDS	14:20	18.11	1.81	40	RABDS	16:08	17.51	2.48
13	7	14:27	4.03	1.77	41	7	16:13	4.51	2.25
14	6	14:34	11.24	1.78	42	6	16:18	11.63	2.17
15	1	14:41	4.75	1.91	43	1	16:25	5.08	2.24
16	2	14:46	12.16	1.93	44	2	16:30	12.48	2.25
17	R1BUS	14:59	13.48	2.52	45	R1BUS	16:45	13.36	2.64
18	R1BDS	14:57	16:34	2.16	46	R1BDS	16:42	16:45	2.26
19	3	14.51	5.56	1.95	47	3	16:35	5.80	2.19
20	11	14:53	4.37		48	11	16:38	4.60	
21	12	14:54	11.19		49	12	16:39	11.34	
22	4	15:01	11.62	2.07	50	4	16:46	11.76	2.21
23	5	15:06	4.16	2.10	51	5	16:51	4.24	2.18
24	13	15:18	12.42	2.084	52	13	17:00	12.42	2.084
25	RABUS	15:16	17.61	2.38	53	RABUS	17:02	17.56	2.43
26	RABDS	15:17	17.61	2.38	54	RABDS	17:02	17.61	2.38
27	7	15:23	4.41	2.15	55	7	17:06	4.34	2.08
28	6	15:27	11.60	2.14	56	6	17:10	11.48	2.02

Table B-1: Record of Tide Staff Readings (Run No. 1 Continued)

Date: Oct 26-27, 1994

No.	Staff Number	Time (EDST)	Reading (ft)	Elev. (ft)	No.	Staff Number	Time (EDST)	Reading (ft)	Elev. (ft)
57	1	18:05	4.28	1.44	85	1	20:20	2.57	-0.27
58	2	18:10	11.60	1.37	86	2	20:26	9.88	-0.35
59	R1BUS	18:12	14.25	1.75	87	R1BUS	20:33	15.85	0.15
60	R1BDS	18:16	17.05	1.45	88	R1BDS	20:36	18.45	0.05
61	3	18:20	4.86	1.25	89	3	20:39	3.23	-0.38
62	11	18:25	3.79		90	11			
63	12	18:23	10.42		91	12			
64	4	18:32	10.74	1.19	92	4			
65	5	18:38	3.10	1.04	93	5	20:49	1.595	-0.465
66	13	18:47	11.29	0.954	94	13	21:03	9.81	-0.526
67	RABUS	18:52	18.79	1.20	95	RABUS	20:58	20.11	-0.12
68	RABDS	18:50	18.78	1.21	96	RABDS	21:00	20.20	-0.21
69	7	18:59	3.07	0.81	97	7	21:09	1.68	-0.58
70	6	19:05	10.20	0.80	98	6	21:17	8.74	-0.72
71	1	19:11	3.41	0.57	99	1	21:29	1.89	-0.95
72	2	19:16	10.74	0.51	100	2	21:36	Too Low	
73	R1BUS	19:22	14.91	1.09	101	R1BUS	21:43	16.54	-0.54
74	R1BDS	19:26	17.81	0.69	102	R1BDS	21:46	19.25	-0.75
75	3	19:27	3.82	0.21	103	3	21:49	2.54	-1.07
76	11				104	11			
77	12				105	12			
78	4				106	4			
79	5	19:47	2.24	0.18	107	5	22:04	0.92	-1.14
80	13	20:00	10.47	0.134	108	13	22:17	9.46	-0.876
81	RABUS	19:55	19.47	0.52	109	RABUS	22:14	20.67	-0.68
82	RABDS	19:58	19.53	0.46	110	RABDS	22:16	20:79	-0.80
83	7	20:07	2.30	0.04	111	7	22:25	1.08	-1.18
84	6	20:12	9.50	0.04	112	6	22:34	8.20(Es.)	-1.26

Table B-1: Record of Tide Staff Readings (Run No. 1 Continued)

Date: Oct 26-27, 1994

No.	Staff Number	Time (EDST)	Reading (ft)	Elev. (ft)	No.	Staff Number	Time (EDST)	Reading (ft)	Elev. (ft)
113	1	23:07	1.7(Es.)	-1.14	141	1	1:27	3.21	0.37
114	2		Too Low		142	2	1:34	10.63	0.40
115	R1BUS	23:29	16.49	-0.49	143	R1BUS	1:41	15.00	1.00
116	R1BDS	23:27	19.21	-0.71	144	R1BDS	1:39	17.69	0.81
117	3	23:23	2.60	-1.01	145	3	1:38	4.10	0.49
118	11				146	11			
119	12				147	12			
120	4				148	4	1:51	10.20	0.65
121	5	23:40	1.20	-0.86	149	5	2:01	2.78	0.52
122	13	23:51	9.48	-0.856	150	13	2:14	11.08	0.744
123	RABUS	23:52	20.55	-0.56	151	RABUS	2:11	18.96	1.03
124	RABDS	23:57	20.57	-0.54	152	RABDS	2:12	18.97	1.02
125	7	10/27 0:05	1.56	-0.70	153	2:20	21:09	3.20	0.94
126	6	0:11	8.80	-0.66	154	6	2:25	10.43	0.97
127	1	0:20	2.36	-0.48	155	1	2:33	3.92	1.08
128	2	0:27	9.70	-0.53	156	2	2:39	11.30	1.07
129	R1BUS	0:35	17.87	-1.87	157	R1BUS	2:47	14.30	1.70
130	R1BDS	0:34	18.60	-0.10	158	R1BDS	2:45	17.05	1.45
131	3	0:33	3.22	-0.39	159	3	2:44	4.76	1.15
132	11				160	11			
133	12				161	12			
134	4				162	4	2:56	11.93	2.38
135	5	0:46	1.84	-0.22	163	5	3:04	3.40	1.14
136	13	0:59	10.15	-0.186	164	13	3:17	11.72	1.384
137	RABUS	0:56	19.91	0.08	165	RABUS	3:15	18.30	1.69
138	RABDS	0:57	19.91	0.08	166	RABDS	3:16	18.32	1.67
139	7	1:05	2.22	-0.04	167	7	3:22	3.79	1.53
140	6	1:20	9.62	0.16	168	6	3:27	11.02	1.56

Table B-1: Record of Tide Staff Readings (Run No. 1 Continued)

Date: Oct 26-27, 1994

No.	Staff Number	Time (EDST)	Reading (ft)	Elev. (ft)	No.	Staff Number	Time (EDST)	Reading (ft)	Elev. (ft)
169	1	3:52	4.63	1.79	197	1	5:44	4.68	1.84
170	2	3:59	12.06	1.83	198	2	5:50	12.00	1.77
171	R1BUS	4:05	13.92	2.58	199	R1BUS	5:54	13.75	2.25
172	R1BDS	4:08	16.31	2.19	200	R1BDS	5:57	16.45	2.05
173	3	4:11	5.52	1.91	201	3	5:59	5.37	1.76
174	11				202	11			
175	12				203	12			
176	4				204	4			
177	5	4:16	4.00	1.94	205	5	6:06	3.76	1.70
178	13	4:30	12.31	1.994	206	13	6:16	11.95	1.614
179	RABUS				207	RABUS			
180	RABDS	4:27	17.72	2.27	208	RABDS	6:15	18.03	1.96
181	7	4:36	4.29	2.03	209	2:20	6:21	3.80	1.54
182	6	4:41	11.47	2.01	210	6	6:26	10.90	1.44
183	1	4:48	4.88	2.04	211	1	6:33	4.20	1.36
184	2	4:55	12.25	2.02	212	2	6:39	11.51	1.28
185	R1BUS	5:00	13.40	2.60	213	R1BUS	6:44	14.19	1.81
186	R1BDS	5:02	16.21	2.29	214	R1BDS	6:46	17.03	1.47
187	3	5:04	5.56	1.95	215	3	6:49	4.76	1.15
188	11				216	9	7:18	11.18	
189	12				217	10	7:19	10.26	
190	4				218	4			
191	5	5:11	4.00	1.94	219	5	6:55	3.16	1.10
192	13	5:25	12.22	1.884	220	13	7:06	11.32	0.984
193	RABUS				221	RABUS			
194	RABDS	5:24	17.80	2.19	222	RABDS	7:05	18.70	1.29
195	7	5:31	4.17	1.91	223	7	7:12	3.20	0.94
196	6	5:37	11.27	1.81	224	6	7:24	10.18	0.72

Table B-1: Record of Tide Staff Readings (Run No. 1 Continued)

Date: Oct 26-27, 1994

No.	Staff Number	Time (EDST)	Reading (ft)	Elev. (ft)	No.	Staff Number	Time (EDST)	Reading (ft)	Elev. (ft)
225	1	8:25	2.86	0.02	253	1	10:21	1.96	-0.88
226	2	8:28	10.22	-0.01	254	2			
227	R1BUS	8:36	15.58	0.42	255	R1BUS	10:30	16.46	-0.46
228	R1BDS	8:35	18.28	0.22	256	R1BDS	10:29	19.11	-0.61
229	3	8:33	3.59	-0.02	257	3	10:28	2.70	-0.91
230	11				258	11			
231	12				259	12			
232	4	8:44	9.46	-0.09	260	4	10:37	8.70	-0.85
233	5	8:50	1.92	-0.14	261	5	10:42	1.18	-0.88
234	13	8:53	10.12	-0.216	262	13	10:56	9.41	-0.926
235	RABUS	9:00	19.90	0.09	263	RABUS	10:52	20.60	-0.61
236	RABDS	8:53	19.92	0.07	264	RABDS	10:55	20.63	-0.64
237	7	9:05	2.00	-0.26	265	2:20	11:12	1.43	-0.83
238	6	9:16	9.04	-0.42	266	6	11:19	8.60	-0.86
239	1	9:22	2.31	-0.53	267	1	11:37	2.08	-0.76
240	2				268	2	11:41	Too Low	
241	R1BUS	9:35	16.35	-0.35	269	R1BUS	11:48	16.24	-0.24
242	R1BDS	9:33	18.97	-0.47	270	R1BDS	11:46	18.91	-0.41
243	3	9:30	3.05	-0.56	271	3	11:50	2.86	-0.75
244	11				272	9			
245	12				273	10			
246	4	9:46	8.97	-0.58	274	4	11:51	8.84	-0.71
247	5	9:53	1.38	-0.68	275	5	11:57	1.39	-0.67
248	13	10:01	9.62	-0.726	276	13	12:05	9.58	-0.756
249	RABUS	10:02	20.36	-0.37	277	RABUS	12:06	20.45	-0.46
250	RABDS	10:03	20.42	-0.43	278	RABDS	12:08	20.46	-0.47
251	7	10:07	1.52	-0.74	279	7	12:13	1.67	-0.59
252	6	10:12	8.80	-0.66	280	6	12:19	8.89	-0.57

Table B-1: Record of Tide Staff Readings (Run No. 1 Continued)

Date: Oct 26-27, 1994

No.	Staff Number	Time (EDST)	Reading (ft)	Elev. (ft)	No.	Staff Number	Time (EDST)	Reading (ft)	Elev. (ft)
281	1	12:25	2.39	-0.45					
282	2	12:30	9.80	-0.43					
283	R1BUS	12:35	15.92	0.08					
284	R1BDS	12:37	18.58	0.08					
285	3	12:39	3.26	-0.35					
286	11								
287	12								
288	4	12:40	9.22	-0.33					
289	5	12:49	1.81	-0.25					
290	13	12:56	10.02	-0.316					
291	RABUS	12:56	19.96	0.03					
292	RABDS	12:58	19.97	0.02					
293	7	13:04	2.18	-0.08					
294	6	13:09	9.44	-0.02					
295	1	13:16	3.00	0.12					
296	2	13:21	10.39	0.16					
297	R1BUS	13:26	15.20	0.80					
298	R1BDS	13:29	17.92	0.58					
299	3	13;31	3.99	0.38					
300	9	13:59	11.14						
301	10	14:01	10.18						
302	4	13:25	9.80	0.25					
303	5	13:38	2.49	0.43					
304	13	13:46	10.76	0.424					
305	RABUS	13:47	19.20	0.79					
306	RABDS	13:49	19.21	0.78					
307	7	13:54	2.95	0.69					
308	6	14:05	10.25	0.79					

Table B-2: Record of Tide Staff Readings (Run No. 2)

Date: Dec 1-2, 1994

No.	Staff Number	Time (EDST)	Reading (ft)	Elev. (ft)	No.	Staff Number	Time (EDST)	Reading (ft)	Elev. (ft)
1	1	12/1 8:59	5.62	2.78	29	1	10:45	4.35	1.51
2	2	9:06	13.40	3.17	30	2	10:49	11.70	1.47
3	3	9:14	6.42	2.81	31	3	10:58	4.98	1.37
4	R1BUS	9:11	12.73	3.27	32	R1BUS	10:54	14.09	1.91
5	R1BDS	9:14	15.41	3.09	33	R1BDS	10:56	16.87	1.63
6	4	9:11	12.43	2.87	34	4	10:56	11.03	1.48
7	5	9:20	4.96	2.90	35	5	11:04	3.36	1.30
8	13	9;28	13.16	2.824	36	13	11:12	11.59	1.254
9	RABUS	9:29	16.85	3.14	37	RABUS	11:12	18.45	1.54
10	RABDS	9:30	16.90	3.09	38	RABDS	11:13	18.51	1.48
11	7	9:34	5.04	2.78	39	7	11:19	3.37	1.11
12	6	9:45	12.09	2.63	40	6	11:29	10.25	0.79
13	9	9:40	12.74		41	9	11:23	11.19	
14	10	9:41	12.16		42	10	11:25	10.33	
15	1	9:52	5.28	2.44	43	1	11:36	3.31	0.47
16	2	9:57	12.69	2.46	44	2	11:41	10.66	0.43
17	3	10:08	5.91	2.30	45	3	11:50	3.92	0.31
18	R1BUS	10:02	13.11	2.89	46	R1BUS	11:45	15.15	0.85
19	R1BDS	10:04	15.92	2.58	47	R1BDS	11:47	18.01	0.49
20	4	10:02	11.70	2.15	48	4	11:45	10.05	0.50
21	5	10:13	4.38	2.32	49	5	11:55	2.38	0.32
22	13	10:21	12.60	2.264	50	13	12:03	10.03	-0.306
23	RABUS	10:21	17.44	2.55	51	RABUS	12:04	19.52	0.47
24	RABDS	10:22	17.45	2.54	52	RABDS	12:05	19.45	0.54
25	7	10:27	4.42	2.16	53	7	12:10	2.42	0.16
26	6	10:38	11.33	1.87	54	6	12:21	9.32	-0.14
27	9	10:31	12.10		55	9	12:15	11.18	
28	10	10:33	11.44		56	10	12:17	Too Low	

Table B-2: Record of Tide Staff Readings (Run No. 2 Continued)

Date: Dec 1-2, 1994

No.	Staff Number	Time (EDST)	Reading (ft)	Elev. (ft)	No.	Staff Number	Time (EDST)	Reading (ft)	Elev. (ft)
57	1	13:07	2.00(Es.)	-0.84	85	1	15:19	0.60(ES.)	-2.24
58	2	13:12	9.50(Es.)	-0.73	86	2			
59	3	13:20	2.55	-1.06	87	3			
60	R1BUS	13:26	16.68	-0.68	88	R1BUS	15:25	17.59	-1.59
61	R1BDS	13:27	19.51	-0.99	89	R1BDS	15:27	20.44	-1.94
62	4	13:28	8.45	-1.10	90	4			
63	5	13:40	0.86	-1.20	91	5			
64	13	13:47	9.52	-0.81	92	13	15:36	9.16	-1.176
65	RABUS	13:51	20.48	-0.49	93	RABUS	15:38	20.79	-0.80
66	RABDS	13:49	20.52	-0.53	94	RABDS	15:36	20.85	-0.86
67	7	13:57	1.15	-1.11	95	7	15:44	0.62	-1.64
68	6				96	6			
69	9				97	9			
70	10				98	10			
71	1	14:26	1.00(ES.)	-1.84	99	1	16:04	0.81(ES.)	-2.03
72	2				100	2			
73	3				101	3			
74	R1BUS	14:33	17.32	-1.32	102	R1BUS	16:12	17.63	-1.63
75	R1BDS	14:36	20.13	-1.63	103	R1BDS	16:14	20.27	-1.77
76	4				104	4			
77	5				105	5			
78	13	15:02	9.22	-1.116	106	13	16:33	9.12	-1.216
79	RABUS	15:04	20.74	-0.75	107	RABUS	16:29	20.85	-0.86
80	RABDS	15:02	20.78	-0.79	108	RABDS	16:31	20.90	-0.91
81	7	15:11	0.73	-1.53	109	7	16:41	0.59	-1.67
82	6				110	6	16:47	Too Low	
83	9				111	9			
84	10				112	10			

Table B-2: Record of Tide Staff Readings (Run No. 2 Continued)

Date: Dec 1-2, 1994

No.	Staff Number	Time (EDST)	Reading (ft)	Elev. (ft)	No.	Staff Number	Time (EDST)	Reading (ft)	Elev. (ft)
113	1	16:57	1.41(Es.)	-1.43	141	1	20:48	4.81	1.97
114	2				142	2	20:53	12.22	1.99
115	3	17:11	2.36	-1.25	143	3	21:05	5.63	2.02
116	R1BUS	17:05	16.81	-0.81	144	R1BUS	21:09	13.49	2.51
117	R1BDS	17:07	19.56	-1.06	145	R1BDS	21:07	16.33	2.17
118	4				146	4	21:00	11.61	2.05
119	5	17:20	0.93	-1.13	147	5	21:15	4.15	2.09
120	13	17:31	9.31	-1.026	148	13	21:22	12.40	2.064
121	RABUS	17:28	20.75	-0.76	149	RABUS	21:25	17.60	2.39
122	RABDS	17:30	20.74	-0.75	150	RABDS	21:23	17.63	2.36
123	7	17:37	1.43	-0.83	151	7	21:30	4.32	2.07
124	6	17:44	8.78	-0.77	152	6	21:41	11.42	1.96
125	9				153	9	21:35	12:04	
126	10				154	10	21;36	11:49	
127	1	17:50	2.42	-0.42	155	1	21:47	4.83	1.99
128	2	17;56	9.96	-0.27	156	2	21:52	12.19	1.96
129	3	18:05	3.40	-0.21	157	3	21:59	5.52	1.99
130	R1BUS	18:00	15.89	0.11	158	R1BUS	22:02	13.62	2.38
131	R1BDS	18:02	18.50	0.0	159	R1BDS	22:01	16.47	2.03
132	4	18:02	9.30	-0.25	160	4	21:56	11.51	1.96
133	5	18:11	1.96	-0.10	161	5	22:07	3.97	1.91
134	13	18:21	10.25	-0.086	162	13	22:15	12.21	1.874
135	RABUS	18:20	19.75	0.24	163	RABUS	22:16	17.81	2.18
136	RABDS	18:22	19.74	0.25	164	RABDS	22:14	17.83	2.16
137	7	18:27	2.45	0.19	165	7	22:22	4.10	1.85
138	6	18:34	9.79	0.33	166	6	22:26	11.20	1.74
139	9				167	9			
140	10				168	10			

Table B-3: Record of Tide Staff Readings (Run No. 3)

Date: April 20, 1995

Staff 1				Staff 8			
No	Time (EDST)	Reading (ft)	Elev. (ft)	No	Time (EDST)	Reading (ft)	Elev. (ft)
1	4/19 21:50	4.72	-1.24	1	4/19 22:00	1(Es.)	-0.76
2	22:08	4.93	-1.03	2	22:26	1.1(Es.)	-0.66
3	22:42	5.17	-0.79	3	22:52	1.5(Es.)	-0.26
4	23:54	6.69	0.73	4	4/20 0:03	2.47	0.79
5	4/20 0:17	1.23	2.66	5	0:25	3.01	1.25
6	1:08	8.00	2.04	6	1:10	3.63	1.87
7	1:15	8.14	2.18	7	1:28	3.96	2.20
8	1:28	8.22	2.26	8	1:44	4.12	2.36
9	1:45	8.52	2.56	9	2:01	4.28	2.52
10	1:59	8.61	2.65	10	2:17	4.42	2.66
11	2:10	8.72	2.76	11	2:30	4.55	2.79
12	2:15	8.73	2.77	12	2:55	4.72	2.96
13	2:30	8.83	2.87	13	3:07	4.80	3.04
14	2:45	8.80	2.84	14	3:21	4.86	3.10
15	3:00	9.00	3.04	15	3:31	4.88	3.14
16	3:15	8.90	2.94	16	3:42	4.85	3.09
17	3:30	8.97	3.01	17	3:57	4.76	3.00
18	3:45	8.91	2.95	18	4:12	4.68	2.92
19	4:00	8.82	2.86	19	5:20	3.83	2.07
20	5:36	7.32	1.36	20	7:32	2.6(Es.)	0.84
21	8:00	4.88	-1.08	21			
22	8:46	4.35	-1.61	22			
23	9:15	4.13	-1.83	23			
Staff 7				**Staff 9**			
1	4/19 22:05	2.32	-1.23	1	4/20 7:42	10.57	-0.28
2	22:32	2.65	-0.90	2	8:12	10.31	-0.54
3	22:59	2.93	-0.62	3	8:30	10.21	-0.64
4	0:08	4.40	0.85	4	9:00	10.08	-0.77
5	0:31	4.89	1.34	5	9:27	10.00	-0.85
6	4:/20 5:28	5.31	1.76	6	9:35	9.99	-0.86
7	7:51	2.87	-0.68	7	9:42	9.98	-0.87
8	8:38	2.40	-1.15	8			
9	9:08	2.20	-1.35	9			

Table B-3: Record of Tide Staff Readings (Run No. 3 Continued)

Date: April 20, 1995

Staff 17				Staff 18			
No	Time (EDST)	Reading (ft)	Elev. (ft)	No	Time (EDST)	Reading (ft)	Elev. (ft)
1	4/20 1:34	10.28	2.30	1	1:31	10.19	2.23
2	1:42	10.36	2.38	2	1:46	10.30	2.34
3	1:49	10.37	2.39	3	2:02	10.43	2.47
4	1:59	10.53	2.55	4	2:16	10.59	2.63
5	2:16	10.64	2.66	5	2:32	10.73	2.77
6	2:30	10.78	2.80	6	2:47	10.88	2.92
7	2:46	10.91	2.93	7	3:01	10.97	3.01
8	3:00	11.00	3.02	8	3:17	11.04	3.08
9	3:16	11.06	3.08	9	3:32	11.06	3.10
10	3:30	11.06	3.08	10	3:46	11.00	3.04
11	3:46	11.00	3.02	11	4:01	10.92	2.96
12	4:00	10.93	2.95	12	4:17	10.82	2.86
13	4:16	10.83	2.85	13	4:31	10.70	2.74
14	4:30	10.71	2.73	14	4:46	10.58	2.62
15	4:45	10.5	2.58	15	5:01	10.44	2.48
16	5:00	10.40	2.42	16			
17	5:05	10.30	2.32	17			
Staff 19				**Staff 20**			
1	1:30	2.10	2.18	1	1:50	9.28	2.32
2	1:45	2.18	2.26	2	1:58	9.42	2.46
3	2:00	2.38	2.46	3	2:15	9.57	2.61
4	2:15	2.52	2.60	4	2:20	9.71	2.75
5	2:30	2.66	2.74	5	2:44	9.83	2.87
6	2:45	2.79	2.87	6	2:59	9.93	2.97
7	2:59	2.89	2.97	7	3:15	10.01	3.05
8	3:15	2.96	3.04	8	3:29	10.04	3.08
9	3:29	2.98	3.06	9	3:44	9.99	3.03
10	3:45	2.94	3.02	10	3:59	9.90	2.94
11	3:59	2.86	2.94	11	4:14	9.81	2.85
12	4:15	2.76	2.84	12	4:29	9.69	2.73
13	4:30	2.64	2.72	13	4:44	9.53	2.57
14	4:44	2.50	2.58	14	4:59	9.41	2.45
15	4:59	2.36	2.44	15	5:05	9.34	2.38

Table B-4: Record of Water Depth and Velocity (Run No. 3)

Survey Data: April 19, 1995
Location: DS of R1 Road

Position	No.	Time (EDST)	D_b (ft)	D_s (ft)	Water Depth (ft)	0.6H (ft)	NRV	Δt (Sec.)	Velocity (ft/s)
Station1	1	4/19 23:26	21.40	18.21	2.69	1.60	20	48	0.928
Num.2	2	23:46		17.59	3.31	1.98	25	50	1.11
	3	4/20 0:05		17.25	3.65	2.2	25	53	1.05
	4								
	5								
	6								
	7								
	8								
	9								
	10								
Station2	1	4/19 23:30	22.09	18.40	3.69	2.20	35	55	1.407
Num.5	2	23:44		17.90	4.19	2.50	40	57	1.549
	3	4/20 0:06		17.61	4.48	2.70	35	45.5	1.696
	4								
	5								
	6								
	7								
	8								
	9								
	10								
Station3	1	4/19 23:41	22.09	18.6	3.49	2.10	20	61	0.734
Num.6	2	13:53		17.9	4.19	2.50	20	56	0.798
	3	4/20 0:12		17.63	4.46	2.70	30	52	1.276
	4								
	5								
	6								
	7								
	8								
	9								
	10								

D_b—Distance between the Berm of R1 Bridge and River Bottom.
D_s—Distance between the Berm of R1 Bridge and Water Surface.

Table B-4: Record of Water Depth and Velocity (Run No. 3 Continued)

Date: April 20, 1995
Location: DS of R1 Bridge

Position	No.	Time (EDST)	D_b (ft)	D_s (ft)	Water Depth (ft)	0.6H (ft)	NRV	Δt (Sec.)	Velocity (ft/s)
Station1	1	4/20 5:42	21.40	16.70	4.70	2.82	30	47	1.41
Num.2	2	5:54		16.98	4.42	2.65	30	51	1.30
	3	6:03		17.10	4.30	2.59	30	51	1.30
	4	6:14		17.41	3.99	2.40	30	60	1.11
	5								
	6								
	7								
	8								
	9								
	10								
Station2	1	4/20 5:45	22.07	17.11	4.96	2.98	40	56	1.58
Num.4	2	5:57		17.25	4.82	2.89	35	58	1.34
	3	6:07		17.49	4.58	2.76	30	52	1.28
	4	6:17		17.68	4.39	2.64	30	47	1.41
	5	6:24		17.86	4.21	2.52	30	55	1.21
	6								
	7								
	8								
	9								
	10								
Station3	1	4/20 5:49	22.09	17.50	4.59	2.76	30	49	1.35
Num.6	2	5:59		17.78	4.31	2.59	30	51	1.30
	3	6:10		17.90	4.19	2.52	35	67	1.16
	4	6:20		18.13	3.96	2.40	30	56	1.19
	5								
	6								
	7								
	8								
	9								
	10								

D_b—Distance between the Berm of R1 Bridge and River Bottom.
D_s—Distance between the Berm of R1 Bridge and Water Surface.

Table B-5: Record of Tide Staff Readings
Velocity Measurement (Run No. 3)

Date: April 20, 1995
Location: US of Railway B.

Position	No.	Time (EDST)	D_b (ft)	D_s (ft)	Water Depth (ft)	0.6H (ft)	NRV	Δt (Sec.)	Velocity (ft/s)
Station1	1	4/20 8:10	21.18	20.20	0.98		20	48	0.827
Num.2	2	8:25		20.31	0.87		20	50	0.735
	3	8:36		20.43	0.75		15	53	0.661
	4	8:47		20.50	0.68		15		0.604
	5	8:56		20.49	0.69		15		0.661
	6	9:28		20.54	0.64		15		0.674
	7	9:38		20.57	0.61		15		0.626
	8								
	9								
	10								
Station2	1	4/20 8:18	22.97	20.26	2.71	1.63	20	53	0.843
Num.4	2	8:29		20.31	2.66	1.60	20	44.5	0.989
	3	8:38		20.48	2.49	1.59	15	35.7	0.964
	4	8:49		20.48	2.49	1.59	15	36.8	0.908
	5	9:22		20.59	2.38	1.43	15	31.6	1.054
	6	9:32		20.58	2.39	1.43	15	33.5	0.976
	7	9:42		20.61	2.36	1.41	15	38.8	0.842
	8								
	9								
	10								
Station3	1	4/20 8:21	23.22	20.28	2.94	1.76	25	49.8	1.11
Num.5	2	8:33		20.40	2.82	1.69	20	39.4	1.11
	3	8:42		20.45	2.77	1.66	20	39.2	1.15
	4	8:52		20.46	2.76	1.65	20	40.0	1.11
	5	9:24		20.53	2.69	1.62	20	43	1.03
	6	9:34		20.60	2.62	1.56	20	42.5	1.04
	7	9:44		20.58	2.64	1.56	20	43	1.03
	8								
	9								
	10								

D_b—Distance between the Berm of Railway Bridge and River Bottom.
D_s—Distance between the Berm of Railway Bridge and Water Surface.

Table B-6: Record of Tide Staff Readings (Run No. 4)

Date: May 16-17, 1995

Staff 1				Staff 4			
No	Time (EDST)	Reading	Elev. (ft)	No	Time (EDST)	Reading	Elev. (ft)
1	5/16 19:48	4.96	-1.00	1	5/16 19:54	11.68(Es.)	-0.99
2	20:18	5.33	-0.63	2	20:25	12.10	-0.57
3	22:23	7.98	2.02	3	22:45	14.90	2.23
4	23:22	8.88	2.94	4	23:22	15.76	3.09
5	5/17 0:15	3.49	2.66	5	5/17 0:24	16.15	3.58
6	1:18	9.73	3.79	6	0:28	16.50	3.83
7	2:18	9.27	3.33	7	1:28	15.96	3.29
8	3:17	8.13	2.17	8	2:29	15.07	2.40
9	4:18	6.89	0.93	9	3:24	13.62	0.95
10	5:08	5.88	-0.08	10	4:25	12.66	-0.01
11	6:16	4.88	-1.08	11	5:15	11.70	-0.97
12	7:20	4.32	-1.64	12	7:31	11.10	-1.57
13				13			
Staff 7				**Staff 8 OR 9**			
1	5/16 20:09	2.62	-0.93	1(9)	5/16 20:00	9.90(E.)	-0.95
2	20:38	3.00	-0.55	2(9)	20:32	10.30	-0.55
3	23:12	6.04	2.49	3	23:07	4.27	2.51
4	5/17 0:03	6.66	3.11	4	23:56	4.80	3.04
5	1:05	7.22	3.67	5	5/17 0:59	5.45	3.69
6	2:07	7.02	3.47	6	2:01	5.41	3.65
7	3:07	6.37	2.82	7	3:00	4.83	3.07
8	4:05	5.08	1.53	8	3:59	3.74	1.98
9	4:58	3.87	0.32	9	4:52	2.40	0.64
10	6:07	2.87	-0.68	10	6:02	2.60(E.)	0.84
11	7:10	2.31	-1.24	11(9)	7:00	10.12	-0.73
12				12			
13				13			

Table B-6: Record of Tide Staff Readings(Run No. 4 Continued)

Date: May 16-17, 1995

Staff 17				Staff 18			
No	Time (EDST)	Reading	Elev. (ft)	No	Time (EDST)	Reading	Elev. (ft)
1	5/16 23:19	10.64	2.66	1	5/16 23:20	10.51	2.55
2	23:51	10.96	2.98	2	23:47	10.91	2.95
3	23:59	11.11	3.13	3	5/17 0:09	11.22	3.26
4	5/17 0:16	11.34	3.36	4	0:25	11.42	3.46
5	0:36	11.57	3.59	5	0:43	11.57	3.61
6	0:49	11.65	3.67	6	0:55	11.68	3.72
7	1:01	11.72	3.74	7	1:08	11.73	3.77
8	1:18	11.73	3.75	8	1:24	11.78	3.82
9	1:33	11.78	3.80	9	1:40	11.78	3.82
10	1:46	11.73	3.75	10	1:51	11.66	3.70
11	1:58	11.62	3.64	11			
12				12			
Staff 19				**Staff 20**			
1	5/16 23:23	2.45	2.53	1	5/16 23:17	9.53	2.57
2	23:45	2.82	2.90	2	23:45	9.87	2.91
3	5/17 0:07	3.20	2.46	3	5/17 0:13	10.24	3.28
4	0:24	3.31	3.39	4	0:32	10.42	3.46
5	0:40	3.46	3.54	5	0:45	10.58	3.62
6	0:53	3.59	3.67	6	0:58	10.66	3.70
7	1:06	3.61	3.69	7	1:13	10.70	3.74
8	1:21	3.68	3.76	8	1:30	10.75	3.79
9	1:38	3.70	3.78	9	1:43	10.72	3.76
10	1:49	3.61	3.69	10	1:56	10.61	3.65
11				11			
12				12			

Table B-7: Record of Water Depth and Velocity (Run No. 4)

Date: May 17, 1995
Location: DS of R1 Road

Position	No.	Time (EDST)	D_b (ft)	D_s (ft)	Water Depth (ft)	0.6H (ft)	NRV	Δt (Sec.)	Velocity (ft/s)
Station1	1	5/17 3:07	21.40	15.40	6.00	3.60	30	36.4	1.816
Num.2	2	3:12		15.78	5.62	3.37	30	32.5	2.032
	3	3:28		16.24	5.16	3.10	30	29.0	2.275
	4	3:38		16.29	5.11	3.06	30	29.6	2.229
	5	4:11		17.08	4.32	2.60	30	33.0	1.983
	6	4:35		17.38	4.02	2.41	30	53.6	1.240
	7	4:58		17.79	3.61	2.17	30	56.8	1.171
	8	5:23		18.15	3.25	1.95	30	55.8	1.192
	9	5:42		18.55	2.85	1.71	15	55.6	0.608
	10								
Station2	1	5/17 3:10	22.07	15.78	6.29	3.80	30	37.0	1.787
Num.4	2	3:20		16.05	6.02	3.61	30	30.8	2.143
	3	3:32		16.43	5.64	3.38	30	31.2	2.116
	4	3:42		16.51	5.56	3.34	30	31.2	2.116
	5	4:26		17.36	4.71	2.83	30	41.8	1.584
	6	4;41		17.80	4.27	2.56	30	43.6	1.520
	7	5:02		18.23	3.84	2.30	30	50.8	1.307
	8	5:28		18.64	3.43	2.05	30	58.2	1.143
	9	5;46		18.90	3.17	1.90	30	57.4	1.159
	10								
Station3	1	5/17 3:15	22.09	16.18	5.91	3.55	30	34.6	1.910
Num.6	2	3:25		16.40	5.69	3.41	30	30.8	2.143
	3	3:35		16.75	5.34	3.20	30	29.5	2.237
	4	3:46		16.96	5.13	3.08	30	30.8	2.143
	5	4:30		17.81	4.28	2.56	30	45.0	1.473
	6	4:46		18.19	3.90	2.34	30	46.5	1.426
	7	5:07		18.54	3.55	2.13	30	56.2	1.183
	8	5:31		18.98	3.11	1.86	30	60.8	1.095
	9	5:49		19.25	2.84	1.70	30	65.6	1.016
	10								

D_b—Distance between the Berm of R1 Bridge and River Bottom.
D_s—Distance between the Berm of R1 Bridge and Water Surface.

Table B-8: Freshwater Runoff (Run No. 4)

Date: May 17, 1995
Climate: Clear abd Dry

Position	No.	D_i (ft)	Water Depth (ft)	Mea. Point	NRV	Δt (Sec.)	Velocity (ft/s)
Culvert	1	1	1.4	0.5	10	42.3	0.263
(Width=9ft)	2	2	1.4	0.5	10	47.7	0.237
	3	5	1.8	0.6	15	32.6	0.479
	4	7	1.4	0.6	15	32.4	0.482
	5	8	1.4	0.6	15	30.0	0.517
	6	3	1.9	0.6	15	33.0	0.474
	7	6	1.4	0.6	10	33.1	0.326
	8						
	9						
	1						
Wood Bridge	1	2	2.6	0.6	10	48.8	0.235
Width=8ft	2	4	2.4	0.6	10	65.5	0.180
	3	6	2.6	0.6	10	51.3	0.223
	4						
	5						
	6						
	7						
	8						
	9						
	10						
Round Culvert	1	1	0.6	0.6	35	48.8	0.727
Width=8.7 ft	2	2	0.7	0.6	40	23.0	1.713
	3	3	0.65	0.6	40	21.0	1.873
	4	4	0.80	0.6	40	30.0	1.321
	5	5	0.85	0.6	40	31.3	1.268
	6	6	0.60	0.6	40	37.3	1.069
	7						
	8						
	9						
	10						